OBSERVERS AS A TOOL TO REDUCE INFORMATION EXCHANGE AND INCREASE CONVERGENCE RATE IN MULTI-AGENT SYSTEMS

By

Dhrubajit Chowdhury

A DISSERTATION

Submitted to
Michigan State University
in partial fulfillment of the requirements
for the degree of

Electrical Engineering – Doctor of Philosophy

2020

ABSTRACT

OBSERVERS AS A TOOL TO REDUCE INFORMATION EXCHANGE AND INCREASE CONVERGENCE RATE IN MULTI-AGENT SYSTEMS

By

Dhrubajit Chowdhury

Observers form an integral part of output feedback control of linear and nonlinear systems. This dissertation investigates the use of observers in multi-agent systems to reduce information exchange and increase the convergence rate. Multi-agent systems have been immensely popular since the last two decades due to their broad applicability in practical problems, some of them being distributed sensor networks, formation control, and cooperative robotics. The controller for each agent is distributed in nature, which means that it only depends on the local information available to it. The distributed approach has several advantages such as less computational effort, reliability, etc., compared to the centralized one where there is a central agent that does all the computations and then makes the decision.

The convergence rate of consensus algorithms is an important performance measure. We show that by using observers, we can increase the convergence rate of the consensus algorithm. The observer is used for estimating the missing links at each agent. We also study the effect of increasing network size on the consensus algorithm. For networks without a leader, the rate of convergence of the consensus protocol becomes slow for certain classes of graphs, while for networks with a single leader, the convergence rate becomes slow for undirected graphs. We design scalable consensus algorithms for first-order linear agents and second-order nonlinear heterogeneous agents where the convergence rate remains almost invariant of the network size.

We consider the case of reduced information exchange in a network of nonlinear hetero-

geneous agents having the same relative degree r. We use observers along with feedback control to compensate for the heterogeneity at each agent. Finally, motivated by the practical application of multi-agent systems to power systems frequency synchronization, we fuse dynamic consensus algorithms with observers to achieve practical frequency synchronization under time-varying power-demand. We show that the frequency synchronization error can be made arbitrarily small by tuning controller and observer parameters.

This dissertation is dedicated to my beloved parents.

ACKNOWLEDGMENTS

First and foremost, I would like to thank one of the essential contributors to this thesis, my advisor Dr. Hassan Khalil. I will always be indebted to him for first accepting me as his student and then for his constant guidance and support throughout my Ph.D. journey. During my time as a Ph.D. student, I was deeply moved by his ability to teach students as well as maintain high-quality research successfully. His constant enthusiasm in answering questions during a research meeting or when teaching in a class has been a real inspiration to me. As I start my academic career, I hope to become not only a well-established researcher but also an inspiring teacher. I also thank him for giving me the flexibility to pursue my research ideas and also work on 'side-projects' over the years. I wish him the best for his retirement life.

My committee members have provided excellent support over the years. I want to thank Dr. Ranjan Mukherjee for allowing me to collaborate with him and work on the control of mechanical systems. He has helped me understand the application of control to mechanical systems. Dr. Xiaobo Tan has always been welcoming when discussing ideas and providing insights into an academic career. The knowledge I have gained while working with him during his class projects is immeasurable. I always enjoyed talking with Dr. Vaibhav Srivastava about state of the art in network systems. He was always available for a quick chat and gave me pointers about new research directions. He serves as a role model for what I want to achieve in the next phase of my career.

I would especially like to thank Dr. Tim Hogan for being flexible with my teaching assignments and all the instructors in my teaching assistantship. I appreciate all ECE department administrators and staff members for their help. I also want to acknowledge the initial funding I received from the National Science Foundation (ECCS - 1128476).

This journey could not have been completed without the support of friends and family. I want to thank all my friends and colleagues at Michigan State University, specially Pratap Bhanu Solanki, Yashesh Dhebar, Gaurav Chauda, Rahul Dey, Dr. Saran Karrupuswami, Suhas Vidhate, Saikat Mondal, Jason Greenberg, Billy Stevers, and Rakshith Lokesh. Thanks to my undergraduate friends Bikiran Guha and Archan Ray, who are also pursuing their Ph.D. in U.S.A. for all the memorable trips. I am also thankful to my friends Suraj, Sunny, Sudip, Shashank, Soumitra, Mukhesh, Tanaya, Monalisa, Sitangshu, Niladri in India for their encouragement and support.

There is a trade-off in everything we do in life. Unfortunately, during this journey, I lost my father, (late) Ajit Kumar Chowdhury, in 2017. I am sure he would be one of the happiest people in the world watching me complete this journey. I will always be indebted to my mother, Swapna Chowdhury, for her unconditional love and support for me. Her life's journey is a source of inspiration for me. I also thank my brother Debashish Chowdhury for his help. Finally, I would like to thank my girlfriend, Paola, for all the love and support.

TABLE OF CONTENTS

LIST OF TABLES . . . **xi**

LIST OF FIGURES . . . **xii**

Chapter 1 Introduction . . . **1**
- 1.1 Literature Review . . . 1
  - 1.1.1 Review on Algebraic Graph Theory . . . 1
  - 1.1.2 Consensus and Synchronization Algorithms Review . . . 3
  - 1.1.3 Application of Consensus Algorithms to Power Systems Review . . . 9
- 1.2 Contribution and Organization . . . 11
  - 1.2.1 Overview of Contribution . . . 11
  - 1.2.2 Thesis Organization . . . 14

Chapter 2 Fast Consensus with Star Topology Using High Gain Observers **16**
- 2.1 Introduction . . . 16
- 2.2 Consensus on Different Network Topologies . . . 18
  - 2.2.1 Consensus with Complete Graph . . . 18
  - 2.2.2 Consensus with Star Graph . . . 19
- 2.3 Design Preliminaries . . . 19
  - 2.3.1 Target System . . . 20
  - 2.3.2 Exploiting the Star Topology Structure . . . 21
- 2.4 Controller Design and Analysis . . . 21
  - 2.4.1 Extended High Gain Observers . . . 22
  - 2.4.2 Peaking . . . 23
  - 2.4.3 Observer Error Dynamics . . . 24
- 2.5 Simulations . . . 32
- 2.6 Conclusion . . . 34

Chapter 3 Scalable Consensus Using High Gain Observers . . . **35**
- 3.1 Introduction . . . 35
- 3.2 Problem Definition . . . 36
- 3.3 State feedback Controller Design . . . 37
- 3.4 Output-Feedback Controller . . . 43
  - 3.4.1 Preliminaries . . . 43
  - 3.4.2 Observer Design . . . 48
  - 3.4.3 Peaking . . . 48
- 3.5 Cyclic Pursuit on Plane . . . 58
- 3.6 Tree Graphs . . . 62
- 3.7 Conclusion . . . 65

Chapter 4 Practical Scalable Synchronization in Leader-Follower Networks 66
4.1 Introduction 66
4.2 Problem Setup 68
4.2.1 Class of Systems 68
4.2.2 Leader 68
4.3 Controller Design With Full Information 71
4.3.1 Controller Design 71
4.3.2 Closed-loop System Analysis 74
4.4 Output Feedback Controller 78
4.4.1 Observer Design 78
4.4.2 Peaking 79
4.4.3 Analysis of the closed loop system 81
4.5 Examples 88
4.5.1 IEEE 300-Bus System 88
4.5.2 Platooning of Vehicles 92
4.6 Conclusion 95

Chapter 5 Practical Synchronization in Networks of Nonlinear Heterogenous Agents under Reduced Information 97
5.1 Introduction 97
5.2 Problem Formulation 98
5.2.1 Leader 100
5.3 Relative Dynamics 103
5.4 Synchronization under full information 106
5.5 Synchronization under output feedback 109
5.6 Example 123
5.7 Case with Some Unbounded Leader States 128
5.7.1 State feedback Controller 131
5.7.2 Output feedback Controller 131
5.8 Frequency Control of Power Systems 136
5.9 Conclusion 140

Chapter 6 Power Systems Frequency Synchronization 141
6.1 Introduction 141
6.1.1 System Model 142
6.2 Control Objective 144
6.3 Controller Design Under known Time-Varying Power Demand 147
6.3.1 Communication Topology 147
6.3.2 Dynamic Average Consensus 147
6.3.3 Analysis of the Closed-loop System 149
6.4 Controller Design Under Unknown Time Varying Power Demand 155
6.4.1 Extended High-Gain Observer 155
6.4.2 Analysis of the Closed-loop System 157
6.5 Simulation 162
6.5.1 Case I : Unknown Constant Power Demand 162

6.5.2 Case II : Unknown Time-Varying Power Demand with variable Frequency 164
6.6 Conclusion 165

Chapter 7 Conclusion and Future Work **166**
7.1 Overview of Conclusion 166
7.2 Future Directions 169
7.2.1 Stability of Networks with Signed Laplacians 169
7.2.2 Scalable Formation Control of Mobile Robots 170
7.2.3 Frequency Synchronization in Higher Order Power System Models . . 171

APPENDIX **172**

BIBLIOGRAPHY **175**

LIST OF TABLES

Table 3.1: Laplacian Eigenvalues of Tree-like fractal graphs 64

Table 3.2: Laplacian Eigenvalues of Vicsek fractal graphs 64

LIST OF FIGURES

Figure 2.1: Star Topology 18

Figure 2.2: Consensus on Complete Graph 33

Figure 2.3: Consensus on Star Graph with no Observers 33

Figure 2.4: Consensus on Star Graph with Observers and $\epsilon = 0.001$ 33

Figure 2.5: Deviation of agent 6 trajectory from target trajectory 34

Figure 3.1: A directed circulant graph 59

Figure 3.2: Agent 4 state 60

Figure 3.3: Agent 4 control signal 60

Figure 3.4: Agent 4 control signal with $\mu = 0.1$, $\epsilon = 0.0001$ 61

Figure 3.5: Tree-like Fractal graphs 62

Figure 3.6: Vicsek Fractal graphs 63

Figure 4.1: Diagram of node connections for the IEEE 300-Bus System 89

Figure 4.2: State one synchronization error $e_x = x - x_0$ 90

Figure 4.3: State two synchronization error $e_v = v - v_0$ 90

Figure 4.4: Control signal of the oscillators 91

Figure 4.5: Log-Linear plot of the contol signal for different value of k 91

Figure 4.6: Performance recovery with $k = 300$ 92

Figure 4.7: Line graph representing platoon of vehicles 93

Figure 4.8: Position error of vehicle ten, $\tilde{x}_{10} = x_{10} - x_{10}^{0d}$ 94

Figure 4.9: Velocity error of vehicle ten, $\tilde{e}_{v10} = v_{10} - v_0$ 94

Figure 4.10: Control signal of vehicle ten 94

Figure 5.1: Network interconnection between the agents 123

Figure 5.2: States of the agents under the proposed controller with $\epsilon = 0.001$ 126

Figure 5.3: Control of the agents with $\epsilon = 0.001$ 127

Figure 5.4: States of the agents under the proposed controller with $\epsilon = 0.0001$ 127

Figure 5.5: Control of the agents with $\epsilon = 0.0001$ 128

Figure 5.6: Phase of the buses 139

Figure 5.7: Frequency of the buses 139

Figure 5.8: Control 140

Figure 6.1: Four area network 162

Figure 6.2: Frequency deviation (ω) under unknown constant power demand 163

Figure 6.3: Control (u) under unknown constant power demand 163

Figure 6.4: Frequency deviation (ω) under unknown time-varying power demand . . 164

Figure 6.5: Control (u) under unknown time-varying power demand 165

Chapter 1

Introduction

Multi-agent systems are popular due to their wide applicability in practical problems, some of them being distributed sensor networks [1], [2] and cooperative robotics [3], [4]. The consensus problem in multi-agent systems has been well studied in the last decade. Consensus problems were studied in the field of computer science in distributed computing in which the computer processes are required to reach an agreement on certain data values [5]. The controllers designed for multi-agent systems are distributed in nature and are based on the local information available to the agents, which in turn depends on the communication topology. The communication constraints and the convergence rate of the protocol are given more emphasis while solving the consensus problem.

1.1 Literature Review

1.1.1 Review on Algebraic Graph Theory

The communication topology between the agents is defined by a *time-invariant directed communication graph* which describes the information flow among the agents. A weighted directed graph is denoted by $\mathcal{G} = (\mathcal{V}, \mathcal{E}, \mathcal{A})$, where $\mathcal{V} = \{v_1, v_2, \ldots, v_N\}$ is the set of nodes, one for each of the N agents present in the network, $\mathcal{E} \subseteq \mathcal{V} \times \mathcal{V}$ is the set of edges which represent the interconnection between the agents, and $\mathcal{A}$ is a weighted adjacency matrix with non-negative elements $[\mathcal{A}]_{kj} = a_{kj} \geq 0$. If the edge weights a_{kj} are only zero or one, then the graph is said to be unweighted, otherwise it is said to be weighted. An edge $(v_k, v_j) \in \mathcal{E}$ implies that there is a directed edge from node v_k to node v_j and node v_j receives information from node v_k. Moreover, v_k is called an *in−neighbor* of v_j, and v_j is called an *out−neighbor* of v_k. If $(v_k, v_j) \in \mathcal{E} \implies (v_j, v_k) \in \mathcal{E}$, then the graph is said to be undirected, otherwise it is said to be directed. A path is defined by a sequence of vertices such that for each of its vertices v_k the next vertex in the sequence is a neighbor of v_k. Two nodes v_k and v_j are connected if and only if there exists a directed path from node v_k to node v_j. We assume that there are no self-loops which implies $a_{kk} = 0$ for $k = 1, 2, \ldots, N$. A directed graph contains a directed spanning tree if there exists a node called root such that there exists a directed path from the root node to every other node in the graph. In other words, this implies that the graph is connected.

The Laplacian matrix $L \in \mathbb{R}^{N \times N}$ is defined as $[L]_{kj} = l_{kj}$ where $l_{kk} = \sum\limits_{j=1, j \neq k}^{N} a_{kj}$, $l_{kj} = -a_{kj}$ for $j \neq k$. The Laplacian of an undirected graph can be defined as $L = \mathcal{B}\Gamma_L \mathcal{B}^T$, where Γ_L is a diagonal matrix with the diagonal elements being the weights of edge $(i, j) \in \mathcal{E}$ for all $(i, j) \in \mathcal{V}$, $\mathcal{B} \in \mathbb{R}^{n \times m}$ is the incidence matrix and m is the cardinality of the edge set $\mathcal{E}$, where cardinality is defined as the number of elements in a set. The incidence matrix satisfies $\mathcal{B}^T \mathbf{1} = 0$, where $\mathbf{1} \in \mathbb{R}^n$ represents the vector of all 1's. It can be also be defined as $L = \mathcal{D} - \mathcal{A}$, where $\mathcal{D}$ is called the degree matrix of $\mathcal{G}$.

The structure of the Laplacian matrix is such that the diagonal entries are non-negative, and the off-diagonal entries are non-positive and, for each row, the sum of all the entries on this row is zero. A matrix that satisfies these properties is called Metzler [6] or $\mathcal{M}$ matrix. As a result it has an eigenvalue $\lambda_1(L) = 0$ and the corresponding eigenvector associated with it is a vector of all-ones $\mathbf{1} = \mathrm{col}(1, 1, \ldots, 1)$. We denote the other $N - 1$ eigenvalues of L

as $\lambda_2(L), \ldots, \lambda_N(L)$. A time-invariant directed graph is connected if and only if L has one simple zero eigenvalue $\lambda_1(L) = 0$ and all other eigenvalues $\lambda_2(L), \ldots, \lambda_N(L)$ have positive real parts [7], [8]. If for each node, the number of $in-neighbor$ is equal to the number of $out-neighbor$, we say the graph is balanced, and it follows that $\mathbf{1}^T L = 0$.

For leader-follower networks with a single leader in the network we define the expanded graph as $\bar{\mathcal{G}} = (\bar{\mathcal{V}}, \bar{\mathcal{E}}, \bar{\mathcal{A}})$, where $\bar{\mathcal{V}} = \{v_0, v_1, v_2, \ldots, v_N\}$ and $\bar{\mathcal{E}}$, $\bar{\mathcal{A}}$ contains the edges and edge weights from the leader to the other agents in addition to the edges and edge weights from $\mathcal{E}$ and $\mathcal{A}$, respectively. In this case, the communication topology is described by the grounded Laplacian matrix L_G. The grounded Laplacian matrix is obtained by removing certain rows and columns associated with the leader from the Laplacian matrix. It is also studied in the context of agent stubbornness [9], where an agent can influence the network by exchanging its information with the other agents. Still, in return, it is not influenced since it does not use any information from the other agents in the network. It can also be defined with respect to the Laplacian of the graph $\mathcal{G}$ by $L_G = L + D$, where $D = \text{diag}(d_1, \ldots, d_N)$, and $d_k > 0$ if agent v_k receives information from the leader v_0 otherwise $d_k = 0$. The leader does not receive any information from the agents in the network. If the expanded graph $\bar{\mathcal{G}}$ contains a directed spanning tree with the leader as the root node, then the grounded Laplacian matrix L_G is a nonsingular $\mathcal{M}$-matrix [10].

1.1.2 Consensus and Synchronization Algorithms Review

Consensus and synchronization both describe the effect of reaching agreement in a group of agents in some sense. Consensus-based approaches are used for solving cooperative control problems in multi-agent systems which include formation control [11], [12], connectivity maintenance [13] and flocking [14]. The survey papers [15], [16], and the books [17], [18] provide an exhaustive material on the consensus problems in multi-agent systems.

Consensus in first-order agents was achieved in [19]. The convergence rate is an important factor in the design of the consensus controller. The communication topology through which the agents communicate is important as it decides the convergence rate of the consensus algorithm. The communication topology is generally encoded in a matrix called the graph Laplacian [20], denoted by L. The convergence rate of the consensus algorithm for an undirected graph depends on the second smallest eigenvalue $\lambda_2(L)$ of the graph Laplacian, also known as the algebraic connectivity [7] of the graph. For an undirected graph, the second smallest eigenvalue of the graph Laplacian is non-decreasing if edges are added to the graph [18]. The effect on the convergence rate by adding edges on a directed acyclic graph has been studied in [21].

To increase the convergence rate, a simple solution would be to multiply the consensus equation by a gain. However, if the second smallest eigenvalue of the graph Laplacian of the graph tends to zero, then the gain needs to be very large. Another approach to solving this problem is by redesigning the network topology [22], [23], to increase the second smallest eigenvalue of the graph Laplacian. Redesign of the network topology may lead to a high communication cost as nodes that are at a large geographical distance may need to communicate with each other. Next, we mention other approaches where fast convergence is achieved without using high-gain or redesigning the network topology. Fast consensus is achieved in [24] by recording the past state of a selected agent and its neighbors. In [25], fast convergence is achieved for a strongly connected network of agents with a single leader in the discrete-time setting. The control of the leader is designed by making use of past values of the leader's state, which improves the convergence rate. Some of the other methods estimate the second smallest eigenvalue of the graph Laplacian, which can then be used as a control parameter to achieve fast convergence. Decentralized estimation of the second smallest eigenvalue of the graph Laplacian was achieved for undirected graphs in [26], and strongly connected graphs in [27]. However, these methods require each agent to communicate a vector whose size increases linearly with the number of agents in the network. In [28], the second smallest eigenvalue of the graph Laplacian is estimated, and adaptive control is used to tune the edge weights for undirected graphs. However, the effect of change in edge weights on the control signal is not shown, and the controller requires more information exchange. The decrease of the second smallest eigenvalue of the graph Laplacian also affects finite-time consensus algorithms [29], [30], as the upper bound on the finite time is inversely proportional to the second smallest eigenvalue of the graph Laplacian.

The scalability of consensus laws is also an important factor as with an increase in the network size, the second smallest eigenvalue of the graph Laplacian decreases for many classes of graphs, including planar, lattice, and tree graphs; see [31]. These classes of graphs are contained in the non-expander family [32], where the second smallest eigenvalue of the graph Laplacian decreases towards zero with an increase in the network size. For example, in a circulant undirected graph [17, Chapter 2], where all the agents are arranged in a circle and each agent can communicate with its two adjacent neighbors, the eigenvalues of the Laplacian for this undirected network has a closed-form given by

$$0, 2 - 2\cos\frac{2\pi}{N}, \ldots, 2 - 2\cos\frac{2(N-1)\pi}{N}$$

Therefore as the number of agents (N) increases we have

$$\lim_{N\to\infty} 2 - 2\cos\frac{2\pi}{N} = 0$$

which implies that the second smallest eigenvalue of the graph Laplacian is decreasing towards zero, and the convergence rate of the consensus algorithm is becoming slow. In [18, Chapter 10], a similar conclusion has been drawn for a directed circulant graph. On the contrary, expander family contains classes of graphs where the second smallest eigenvalue of the graph Laplacian is bounded away from zero, with an increase in network size [33], which includes complete graphs, random regular graphs, small-world networks [34], etc. The recent thesis [31] describes this effect. It covers some non-exhaustive classes of graphs where the second smallest eigenvalue of the graph Laplacian decreases with an increase in network size. This property has also been investigated in the platooning of vehicles, where the vehicles are arranged in a line formation, and with an increase in the number of vehicles, the second smallest eigenvalue of the graph Laplacian decreases and, as a result, the closed-loop system becomes unstable [35].

Performance measures of the consensus algorithms are also studied for leader-follower networks. The communication topology is defined by the grounded Laplacian matrix, which is obtained by removing specific rows and columns associated with the leader from the Laplacian matrix. These networks are used for applications such as platooning, where the lead vehicle guides the platoon. The performance measure for these networks depends on the smallest eigenvalue of the grounded Laplacian matrix [36]. For leader-follower networks, the performance measure can degrade with an increase in network size, even if the graph among the followers belongs to the expander family. The decrease in the smallest eigenvalue of the grounded Laplacian matrix or the second smallest eigenvalue of the graph Laplacian also affects other performance measures like the $\mathcal{H}_2$-norm, which is commonly used [37] for studying the robustness of consensus algorithms in the context of linear systems [38], [39]. The $\mathcal{H}_2$-norm is calculated from the difference between the systems output and the average output of the network to the disturbance input. This framework has been applied to analyze the performance of the distributed controllers used for the platooning of vehicles [35]. It was shown in [40], that for first-order systems, the $\mathcal{H}_2$-norm is $O(N)$, where N is the network size, for the case when the underlying graph among the followers is a random regular graph, which belongs to the expander family. This occurs due to the smallest eigenvalue of the grounded Laplacian matrix approaching zero with an increase in network size. Similarly, observations were made in [32], which also comments on the loss of stability for agents of order greater or equal to three.

In synchronization problems, the emphasis is on the individual dynamics rather than on the communication constraints; for example, in [41], an all to all communication topology was considered for the synchronization of a group of Kuramoto oscillators. The synchronization problem for general linear systems was also solved in [42] by a low gain approach. Later on, a distributed observer-based protocol was designed in [43], which required the exchange of the outputs of the internal states of the controller. However, the topology of the network was restrictive as the edge weights could be only 0 or 1. The results of [43] were extended in [44] where the extension was done for general time-invariant directed topologies. The synchronization problem for a network of integrators connected through a time-varying communication graph was first addressed in [19] and [45]. The extension to time-varying graphs is generally carried out in the framework of switching. The topology switches among a finite set of graphs and there is a dwell-time in between the switches; see [46], [47], [48], [49], [50]. In all of the works mentioned, the state synchronization was done for homogeneous agents, which means that the agent models were identical. It was shown in [51] that an internal model principle is necessary and sufficient for output synchronization of heterogeneous linear systems. Some of the works in output synchronization of heterogeneous multi-agent systems include [52], [53], [54].

The work of [51] was extended to uncertain heterogeneous nonlinear agents in [55] where each agent has a copy of an exosystem and the exosystems were first synchronized and then local controllers were designed at each agent to track the output of the agents respective exosystem. But the design procedure requires an explicit solution of the output regulator equation, which requires solving partial differential equations. The work in [55] was extended in [56] to nonlinear agents in a leader-follower configuration with time-varying topology, with the assumption that each agent knows its output. The work in [57] uses a distributed internal model to convert the problem to a robust stabilization of the augmented system. Then it solves the stabilization problem via distributed dynamic output control law by utilizing and combining a backstepping, high gain feedback control, and distributed high gain observer. An extension to time-varying topologies and non-identical relative degree was recently proposed in [58]. However, similar to [55], the design procedure in [57] and [58] requires an explicit solution of the output regulator equation and assumes that the solution of the output regulator equation along the trajectory of the exosystem is polynomial. In [59] optimal output synchronization in a network of heterogeneous agents was achieved. However, the proposed approach requires the knowledge of leader dynamics to be known at each agent or its approximation using neural networks, which requires the knowledge of basis functions. Moreover, the HJB solution requires knowledge of the system data along the trajectories of the augmented system. In the second part, an off-policy reinforcement learning is proposed, which does not require the system data but requires that each agent knows its state and the dimension of the leaders state. Synchronization in homogeneous nonlinear and heterogeneous linear agents without the exchange of controller states was done in [53]. In [60], almost regulated output synchronization for nonlinear heterogeneous agents with a time-varying graph was achieved. Unlike [55], the paper [60] does not require knowledge of the local output. However, the class of nonlinear systems is a special case of the class of [55] because the input coefficient is taken to be one. In [61] practical synchronization was achieved in a network of nonlinear heterogeneous agents where it was shown that the synchronization error could be made small by increasing the coupling strength of the interconnection. However, the agents were assumed to be semi-passive, and it was assumed that for the emergent dynamics (the dynamics to which all the agents converge to), there exists a compact invariant set that is asymptotically stable.

Distributed observers are used in multi-agent systems when only relative output information is available to the agents. Synchronization was achieved in [43], [52], [62] using distributed observers where the observers were required to exchange the estimates through the communication topology. In [63] synchronization in a network of identical systems was achieved with reduced information exchange using standard Luenberger observers; however, the exchange of controller states was required. In [53] distributed observers were used without the exchange of observer estimates among the agents to achieve synchronization in homogeneous linear and nonlinear agents and heterogeneous linear agents. In a recent work [64], local observers were designed based on LMI approaches to achieve robust output synchronization in linear heterogeneous multi-agent systems.

1.1.3 Application of Consensus Algorithms to Power Systems Review

One of the major applications of the synchronization problem is in power systems, which are studied with the help of swing equations [65]. The power grid is a large network of subsystems called control areas, where each area produces, consumes, and transfers power to adjacent areas to balance power supply and demand in real-time. The frequency of the AC signal should be maintained very close to a nominal value (typically 50 or 60 Hz), to avoid tripping of generators, degraded power quality, etc. Therefore, one of the control objectives in power systems is to minimize the frequency deviation from the nominal value in an economically efficient way in the presence of load fluctuations. The decentralized control is computationally less expensive and can provide efficient control under islanding and self-healing features in scenarios where there is limited communication between the nodes [66].

Frequency control of power systems is a well-established field of research, which has led to standard control designs. The decentralized PI controller is used along with the proportional droop controller to achieve a zero steady-state error, which leads to global stability results [67]. However, it suffers from performance degradation due to measurement bias and clock drifts. Moreover, the steady-state control does not follow equal power-sharing, and therefore, it is not economically efficient. The decentralized leaky-integrator approach, introduced in [68], is robust to biases in the frequency measurements, and the steady-state control leads to equal power-sharing. However, due to the leakage term, the steady-state error is not zero in the case of constant power demand.

To achieve optimal load frequency control (OLFC), the economic dispatch is incorporated with the frequency control problem [67]. Primal-dual gradient controllers achieve OLFC and can handle constraints and convex cost functions; see the survey paper [69]. However, they require knowledge about load and power flow, which are generally unknown. Distributed consensus algorithms are used to achieve OLFC by assuming the existence of a communication layer. A distributed controller strategy called the distributed averaging integral control (DAPI) is well-studied in the context of microgrids [70], [71] and synchronous generators [72]. The DAPI uses a communication network to exchange the integrator states among the controllers, which leads to equal power-sharing, zero steady-state error, and robustness to measurement bias [73]. The DAPI controller has been studied considering the linear [72] and nonlinear [73] models of the power system.

The unknown power demand is assumed to be constant in the above-mentioned approaches. However, an increase in the use of renewable energy sources causes the power demand to fluctuate at the same timescale as the power system dynamics, and therefore approximating the power demand by a constant value becomes unrealistic [74]. This new challenge necessitates the design of controllers that can handle time-varying power demand. One of the strategies developed to deal with time-varying power demand is the distributed internal model approach [74], [75], [76]. However, this approach requires the time-varying power demand to be generated from a known exosystem model, which is difficult to know in advance. More recently, an adaptive internal model-based approach has been developed in [77], where the exosystem is unknown. Still, it uses a linear power system model and assumes that the unknown power demand is a summation of sinusoids.

1.2 Contribution and Organization

1.2.1 Overview of Contribution

The main contribution of this dissertation is to use observers to increase the convergence rate and reduce information exchange in multi-agent systems. The main contributions of this thesis are discussed below.

We first show that observers can be used to construct missing information at each node in a given network topology. We take advantage of the star topology network architecture and design observer-based decentralized controllers that increase the convergence rate of the consensus protocol. This is unlike high-gain consensus approaches where to reach fast consensus, the control gain needs to be high. We also show that for sufficiently small observer parameters, not only the convergence rate of the consensus protocol with the star topology approaches the convergence rate of a complete graph but also the trajectories of the agents with the star topology approach the trajectories of the agents with the complete graph. However, this design procedure is only limited to the star topology.

Next, we study the effect of network size on the convergence rate. For non-expander graphs, the convergence rate of the consensus algorithm becomes slow, with an increase in network size. To solve this issue, we design a scalable consensus algorithm for first-order agents using Proportional Derivative (PD) for general directed graphs in which we guarantee that the convergence rate of the closed-loop system does not change with an increase in network size. Therefore, using the proposed controller, the convergence rate to achieve consensus does not slow down when the network size increases for general directed non-expander graphs. The PD controller is realized using a high-gain observer. We show that the trajectories of the closed-loop system when the high-gain observer is used can be brought arbitrarily close to the trajectories under the PD controller.

The effect of an increase in network size on the system performance also carries over to nonlinear systems since the nature of information exchange between the agents remains the same, i.e., diffusive coupling. For a leader-follower network with a single leader in the network, the smallest eigenvalue of the grounded Laplacian matrix approaches zero with an increase in network size for undirected graphs. The controller gain of standard nonlinear control approaches to achieve synchronization is inversely proportional to the smallest eigenvalue of the grounded Laplacian. Therefore, as the network size increases, these approaches require a significantly high-gain to achieve synchronization. To alleviate this problem, we design a scalable consensus algorithm to achieve practical synchronization in a leader-follower framework for second-order nonlinear heterogeneous systems. We assume that relative state and velocity derivatives are available for feedback, and we realize the controller using a reduced-order high-gain observer. We show that the synchronization error can be made arbitrarily small by tuning a controller and observer parameter, respectively.

Next, we study the use of extended high-gain observers to achieve practical synchronization in a leader-follower network of nonlinear multi-agent systems having the same relative degree r under reduced information exchange. The class of systems considered in the previous cases is a special case of the one considered here. Moreover, the controller designed here uses less information. The agents do not have access to their state or output and only have relative output information from their neighbors. Extended high-gain observer, along with feedback control, is the primary tool used to compensate for the heterogeneous dynamics of each agent and then replace it with the dynamics of the leader. The proposed approach has significant advantages over the other works in literature that solve the synchronization problem for a general class of nonlinear heterogeneous agents: i) It does not require the explicit solution of the output regulator equation. ii) Unlike the classical output synchronization approach, which gives importance only to the steady-state synchronization error, the proposed method also shapes the transient performance of the closed-loop system. iii) The convergence rate can be chosen by first designing the state feedback control. Then, the convergence rate for output feedback can be made arbitrarily close to the convergence rate under state feedback for a sufficiently small observer parameter. This is unlike [61], where the convergence rate depends on the open-loop system. iv) Motivated by practical applications like platooning of vehicles, and frequency synchronization of power systems, we specialize to agents that have relative degree two and the leader having its first state unbounded. This is unlike the scenario in the classical output synchronization approach, which requires the leader or exosystem states to be bounded.

Finally, as an application, we use dynamic consensus and extended high-gain observers to achieve practical frequency synchronization in power systems under unknown time-varying power-demand. The controller design procedure is different from the previous chapter. We do not use feedback linearization to cancel the power system dynamics; rather, we design the controller to only compensate for the time-varying power demand. For stability analysis, we follow a multiple time-scale approach. Unlike other algorithms in the literature, we do not assume that a known model generates power-demand. We show that the steady-state controller approaches the steady-state controller of [74], and the error between them can be made arbitrarily small depending on the tuning of a controller and observer parameters. We show that the synchronization error can be made arbitrarily small by tuning controller and observer parameters. We also consider the communication topology for the exchange of information among the controllers to be directed, which relaxes the communication constraints compared to [68], [72], [74], which assume the communication topology to be undirected.

1.2.2 Thesis Organization

The dissertation is organized as follows. Chapter 2 studies the use of high-gain observers in a star topology to achieve fast consensus. In Chapter 3, we focus on the design of scalable consensus algorithms in first-order agents. In Chapter 4, we design a scalable consensus controller to achieve practical scalable synchronization in second-order nonlinear heterogeneous agents. Chapter 5 studies the practical synchronization of a network of nonlinear heterogeneous agents under reduced information exchange. We study the power systems frequency synchronization problem using dynamic consensus and high-gain observers in Chapter 6. Finally, Chapter 7 discusses the conclusions and future work. Throughout the dissertation, until and otherwise stated $||\cdot||$ would denote the Euclidean norm.

Chapter 2

Fast Consensus with Star Topology Using High Gain Observers

2.1 Introduction

In this chapter, we show that the second smallest eigenvalue of the graph Laplacian can be increased for a fixed star topology [78] by using extended high-gain observers. The star topology is used in wireless sensor networks [79], VSAT communications [80], smart grids in power networks [81] and the leader-follower configuration in multi-agent systems [82]. The star topology is robust against the failures of the individual nodes, i.e., except for the root node, if one of the nodes get disconnected, the graph remains connected and the remaining connected agents can still reach consensus. Furthermore, it has the least number of connections required for a graph to be connected, which reduces the communication cost. Such a configuration also arises in the consensus problem of mobile robots, where the central robot uses an omnidirectional range sensor. In contrast, other robots use single ray range sensors. The sensors are used to measure the relative distance among the robots. The peripheral robots are within the field of view of the central robot, and therefore it can measure its relative distance to the peripheral nodes. The peripheral robots are aligned towards the central robot, and therefore they can measure the relative distance to the central robot. The only information available to the robots is the relative distance among them based on the range sensor measurements, and there is no other communication structure present in this scenario. The consensus problem is solved based on the relative measurements available to the robots by employing the consensus protocol [19].

The second smallest eigenvalue of the graph Laplacian increases with an increase in the number of communication links, but it leads to high communication costs. For example, the fastest convergence rate can be achieved when the communication topology is given by a complete graph, which is costly in terms of the required number of communication links. Therefore one of the trade-offs, as discussed in [19], is that undirected graphs with high communication costs are expected to have a large second smallest eigenvalue of the graph Laplacian and vice-versa. In this chapter, we show that we can increase the second smallest eigenvalue of the graph Laplacian for a fixed star topology by adding observers to each agent expect the root agent. The complete graph is chosen as a reference target system, and we show that the convergence rate of the consensus protocol with the star topology approaches the convergence rate of the consensus protocol with the complete graph for sufficiently small ϵ, which is a high-gain observer parameter. Furthermore, we show that for sufficiently small ϵ, the trajectories of the agents with the star topology approach the trajectories of the agents with the complete virtual graph.

We make the following assumption about the communication topology.

Assumption 2.1: The communication topology is given by a time-invariant, undirected, unweighted, star graph $\mathcal{G}$.

The star topology is illustrated in 2.1

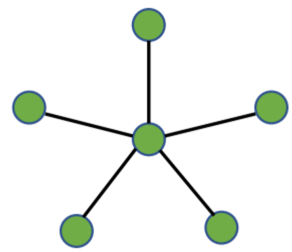

Figure 2.1: Star Topology

We consider agent one as the central or root agent and all the other agents as peripheral agents.

2.2 Consensus on Different Network Topologies

In this section, the convergence rate of the consensus protocol is studied when the communication topology is in the form of complete and star graphs, respectively. The agent dynamics are given by

$$\dot{x}_i = u_i, \quad i = 1, \ldots, N \tag{2.1}$$

The consensus protocol is given by

$$u_i = \sum_{j=1}^{N} (x_j - x_i) \qquad i = 1, \ldots, N. \tag{2.2}$$

2.2.1 Consensus with Complete Graph

If the communication topology is given by a complete graph then the consensus protocol takes the form

$$\dot{x} = -L_c x, \tag{2.3}$$

where $x = [x_1, \ldots, x_N]^T$, and L_c is the graph Laplacian for the complete graph. The eigenvalues of L_c are given by [20]

$$\lambda(L_c) = \{0, N, N, \ldots, N, N\}.$$

where $\lambda(\cdot)$ denotes the eigenvalue. Therefore, the convergence rate of the consensus protocol is proportional to N.

2.2.2 Consensus with Star Graph

Now if the communication topology is given by a star graph we have

$$\dot{x} = -L_s x, \tag{2.4}$$

where L_s is the graph Laplacian. The eigenvalues of L_s are given by $\lambda(L_s) = \{0, 1, 1, \ldots, 1, N\}$. Therefore, the convergence rate of the consensus protocol is proportional to 1. The convergence rate of the consensus protocol for the complete graph is N times faster than the star graph.

2.3 Design Preliminaries

We define our target system as the consensus protocol for the complete graph. The objective of the observer-based controller designed in this chapter is to match the performance of the target system.

2.3.1 Target System

The target system is defined as

$$\dot{x}^* = -L_c x^*, \quad x^*(0) = x(0), \tag{2.5}$$

where $x^*(t)$ is the solution of the target system. Consider the change of variables

$$\alpha^* = x_1^*, \tag{2.6a}$$

$$\delta_i^* = x_{i+1}^* - \alpha^*, \ 1 \le i \le N-1. \tag{2.6b}$$

$\delta^* = [\delta_1^*, \ldots, \delta_{N-1}^*]^T$ is called the disagreement vector and α^* is the consensus manifold. Differentiating (2.6) we have

$$\dot{\alpha}^* = \sum_{i=1}^{N-1} \delta_i^*, \tag{2.7a}$$

$$\dot{\delta}^* = -N\delta^*. \tag{2.7b}$$

We choose a Lyapunov function candidate for the disagreement dynamics (2.7b) as $\bar{V} = \frac{1}{2}\delta^{*T}\delta^*$. Differentiating $\bar{V}$ along (2.7b) we have

$$\dot{\bar{V}} = -N\delta^{*T}\delta^* = -N\|\delta^*\|^2.$$

From which we have

$$\bar{V}(\delta^*(t)) = e^{-2Nt}\bar{V}(\delta^*(0)).$$

Therefore the disagreement vector converges exponentially to zero with a rate N. Hence we can conclude that

$$\lim_{t\to\infty} \delta_i^*(t) = 0 \implies \lim_{t\to\infty} \{x_{i+1}^*(t) - \alpha^*(t)\} = 0, \quad 1 \le i \le N-1.$$

2.3.2 Exploiting the Star Topology Structure

The root agent is numbered as 1 while the other agents are numbered from $2, \ldots, N$ and the root agent is connected to all the other agents in the star network.

In addition to the consensus controller a new decentralized controller will be designed for each agent except the root agent. We do not modify the consensus controller of the root agent as it is connected to all the other agents in the network and it is given by

$$\dot{x}_1 = \sum_{j=2}^{N} (x_j - x_1). \tag{2.8}$$

The controllers in all the other agents will be modified with an observer-based decentralized controller.

2.4 Controller Design and Analysis

In this section we will discuss our strategy of designing the observer-based decentralized controller.

2.4.1 Extended High Gain Observers

We add an extended high gain observer to each agent in the star network except the root agent. The main motivation in adding the observer is that each agent estimates its missing connections from the root agent. The information available to each agent except the root agent is

$$\zeta_{i-1} = x_1 - x_i = -\delta_{i-1}, \qquad i = 2, \ldots, N. \tag{2.9}$$

The control for the peripheral agents are given by

$$u_i = \zeta_{i-1} + \nu_{i-1}, \quad i = 2, \ldots, N$$

where ν_i is the observer based controller to be defined later. Differentiating eq. (2.9) we have

$$\dot{\delta}_{i-1} = -(\dot{x}_1 - \dot{x}_i) = -\sum_{j=2}^{N}(x_j - x_1) + (x_1 - x_i) + \nu_{i-1}.$$

for $i = 2, \ldots, N$. From which we have

$$\dot{\delta}_{i-1} = -2\delta_{i-1} + \sum_{j=2, j\neq i}^{N} (x_1 - x_j) + \nu_{i-1}.$$

If we knew the term

$$\sigma_{i-1} = \sum_{j=2, j\neq i}^{N} (x_1 - x_j) = -\sum_{j=2, j\neq i}^{N} \delta_{j-1}, \quad i = 2, \ldots, N \tag{2.10}$$

the missing connections then could be constructed by the following relation

$$\sum_{j=2, j\neq i}^{N} (x_j - x_i) = -\sigma_{i-1} - (N-2)\delta_{i-1}, \quad i = 2, \ldots, N$$

This gives us the motivation to estimate σ_{i-1} by using an extended high-gain observer. The extended high-gain observer is constructed as [83]

$$\dot{\hat{\delta}}_{i-1} = -2\hat{\delta}_{i-1} + \hat{\sigma}_{i-1} + \nu_{i-1} + \frac{\alpha_1}{\epsilon}(\delta_{i-1} - \hat{\delta}_{i-1}), \tag{2.11a}$$

$$\dot{\hat{\sigma}}_{i-1} = \frac{\alpha_2}{\epsilon^2}(\delta_{i-1} - \hat{\delta}_{i-1}), \tag{2.11b}$$

for $i = 2, \ldots, N$, where ϵ, α_1 and α_2 are positive constants with $\epsilon << 1$. The observer-based controller is given by

$$\nu_{i-1} = -\hat{\sigma}_{i-1} - (N-2)\delta_{i-1}. \tag{2.12}$$

Similar to (2.6), we define the change of variables

$$\alpha = x_1, \tag{2.13a}$$

$$\delta_i = x_{i+1} - \alpha, \quad 1 \leq i \leq N-1. \tag{2.13b}$$

and $\delta = [\delta_1, \ldots, \delta_{N-1}]^T$.

2.4.2 Peaking

When $\delta_{i-1}(0) - \hat{\delta}_{i-1}(0) \neq 0$ the transient response of the observer contains a term of the form $(1/\epsilon)e^{-at/\epsilon}$ for some $a > 0$. This is known as the peaking phenomenon [84]. Its impact in feedback control is overcome by saturating the control outside a compact set of interest.

We define the Lyapunov function $V(\delta) = \frac{1}{2}\delta^T \delta$. Let S be any compact set in $\mathbb{R}^{N-1}$. Choose $c > 0$ such that

$$S \subset \Omega_c = \{V(\delta) \leq c\} \subset \mathbb{R}^{N-1}. \tag{2.14}$$

The observer-based controller is saturated outside the compact set Ω_c. Let

$$M_{i-1} > \max_{\delta \in \Omega_c} |\nu_{i-1}|, \quad 2 \leq i \leq N,$$

The observer-based control is saturated as

$$\bar{\nu}_{i-1} = M_{i-1} \operatorname{sat}\left(\frac{\nu_{i-1}}{M_{i-1}}\right).$$

2.4.3 Observer Error Dynamics

The system (2.1) with the controller

$$u_i = (x_1 - x_i) + \bar{\nu}_{i-1}, \quad \text{for } i = 2, \ldots, N \tag{2.15}$$

in the new coordinates become

$$\dot{\alpha} = \sum_{i=1}^{N-1} \delta_i, \tag{2.16a}$$

$$\dot{\delta} = -\tilde{L}_s \delta + \bar{\nu}, \tag{2.16b}$$

where $\bar{\nu} = [\bar{\nu}_1, \bar{\nu}_2, \ldots, \bar{\nu}_{N-1}]^T$ and $\tilde{L}_s$ is given by

$$\tilde{L}_s = [0 \mid I_{N-1}] L_s \begin{bmatrix} 0 \\ \overline{} \\ I_{N-1} \end{bmatrix} + rr^T, \tag{2.17}$$

where $I_{N-1} \in \mathbb{R}^{N-1 \times N-1}$ is the identity matrix, $r = \mathbf{1} \in \mathbb{R}^{N-1}$ is a column of all 1's and the eigenvalues of $\tilde{L}_s$ are the non-zero eigenvalues of L_s.

With the scaled estimation errors

$$\varphi_{i-1} = \frac{\delta_{i-1} - \hat{\delta}_{i-1}}{\epsilon}, \tag{2.18a}$$

$$\eta_{i-1} = \sigma_{i-1} - \hat{\sigma}_{i-1}, \tag{2.18b}$$

the observer error dynamics are given by

$$\begin{aligned} \epsilon\dot{\varphi}_{i-1} &= \dot{\delta}_{i-1} - \dot{\hat{\delta}}_{i-1} \\ &= -2\delta_{i-1} + \sigma_{i-1} + \nu_{i-1} + 2\hat{\delta}_{i-1} - \hat{\sigma}_{i-1} - \nu_{i-1} - \frac{\alpha_1}{\epsilon}(\delta_{i-1} - \hat{\delta}_{i-1}) \\ &= -\alpha_1\varphi_{i-1} + \eta_{i-1} - 2\epsilon\varphi_{i-1}, \\ \epsilon\dot{\eta}_{i-1} &= -\alpha_2\varphi_{i-1} + \epsilon\dot{\sigma}_{i-1}, \end{aligned}$$

where $\dot{\sigma}_{i-1} = \sum\limits_{j=2, j\neq i}^{N} (\dot{x}_j - \dot{x}_1) = -\sum\limits_{j=2, j\neq i}^{N} \dot{\delta}_{j-1}$.

The foregoing equations can be rewritten as

$$\epsilon\dot{\xi}_{i-1} = A_0\xi_{i-1} + \epsilon\Delta_{i-1}, \tag{2.19}$$

where $\xi_{i-1} = [\varphi_{i-1}, \eta_{i-1}]^T$, $A_0 = \begin{bmatrix} -\alpha_1 & 1 \\ -\alpha_2 & 0 \end{bmatrix}$, $\Delta_{i-1} = \begin{bmatrix} -2\varphi_{i-1} \\ -\sum\limits_{j=2, j\neq i}^{N} \dot{\delta}_{j-1} \end{bmatrix}$ and A_0 is Hurwitz. Let $\hat{\Upsilon} = [\hat{\Upsilon}_1, \ldots, \hat{\Upsilon}_{N-1}]^T$ where $\hat{\Upsilon}_{i-1} = [\hat{\delta}_{i-1}, \hat{\sigma}_{i-1}]^T$ for $i = 2, \ldots, N$, $\Upsilon = [\Upsilon_1, \ldots, \Upsilon_{N-1}]^T$ where $\Upsilon_{i-1} = [\delta_{i-1}, \sigma_{i-1}]^T$ for $i = 2, \ldots, N$, and $\xi = [\xi_1, \ldots, \xi_{N-1}]^T$ where $\xi, \hat{\Upsilon}, \Upsilon \in \mathbb{R}^{2(N-1)}$. We have

$$\hat{\Upsilon} = \Upsilon - D_\epsilon \xi, \tag{2.20}$$

where $D_\epsilon = (I_{N-1} \otimes D_0) \in \mathbb{R}^{2(N-1)\times 2(N-1)}$ and $D_0 = \begin{bmatrix} \epsilon & 0 \\ 0 & 1 \end{bmatrix}$.

Theorem 2.1: *Consider the disagreement dynamics (2.16b) obtained using the feedback controller (2.15) and the extended high-gain observer (2.11), with ϵ, α_1 and α_2 chosen as positive constants. Let S be defined as in (2.14) and Q be any compact set of $\mathbb{R}^{2(N-1)}$. Then, there exists $\epsilon^* > 0$, such that for every $0 < \epsilon \leq \epsilon^*$, the solutions $(\delta(t), \hat{\Upsilon}(t))$ of (2.16b) and (2.11), starting in $S \times Q$, satisfy*

$$\lim_{t\to\infty} \delta(t) = 0 \quad \text{and} \quad \lim_{t\to\infty} \hat{\Upsilon}(t) = 0 \tag{2.21}$$

Proof : We rewrite the closed loop system in the singularly perturbed form,

$$\dot{\alpha} = \sum_{i=1}^{N-1} \delta_i, \tag{2.22a}$$

$$\dot{\delta} = F(\delta, \xi), \tag{2.22b}$$

$$\epsilon\dot{\xi} = A\xi + \epsilon\Delta, \tag{2.22c}$$

where $F(\delta,\xi) = -\tilde{L}_s\delta + \bar{\nu}$, $\Delta = [\Delta_1, \Delta_2, \ldots, \Delta_{N-1}]^T$, $A = (I_{N-1} \otimes A_0) \in \mathbb{R}^{2(N-1)\times 2(N-1)}$. The disagreement dynamics (2.22b) and the observer error dynamics (2.22c) are independent of α.

The Lyapunov function for (2.22c) is defined as $W = \xi^T \bar{P} \xi$, where $\bar{P} = (I_{N-1} \otimes P) \in \mathbb{R}^{2(N-1)\times 2(N-1)}$ and P is the positive definite solution of the Lyapunov equation $PA_0 + A_0^T P = -I$. We define the compact sets $\Sigma = \{W(\xi) \leq \beta\epsilon^2\}$ and $\Lambda = \Omega_c \times \Sigma$. Due to global boundedness of F and Δ in $\hat{\Upsilon}$, for all $\delta \in \Omega_c$ and $\xi \in \mathbb{R}^{2(N-1)}$ we have

$$\|F(\delta,\xi)\| \leq k_1, \quad \|\Delta(\delta,\xi)\| \leq L_1, \tag{2.23}$$

where L_1, k_1 are positive constants independent of ϵ. Because $\delta(0)$ is in the interior of Ω_c there exists $T_1 > 0$ independent of ϵ such that $\delta \in \Omega_c$ for $t \in [0, T_1]$ and during this time interval (2.23) holds. Following the standard analysis for the high-gain observer theory [84, Theorem 1] it can be argued that initially $\xi(0)$ could be outside the set Σ but it quickly reaches the set within a time interval $[0, T(\epsilon)]$ where $T(\epsilon) \to 0$ as $\epsilon \to 0$ and there exists positive constants β and ϵ_1 such that the compact set $\Lambda = \Omega_c \times \Sigma$ is positively invariant for every $0 < \epsilon \leq \epsilon_1$ and for all $\delta(0) \in S$ and $\hat{\Upsilon}(0) \in Q$, the trajectory $(\delta(t), \xi(t))$ enters Λ within the interval $[0, T(\epsilon)]$.

The saturation is no longer effective when the trajectory enters Λ. Therefore we have $\bar{\nu}_{i-1} = \nu_{i-1}$, $\forall\, t \geq T(\epsilon)$, and the closed-loop system is then defined by the linear singularly perturbed form

$$\dot{\alpha} = \sum_{i=1}^{N-1} \delta_i, \tag{2.24a}$$

$$\dot{\delta} = -N\delta - V\xi, \tag{2.24b}$$

$$\epsilon\dot{\xi} = (A + \epsilon R)\xi + \epsilon M\delta, \tag{2.24c}$$

for some matrices V, R and M. We define the following change of variables [85] to separate the fast variables from the slow ones:

$$\chi = \xi + Y(\epsilon)\delta, \tag{2.25}$$

where $Y(\epsilon) = \epsilon A^{-1}M + O(\epsilon^2)$. The transformed system is

$$\dot{\alpha} = \sum_{i=1}^{N-1} \delta_i, \tag{2.26a}$$

$$\dot{\delta} = (-NI_{N-1} + O(\epsilon))\delta - V\chi, \tag{2.26b}$$

$$\epsilon\dot{\chi} = (A + \epsilon R)\chi. \tag{2.26c}$$

From (2.26b) and (2.26c) we have

$$\begin{bmatrix} \dot{\delta} \\ \dot{\chi} \end{bmatrix} = \begin{bmatrix} -NI_{N-1} + O(\epsilon) & -V \\ 0 & (A + \epsilon R)/\epsilon \end{bmatrix} \begin{bmatrix} \delta \\ \chi \end{bmatrix} = \Gamma \begin{bmatrix} \delta \\ \chi \end{bmatrix}. \tag{2.27}$$

The matrix Γ is block triangular and hence its eigenvalues are the eigenvalues of $(-NI_{N-1} + O(\epsilon))$ and $(A+\epsilon R)/\epsilon$. We can find $\epsilon^* > 0$ such that for all $\epsilon \in (0, \epsilon^*)$ the matrix Γ is Hurwitz.

Therefore,

$$\lim_{t\to\infty} \delta(t) = 0 \text{ and } \lim_{t\to\infty} \chi(t) = 0. \tag{2.28}$$

From (2.25) we can conclude that $\lim_{t\to\infty} \xi(t) = 0$; hence (2.21) follows from (2.20). ■

Remark 2.1: The convergence rate of the star topology will increase to b if the consensus controller (2.2) is multiplied by a gain b. However there is a limit on how high the gain could be and it depends on the physical constraints of the control. The observer based method presented in this chapter speeds up the convergence rate not by increasing the gain in the consensus equation but by providing more information to the nodes.

Theorem 2.2: *Suppose Theorem 2.1 holds and let the target system be defined as in (2.5). Then, given any $\mu > 0$ there exists $\epsilon^{**} > 0$ such that for all $\epsilon \in (0, \epsilon^{**})$*

$$\|x(t) - x^*(t)\| \leq \ \mu \ \ \forall\ t \geq 0, \tag{2.29}$$

Proof: As $\delta(0)$ is in the interior of Ω_c we have $\|\delta(t) - \delta(0)\| \leq k_1 t$ during the interval $[0, T(\epsilon)]$, for some $k_1 > 0$. Similarly it can be shown that $\|\delta^*(t) - \delta^*(0)\| \leq k_1 t$ during the same time interval. As $\delta(0) = \delta^*(0)$ we have

$$\|\delta(t) - \delta^*(t)\| \leq 2k_1 T(\epsilon), \quad \forall\ t \in [0, T(\epsilon)].$$

Since $T(\epsilon) \to 0$ as $\epsilon \to 0$, there exists $0 < \epsilon_2 \leq \epsilon^*$ such that, for every $0 < \epsilon \leq \epsilon_2$, we have

$$\|\delta(t) - \delta^*(t)\| = O(T(\epsilon)), \quad \forall\ t \in [0, T(\epsilon)]. \tag{2.30}$$

Subtracting (2.7a) from (2.26a) we have

$$\dot{\alpha}(t) - \dot{\alpha}^*(t) = r^T[\delta(t) - \delta^*(t)]. \tag{2.31}$$

Integrating (2.31) and using $\alpha(0) = \alpha^*(0)$ results in

$$\alpha(t) - \alpha^*(t) = r^T \int_0^t [\delta(\tau) - \delta^*(\tau)]d\tau.$$

Taking the absolute value we have

$$|\alpha(t) - \alpha^*(t)| = O(T^2(\epsilon)), \quad \forall\, t \in [0, T(\epsilon)]. \tag{2.32}$$

We know that

$$\|e^{-NI_{N-1}t}\| \leq k_2 e^{-\lambda_1 t} \quad \text{and} \quad \|e^{(-NI_{N-1}+O(\epsilon))t}\| \leq k_3 e^{-\lambda_2 t}, \tag{2.33}$$

where k_2, k_3, λ_1 and λ_2 are positive constants and for ϵ small enough λ_2 can be chosen such that $\lambda_2 < \lambda_1$. From (2.26c) we have

$$\|\chi(t)\| \leq k_4 e^{-\lambda_3 (t - T(\epsilon))/\epsilon} \|\chi(T(\epsilon))\|, \tag{2.34}$$

where k_4 and λ_3 are positive constants. Next we define the deviation of the system trajectory from the target trajectory as $\psi(t) = \delta(t) - \delta^*(t)$. Differentiating $\psi(t)$ we have

$$\dot{\psi}(t) = (-NI_{N-1} + O(\epsilon))\psi(t) + O(\epsilon)\delta^*(t) - V\chi(t).$$

Integrating $\dot{\psi}(t)$ we have

$$\psi(t) = e^{(-NI_{N-1}+O(\epsilon))(t-T(\epsilon))}\psi(T(\epsilon)) + \int\limits_{T(\epsilon)}^{t} e^{(-NI_{N-1}+O(\epsilon))(t-\tau)}[O(\epsilon)\delta^*(\tau) - V\chi(\tau)]d\tau. \tag{2.35}$$

From (2.30) we have,

$$\|\psi(T(\epsilon))\| = \|\delta(T(\epsilon)) - \delta^*(T(\epsilon))\| = O(T(\epsilon)).$$

From (2.35),

$$\|\psi(t)\| \leq k_3 e^{-\lambda_2(t-T(\epsilon))}O(T(\epsilon)) + \frac{\epsilon k_3 k_5}{(\lambda_1 - \lambda_2)}[e^{-\lambda_2(t-T(\epsilon))} - e^{-\lambda_1(t-T(\epsilon))}]$$

$$+\frac{\epsilon k_3 k_6}{(\lambda_3 - \epsilon\lambda_2)}\left[e^{-\lambda_2(t-T(\epsilon))} - e^{-\lambda_3(t-T(\epsilon))/\epsilon}\right],$$

where k_5, k_6 and λ_3 are positive constants. From the above inequality it can be shown that

$$\|\psi(t)\| \leq (O(T(\epsilon)) + \epsilon k_7)e^{-\lambda_2(t-T(\epsilon))} \quad \forall\ t \geq T(\epsilon), \tag{2.36}$$

where k_7 is a positive constant. Since $T(\epsilon) \to 0$ as $\epsilon \to 0$, there exists $0 < \epsilon_3 \leq \epsilon_2$ such that, for every $0 < \epsilon \leq \epsilon_3$, we can conclude that

$$\|\delta(t) - \delta^*(t)\| \leq \mu, \quad \forall\ t \geq 0. \tag{2.37}$$

Integrating (2.31) from the time $T(\epsilon)$ we have

$$\alpha(t) - \alpha^*(t) = [\alpha(T(\epsilon)) - \alpha^*(T(\epsilon))] + r^T \int_{T(\epsilon)}^{t} [\delta(\tau) - \delta^*(\tau)]d\tau.$$

Using $|\alpha(T(\epsilon)) - \alpha^*(T(\epsilon))| = O(T^2(\epsilon))$ shows that

$$|\alpha(t) - \alpha^*(t)| \leq O(T^2(\epsilon)) + \|r^T\| \frac{(O(T(\epsilon)) + \epsilon k_7)}{\lambda_2}. \tag{2.38}$$

Since $T(\epsilon) \to 0$ as $\epsilon \to 0$, there exists $0 < \epsilon_4 \leq \epsilon_3$ such that, for every $0 < \epsilon \leq \epsilon_4$, we can conclude that

$$|\alpha(t) - \alpha^*(t)| \leq \mu \quad \forall\, t \geq 0. \tag{2.39}$$

Take $\epsilon^{**} = \min\{\epsilon_3, \epsilon_4\}$. Then (2.29) follows from (2.37) and (2.39). ■

Remark 2.2: The consensus limit achieved by using a controller of the form (2.22) is the average of the initial conditions of the system [19]. From Theorem 2.1 we can only conclude that the agents achieve consensus. Theorem 2.2 shows that the consensus limit achieved by using the observer-based controller can be made arbitrarily close to the one achieved by using a standard consensus controller.

2.5 Simulations

The simulation results are provided for a network of 10 agents with agent 1 as the root agent. The initial conditions for the agents are chosen as $x_{i+1}(0) = 5i$, for $i = 0, 1, \ldots, 9$.

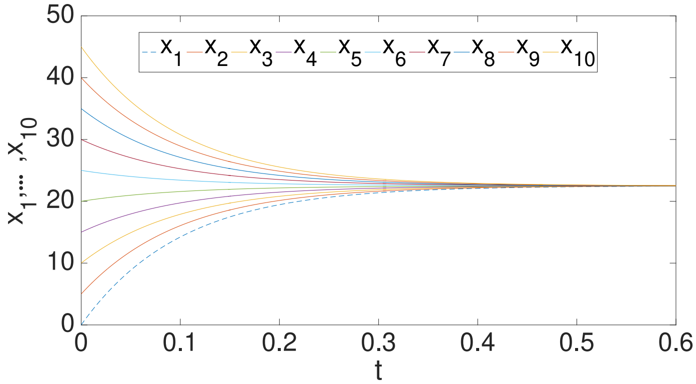

Figure 2.2: Consensus on Complete Graph

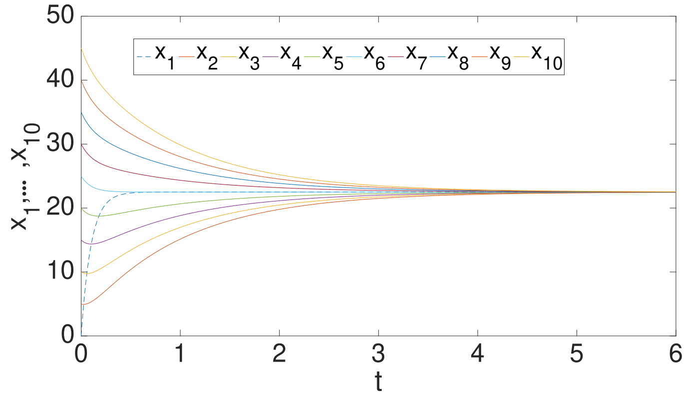

Figure 2.3: Consensus on Star Graph with no Observers

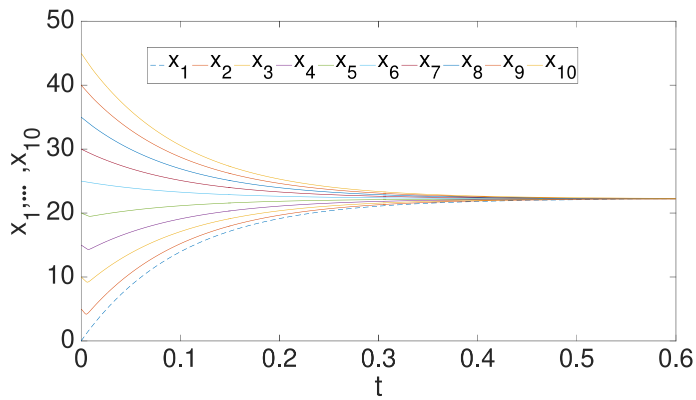

Figure 2.4: Consensus on Star Graph with Observers and $\epsilon = 0.001$

Fig. 2.2 shows the trajectories of the agents under a complete graph. Fig. 2.3 shows the trajectories of the agents under a star graph without observer where the convergence rate is 10 times slower than the complete graph. Fig. 2.4 shows the trajectories of the agents under a star graph with observers. Fig. 2.2 and 2.4 have the same time scale as they achieve consensus with a rate of 10.

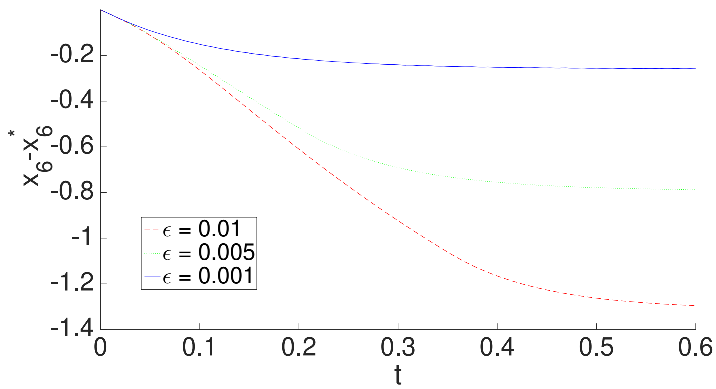

Figure 2.5: Deviation of agent 6 trajectory from target trajectory

Fig. 2.5 illustrates the fact that as ϵ decreases the deviation of the consensus limit of the star topology with observers compared to the complete topology decreases and this trend is representative for all other agent trajectories.

2.6 Conclusion

This chapter presented an algorithm which increases the convergence rate of the consensus protocol on star topology using observers. The trajectories of the agents under the star topology approach the trajectories of the agents under a complete graph for sufficiently small ϵ. However adding observers increases the controller complexity as the closed loop system also comprises the observer dynamics.

Chapter 3

Scalable Consensus Using High Gain Observers

3.1 Introduction

In this chapter, we design a PD consensus controller for general directed graphs in which we guarantee that the convergence rate of the closed-loop system does not change with an increase in network size. The effect of network size on the convergence rate is not known for the case of general directed graphs. However, using the proposed controller, we can guarantee that the convergence rate remains unchanged [86] with an increase in network size. Moreover, the closed-loop system matrix has the properties of a Laplacian matrix. Therefore, it is named as Virtual Laplacian matrix, which represents the virtual connections among the agents for the closed-loop system. The real parts of the eigenvalues of the Virtual Laplacian matrix approach one while the imaginary parts approach zero as a design parameter increases. We realize the PD controller using a high-gain observer and show that the trajectories of the closed-loop system when the high-gain observer is used can be brought arbitrarily close to the trajectories under the PD controller.

3.2 Problem Definition

We consider the consensus problem in a network of N agents where a single integrator represents each agent

$$\dot{x}_i = v_i, \quad i = 1, \ldots, N. \tag{3.1}$$

The communication topology is defined by $\mathcal{G} = (\mathcal{V}, \mathcal{E}, \mathcal{A})$. The agents can only measure relative information, and we define a signal which represents the weighted sum of all the measurements at agent i,

$$\zeta_i = \sum_{j=1}^{N} a_{ij}(x_j - x_i) \tag{3.2}$$

where $a_{ij} \geq 0$. Equation (3.2) in matrix form can be written as $\zeta = -Lx$, where $\zeta = \mathrm{col}(\zeta_1, \ldots, \zeta_N)$.

Assumption 3.1: The communication topology is defined by a weighted directed graph $\mathcal{G}$ which contains a globally reachable node, i.e., $\mathcal{G}$ contains a node which can be reached from any another node by traversing a directed path.

The above assumption implies that zero is a simple eigenvalue of the graph Laplacian L and all other eigenvalues have positive real parts [20]. This is the most general assumption considered in the literature for time-invariant graphs. The objective of the consensus algorithm is defined as

$$\lim_{t\to\infty} \{x_i(t) - x_j(t)\} = 0, \text{ for } i \neq j \text{ and } i, j = 1, \ldots, N$$

for which a standard consensus controller [19] is

$$v_i = k_s \sum_{j=1}^{N} a_{ij}(x_j - x_i) \tag{3.3}$$

where k_s is a positive constant, which we introduce as a tunable controller gain. The closed-loop system of (3.1) with the controller (3.3) is

$$\dot{x} = -k_s L x \tag{3.4}$$

where the convergence rate for undirected graphs [18, Chapter 7] is given by $k_s \lambda_2(L)$. The convergence rate decreases for certain classes of undirected graphs where increase in network size results in $\lambda_2(L) \to 0$. Therefore, as the second smallest eigenvalue of the graph Laplacian tends to zero the magnitude of the control signal needs to be very large to attain a specific convergence rate.

3.3 State feedback Controller Design

In this section we design PD control for a network of N agents described in (3.1), assuming that the state derivatives are available to the agents. Differentiating (3.2) in matrix form we have

$$\dot{\zeta} = -Lv$$

where $v = \mathrm{col}(v_1, \ldots, v_N)$ and for each agent i we have

$$\dot{\zeta}_i = \sum_{j=1}^{N} a_{ij}(v_j - v_i)$$

Next we define a signal σ_i to be $\sigma_i = \dot{\zeta}_i$, which can be written as $\sigma = -Lv$, where $\sigma = \mathrm{col}(\sigma_1, \ldots, \sigma_N)$. The control at each node is taken as

$$v_i = k_d \sigma_i + k_p \zeta_i \tag{3.5}$$

where k_p and k_d are positive constants. In this section we assume that σ_i is available for feedback. Substituting for σ_i we have,

$$v_i = k_d \sum_{j=1}^{N} a_{ij}(v_j - v_i) + k_p \zeta_i$$

The above controller is distributed in nature as it relies only on local information. Next we write the equations in matrix form,

$$(I + k_d L)v = k_p \zeta$$

The matrix $(I + k_d L)$ is nonsingular because $\lambda_i(I + k_d L) = 1 + k_d \lambda_i(L)$, where $\mathrm{Re}\,(\lambda_i(L)) \geq 0$, from Assumption 3.1. Choosing $k_d = k$ and $k_p = \gamma k$, we have the control as $v = \gamma \left(\frac{1}{k} I + L \right)^{-1} \zeta$, which results in the closed-loop system

$$\dot{x} = -\gamma \left(\frac{1}{k} I + L \right)^{-1} L x = -\gamma \hat{L} x \tag{3.6}$$

where $\hat{L}$ represents the Virtual Laplacian matrix, defined as

$$\hat{L} = \left(\frac{1}{k} I + L \right)^{-1} L \tag{3.7}$$

Remark 3.1: The matrix L encodes the physical exchange of information among the agents while the matrix $\hat{L}$ encodes the virtual connections among the agents for the closed-loop system.

Properties of a matrix of the form $(I+eL)^{-1}L$ for $e \geq 0$, were identified in [87, Section II.B], for the case of undirected graphs. In the next Lemma we show a property of $\hat{L}$ for general directed graphs.

Lemma 3.1: *The matrix $\hat{L}$ is a Laplacian matrix.*

Proof: A matrix is a Laplacian matrix if [18, Chapter 6], i) its row-sums are zero, ii) its diagonal entries are non-negative, and iii) its non-diagonal entries are non-positive. We now show that $\hat{L}$ satisfies the three properties. Using the identity

$$(I + A)^{-1} = I - (I + A)^{-1} A$$

where $A \in \mathbb{R}^{N \times N}$, equation (3.7) can be simplified to

$$\hat{L} = I - (I + kL)^{-1} .$$

The Laplacian matrix L is a singular Metzler or $\mathcal{M}$ matrix [6], which implies that $(I + kL)$ is a nonsingular $\mathcal{M}$ matrix. It follows from [88, Section III.G] that $(I + kL)^{-1}$ is a positive matrix. We first show that the row sums of $\hat{L}$ are zero by

$$\hat{L}\mathbf{1} = \left[I - (I + kL)^{-1}\right] \mathbf{1} = \left(\frac{1}{k} I + L\right)^{-1} L\mathbf{1} = \mathbf{0}$$

where $(\mathbf{1}, \mathbf{0})$ are columns of all 1's and 0's of appropriate dimension. From which we conclude that $(I + kL)^{-1} \mathbf{1} = \mathbf{1}$.

Next, let $\tilde{w}_{ij}$ be an element of the matrix $(I+kL)^{-1}$. Since $(I+kL)^{-1}$ is a positive matrix it implies $\tilde{w}_{ij} \geq 0$. Moreover, from $(I+kL)^{-1}\mathbf{1} = \mathbf{1}$, we have $\sum_{j=1}^{n} \tilde{w}_{ij} = 1$. The matrix $\hat{L}$ has the diagonal elements as $1-\tilde{w}_{ii}$ and the off-diagonal elements as $-\tilde{w}_{ij}$ for $i \neq j$. Using the properties $\tilde{w}_{ij} \geq 0$ and $\sum_{j=1}^{n} \tilde{w}_{ij} = 1$ we can conclude that $1-\tilde{w}_{ii}$ is non-negative and $-\tilde{w}_{ij}$ is non-positive, which satisfies property (ii) and (iii) and therefore we conclude that $\hat{L}$ is a Laplacian matrix. ■

In the next Theorem we show properties of the eigenvalues of $\hat{L}$ for general directed graphs.

Theorem 3.1: *Consider the closed-loop system (3.6), with initial condition $x(0) \in \mathbb{R}^N$, obtained using the state feedback controller (3.5), with $k_p = \gamma k$, and $k_d = k$ where k and γ are chosen as positive constants. Let the graph $\mathcal{G}$ be a weighted directed graph satisfying Assumption 3.1, then for sufficiently large k,*

$$\mathrm{Re}(\lambda_i(\hat{L})) = 1 - \frac{1}{k}\mathrm{Re}\left(\frac{1}{\lambda_i(L)}\right) + O\left(\frac{1}{k^2}\right), \tag{3.8a}$$

$$\mathrm{Im}(\lambda_i(\hat{L})) = -\frac{1}{k}\mathrm{Im}\left(\frac{1}{\lambda_i(L)}\right) + O\left(\frac{1}{k^2}\right), \tag{3.8b}$$

for $i = 2, \ldots, N$, where $\lambda_i(\hat{L})$ and $\lambda_i(L)$ are the eigenvalues of $\hat{L}$ and L, respectively. Moreover, the control signal $v = -\gamma\hat{L}x$ is bounded uniformly in k.

Proof : First we decompose L in its Jordan form

$$L = \tilde{P}J\tilde{P}^{-1}$$

where $J = \mathrm{blkdiag}(0, J_2, \ldots, J_m)$ and $m \leq N$ is the number of Jordan blocks. The first Jordan block is the scalar zero and the other Jordan blocks $J_2, \ldots, J_m$ contain the eigenvalues with strict positive real parts. From the Jordan decomposition of L we have

$$\hat{L} = \left[\frac{1}{k}\tilde{P}\tilde{P}^{-1} + \tilde{P}J\tilde{P}^{-1}\right]^{-1}\tilde{P}J\tilde{P}^{-1} = \tilde{P}\left[\frac{1}{k}I + J\right]^{-1}J\tilde{P}^{-1}$$

$\frac{1}{k}I + J$ is a triangular matrix with diagonal elements $\frac{1}{k} + \lambda_i(L)$ and J is a triangular matrix with diagonal elements $\lambda_i(L)$. Therefore the eigenvalues of $\hat{L}$ are given by

$$\lambda_i(\hat{L}) = \frac{\lambda_i(L)}{\frac{1}{k} + \lambda_i(L)} = \frac{1}{1 + \frac{1}{k\lambda_i(L)}}.$$

For suffciently large k we have

$$\frac{1}{1 + \frac{1}{k\lambda_i(L)}} = 1 - \frac{1}{k\lambda_i(L)} + \left(\frac{1}{k\lambda_i(L)}\right)^2 - \left(\frac{1}{k\lambda_i(L)}\right)^3 + \dots$$

for $i = 2, \dots, N$, from which

$$\mathrm{Re}\left(\frac{\lambda_i(L)}{\frac{1}{k} + \lambda_i(L)}\right) = 1 - \frac{1}{k}\mathrm{Re}\left(\frac{1}{\lambda_i(L)}\right) + O\left(\frac{1}{k^2}\right),$$

$$\mathrm{Im}\left(\frac{\lambda_i(L)}{\frac{1}{k} + \lambda_i(L)}\right) = -\frac{1}{k}\mathrm{Im}\left(\frac{1}{\lambda_i(L)}\right) + O\left(\frac{1}{k^2}\right)$$

Therefore, (3.8) follows from the above equations.

To show that the control signal is bounded we write it as $v = -\tilde{K}x$, where $\tilde{K} = \gamma\hat{L}$. We show that the norm of $\tilde{K}$ is bounded uniformly in k. First, we rewrite $\tilde{K}$ as $\tilde{K} = \gamma I - \gamma(I + kL)^{-1}$. The matrix $(I + kL)$ is a nonsingular $\mathcal{M}$ matrix and it is strictly diagonally dominant, therefore it follows from [89] that

$$||(I + kL)^{-1}||_\infty = 1.$$

From which we have

$$||\tilde{K}||_\infty \leq 2\gamma$$

Therefore, the infinity norm of $\tilde{K}$ is independent of k. For sufficiently large k, the matrix $\tilde{J}_i = \left[\frac{1}{k}I + J_i\right]^{-1} J_i$ is given by $\tilde{J}_i = I + O(1/k)$ and the solution of (3.6) is given by

$$x(t) = \tilde{P}\bar{L}\tilde{P}^{-1}x(0) + O\left(\frac{1}{k}\right)$$

where $\bar{L} = \text{diag}(1, e^{-\gamma t}, \ldots, e^{-\gamma t})$. From which it can be shown that

$$||x(t)||_\infty \leq a_1 + (a_2 + a_3 e^{-\gamma t})||x(0)||_\infty$$

where a_1, a_2 and a_3 are positive constants independent of k. Therefore,

$$||v(t)||_\infty \leq ||\tilde{K}||_\infty \cdot ||x(t)||_\infty \leq 2\gamma[a_1 + (a_2 + a_3 e^{-\gamma t})||x(0)||_\infty]$$

From which we can conclude that the control signal is bounded uniformly in k. ■

Remark 3.2: For sufficiently large k, the eigenvalues of the Virtual Laplacian matrix $\hat{L}$ approach 1+0i, and therefore the directedness of the graph is irrelevant. The eigenvalues of the closed-loop system (3.6) approach $-\gamma$ for sufficiently large k. Therefore, the convergence rate approaches γ and will not deteriorate as the network size grows, provided k is sufficiently large. The convergence rate can further be increased by increasing γ, however with increase in γ, the magnitude of the control signal increases.

Remark 3.3: A special case arises when the graph $\mathcal{G}$ is connected and undirected with Laplacian $L = U\Lambda_L U^T$, where U is orthonormal and $\Lambda_L = \mathrm{diag}(0, \lambda_2, \ldots, \lambda_N)$. Then for this case, L is irreducible [18], which implies that $(I + kL)$ is also irreducible. Therefore, it follows from [88, Section III.G] that $(I + kL)^{-1}$ is a strictly positive matrix. Since, $(I + kL)^{-1}$ strictly positive, it implies that all the matrix elements are non-zero. Therefore, we can conclude the virtual Laplacian matrix $\hat{L}$ is symmetric with all the connections (virtual complete graph). Moreover, with sufficiently large k

$$\left(\frac{1}{k}I + L\right)^{-1} = L^{+} - \frac{1}{k}L^{+} + O\left(\frac{1}{k^2}\right)$$

where L^{+} is the pseudoinverse Laplacian matrix, see [18, Chapter 6], with $L^{+} = U\Lambda_P U^T$, where $\Lambda_P = \mathrm{diag}(0, 1/\lambda_2, \ldots, 1/\lambda_N)$. Therefore, we have

$$\hat{L} = L^{+}L + O\left(\frac{1}{k}\right) = \left[I - \frac{1}{N}\mathbf{1}\mathbf{1}^T\right] + O\left(\frac{1}{k}\right) \tag{3.9}$$

3.4 Output-Feedback Controller

3.4.1 Preliminaries

For the design of the output feedback controller we first discuss the following controller

$$\mu\dot{v}_i = -v_i + k\sigma_i + \gamma k\zeta_i \tag{3.10}$$

which in vector form becomes

$$\mu \dot{v} = -v + k\sigma + \gamma k \zeta$$

The motivation for using a controller of the form (3.10) is because the analysis of the output feedback requires the boundedness of the derivative of the control ($\dot{v}$) which is achieved by (3.10). First, we discuss the case when σ is available for feedback. The quasi-steady state of (3.10) when $\mu = 0$ is given by

$$v = k\sigma + \gamma k \zeta = -kLv - \gamma kLx \implies v = -\gamma \hat{L} x$$

which implies that for sufficiently small μ we recover the PD controller properties. From the change of variable $y = v + \gamma \hat{L} x$, we have

$$\mu \dot{y} = [A + \mu \gamma \hat{L}] y - \mu \gamma^2 \hat{L}^2 x \tag{3.11}$$

where $A = -(I + kL)$. We define a change of coordinates

$$y = \begin{bmatrix} 1 & \mathbf{0}^T \\ \mathbf{1} & I \end{bmatrix} z \triangleq T \bar{y}$$

From which we have

$$\tilde{\mathcal{L}} = T^{-1} \hat{L} T = \begin{bmatrix} 0 & \tilde{\mathcal{L}}_{12} \\ \mathbf{0} & \tilde{\mathcal{L}}_{22} \end{bmatrix}, \ \bar{\mathcal{L}} = T^{-1} L T = \begin{bmatrix} 0 & \bar{\mathcal{L}}_{12} \\ \mathbf{0} & \bar{\mathcal{L}}_{22} \end{bmatrix}$$

where the eigenvalues of the matrix $\tilde{\mathcal{L}}_{22}$, $\bar{\mathcal{L}}_{22}$ are the non-zero eigenvalues of $\hat{L}$ and L, respectively. Using the transformations $x = \tilde{P}z$ and $y = T\bar{y}$, the closed-loop system becomes

$$\dot{z}_1 = R_1\bar{y} \tag{3.12a}$$

$$\dot{\tilde{z}} = -\gamma\tilde{J}\tilde{z} + R_2\bar{y} \tag{3.12b}$$

$$\mu\dot{\bar{y}} = \tilde{A}\bar{y} + kE\bar{y} + \mu\gamma R_3\bar{y} + \mu\gamma^2 R_4\tilde{z} \tag{3.12c}$$

where

$$\tilde{A} = \begin{bmatrix} -1 & 0 \\ 0 & -(I + k\bar{\mathcal{L}}_{22}) \end{bmatrix}, \ E = \begin{bmatrix} 0 & -\bar{\mathcal{L}}_{12} \\ \mathbf{0} & \mathbf{0}_{N-1\times N-1} \end{bmatrix},$$

where $\tilde{A}$ is Hurwitz, $\mathbf{0}_{N-1\times N-1}$ is a matrix of all 0's, $z = \text{col}(z_1, \tilde{z})$, for some matrices R_1, R_2, R_3, and R_4 where the norm of these matrices are bounded uniformly in k and $\tilde{J} = \text{blkdiag}(\tilde{J}_2, \ldots, \tilde{J}_m)$. For sufficiently large k, we have

$$\tilde{J} = I + O(1/k)$$

Remark 3.4: The system (3.12b)-(3.12c) is a linear singularly perturbed system and it can be easily shown following the standard singular perturbation results that for sufficiently small μ, the origin of (3.12b)-(3.12c) is exponentially stable. We follow a Lyapunov analysis for (3.12b)-(3.12c) for two reasons i) The analysis of the system (3.12) determines the saturation levels that have to be used in output feedback to deal with the observer peaking. ii) To show that an upper bound on parameter μ is independent of k.

Next we define a composite Lyapunov function for (3.12b)-(3.12c) as

$$V = \tilde{z}^T \tilde{z} + \bar{y}^T P \bar{y}$$

where P is a symmetric positive definite matrix given by

$$P = \begin{bmatrix} b/2 & \mathbf{0}^T \\ \mathbf{0} & W \end{bmatrix}$$

where $b > 0$ and $W = W^T > 0$ is the solution to the Lyapunov equation $W\bar{\mathcal{L}}_{22} + \bar{\mathcal{L}}_{22}^T W = I$. From which we have $P\tilde{A} + \tilde{A}^T P = -Q$, where Q is a symmetric positive definite matrix given by

$$Q = \begin{bmatrix} b & \mathbf{0}^T \\ \mathbf{0} & (2W + kI) \end{bmatrix}$$

We define the set of initial conditions as $\Gamma = \{V \leq c\}$, where c is any positive constant.

Lemma 3.2: *Consider the closed-loop system (3.12) obtained using the system (3.1) and controller (3.10). Let $(\tilde{z}(0), \bar{y}(0)) \in \Gamma$ and $z_1(0)$ lie in any compact set of $\mathbb{R}$. Then, there exists $\mu^* > 0$, such that for all $\mu \in (0, \mu^*]$, the set Γ is positively invariant and the trajectories of the system (3.12) are bounded. Moreover we have*

$$\lim_{t\to\infty} \tilde{z}(t) = 0, \ \lim_{t\to\infty} \bar{y}(t) = 0, \ \text{and} \ \lim_{t\to\infty} z_1 = \text{constant} \tag{3.13}$$

Proof : Taking the time-derivative of V along (3.12b)-(3.12c), we have

$$\dot{V} = -\gamma\tilde{z}^T[\tilde{J} + \tilde{J}^T]\tilde{z} + 2\tilde{z}^T R_2\bar{y} - (1/\mu)[\tilde{y}^T(2W + kI)\tilde{y}^T + b\bar{y}_1^2] - (1/\mu)bk\bar{y}_1\bar{\mathcal{L}}_{12}\tilde{y} + 2\gamma\bar{y}^T PR_3\bar{y} + 2\gamma^2\bar{y}^T PR_4\tilde{z}$$

where $\bar{y} = \mathrm{col}(y_1, \tilde{y})$, $\tilde{y} = \mathrm{col}(\bar{y}_2, \ldots, \bar{y}_N)$. From which we have

$$\dot{V} \le -2\gamma||\tilde{z}||^2 + \gamma(e_1/k)||\tilde{z}||^2 + e_2||\tilde{z}||\cdot||\bar{y}|| + e_3||\bar{y}||^2 - (1/\mu)[\bar{y}_1\ \tilde{y}] \begin{bmatrix} b & -bke_4/2 \\ -bke_4/2 & 2\lambda_{\min}(W) \end{bmatrix} \begin{bmatrix} \bar{y}_1 \\ \tilde{y} \end{bmatrix}$$

for some positive constants e_1, e_2, e_3 and e_4 independent of k. Choosing $b \le 8\lambda_{\min}(W)/(k_{\min}^2 e_4^2)$, where $k_{\min}$ is a lower bound on k, which without the loss of generality can be chosen as $k_{\min} = 1$, from which we have

$$-[\bar{y}_1\ \tilde{y}] \begin{bmatrix} b & -bke_4/2 \\ -bke_4/2 & 2\lambda_{\min}(W) \end{bmatrix} [\bar{y}_1\ \tilde{y}]^T \le -b_1||\bar{y}||^2$$

where b_1 is a positive constant independent of k. For $k \ge e_1$, we have

$$\dot{V} \le -[\tilde{z}\ \bar{y}] \begin{bmatrix} \gamma & -e_2/2 \\ -e_2/2 & \dfrac{b_1}{\mu} - e_3 \end{bmatrix} \begin{bmatrix} \tilde{z} \\ \bar{y} \end{bmatrix}$$

Therefore, there exists $\mu^* > 0$ such that for all $\mu \in (0, \mu^*]$, the above matrix positive is positive definite. From which it follows that

$$\lim_{t\to\infty} \tilde{z}(t) = 0, \ \lim_{t\to\infty} \bar{y}(t) = 0$$

Moreover, the set Γ is positively invariant as $\dot{V} < 0$ on the boundary $\{V = c\}$.

Because of the exponential stability of the system (3.12b)-(3.12c), $z_1(t)$ remains bounded and all the agents converge to the consensus value $\lim_{t\to\infty} z_1(t) = \text{constant}$. From which we can conclude that (3.13) follows. ■

3.4.2 Observer Design

The controller (3.10) assumes the availability of the state derivatives. In this section we estimate the extended state by adding a high-gain observer to each agent in the network to estimate the signal σ_i. The driving signal to the observer is ζ_i. The high-gain observer [90] is constructed as

$$\dot{\hat{\zeta}}_i = \hat{\sigma}_i + \frac{\alpha_1}{\epsilon}(\zeta_i - \hat{\zeta}_i) \tag{3.14a}$$

$$\dot{\hat{\sigma}}_i = \frac{\alpha_2}{\epsilon^2}(\zeta_i - \hat{\zeta}_i) \tag{3.14b}$$

where ϵ, α_1 and α_2 are positive constants with $\epsilon << 1$ for $i = 1, \ldots, N$.

3.4.3 Peaking

When the initial condition of the estimate $\hat{\zeta}_i(0)$ is not the same as $\zeta_i(0)$, then during the transient period, the observer estimates will peak; see [90]. In order to mitigate this effect, the control is saturated outside a positively invariant set under the state feedback controller so that peaking does not affect the plant. We find the maximum value of the control by finding the maximum value of $v = y - \gamma \hat{L} x = Q_1 \bar{y} + Q_2 \tilde{z}$ inside the positively invariant set

Γ, where Q_1 and Q_2 are some matrices independent of k. Let

$$M_i > \max_{(\tilde{z},\bar{y})\in\Gamma} |(Q_1)_i \bar{y}| + \ |(Q_3)_i \tilde{z}|$$

where $(Q_1)_i, (Q_2)_i$ denotes the i^{th} rows of Q_1 and Q_2. The constants M_i are independent of k as the set $\{V \leq c\}$ is independent of k. The output feedback controller is given by

$$\mu \dot{v}_i = -v_i + M_i \text{sat}\left(\frac{k\hat{\sigma}_i + \gamma k \hat{\zeta}_i}{M_i}\right) \tag{3.15}$$

where sat$(\cdot)$ is the saturation function defined as $\text{sat}(y) = \text{sign}(y)\min\{1, |y|\}$.

The change of variables $y = v + \gamma \hat{L} x$ transforms (3.15) to

$$\mu \dot{y} = [A + \mu\gamma\hat{L}]y - \mu\gamma^2 R_3 \tilde{z} - \Delta$$

where $\Delta = \left[(k\sigma + \gamma k\zeta) - M\mathbf{sat}\left(\frac{k\hat{\sigma} + \gamma k\hat{\zeta}}{M}\right)\right]$, $M = \text{diag}(M_1, \ldots, M_N)$ and $\mathbf{sat} = \text{col}\left(\text{sat}\left(\frac{k\hat{\sigma}_1 + \gamma k\hat{\zeta}_1}{M_1}\right), \ldots, \text{sat}\left(\frac{k\hat{\sigma}_N + \gamma k\hat{\zeta}_N}{M_N}\right)\right)$.

The observer scaled estimation error is defined as

$$\delta_i = \frac{\zeta_i - \hat{\zeta}_i}{\epsilon} \quad \text{and} \quad \eta_i = \sigma_i - \hat{\sigma}_i$$

and using the change of coordinates $x = \tilde{P}z$ and $y = T\bar{y}$ the closed-loop system under the output feedback controller (3.15) is given by

$$\dot{z}_1 = R_1 \bar{y} \tag{3.16a}$$

$$\dot{\tilde{z}} = -\gamma \tilde{J} \tilde{z} + R_2 \bar{y} \tag{3.16b}$$

$$\mu \dot{\bar{y}} = \tilde{A}\bar{y} + kE\bar{y} + \mu\gamma R_3 \bar{y} + \mu\gamma^2 R_4 \tilde{z} + R_5 \Delta \tag{3.16c}$$

$$\epsilon \dot{\psi} = A_0 \psi + (\epsilon/\mu) \begin{bmatrix} \mathbf{0} \\ -LAT\bar{y} + L\Delta \end{bmatrix} \tag{3.16d}$$

where $A_0 = \begin{bmatrix} -\alpha_1 I & I \\ -\alpha_2 I & \mathbf{0}_{N\times N} \end{bmatrix}$ is Hurwitz, $\psi = \mathrm{col}(\delta, \eta)$, $\delta = \mathrm{col}(\delta_1, \ldots, \delta_N)$, $\eta = \mathrm{col}(\eta_1, \ldots, \eta_N)$ and R_5 is some matrix which is bounded uniformly in k.

Next we define the Lyapunov functions $V_\psi = \psi^T H \psi$, where $H = H^T > 0$ is the solution to the Lyapunov equation $HA_0 + A_0^T H = -I$.

We now state the main Theorems of the chapter.

Theorem 3.2: *Consider the system (3.1) with the output feedback controller (3.15) and the high-gain observer (3.14). Let S be a compact set in the interior of Γ and Q be any compact set of $\mathbb{R}^{2N+1}$. Let $(\tilde{z}(0), \bar{y}(0)) \in S$, and $(z_1(0), \hat{\zeta}(0), \hat{\sigma}(0)) \in Q$, and $\lambda = \max\left\{\mu, \frac{\epsilon}{\mu}\right\}$, then there exists $\lambda^* > 0$, such that for every $0 < \lambda \le \lambda^*$, the trajectories of the closed-loop system (3.16) are bounded for all $t \ge 0$, and*

$$\lim_{t\to\infty} \left[x_i(t) - x_j(t)\right] = 0, \quad \text{for } i \neq j \text{ and } i, j = 1, \ldots, N \tag{3.17}$$

Proof : It proceeds in three steps:

Step 1. We show that there exist positive constants κ_1 and $\tilde{\lambda}_1$ such that for $\tilde{\lambda}_1 \leq \lambda$ the set $\Lambda = \{V \leq c\} \times \{V_\psi \leq \kappa_1(\epsilon/\mu)^2\}$ is positively invariant.

Step 2. We show that for any bounded $(\hat{\zeta}(0), \hat{\sigma}(0))$ and any $(\tilde{z}(0), \bar{y}(0))$ in the interior of $\{V \leq c\}$ there exists $\tilde{\lambda}_2 > 0$, such that for $\lambda \leq \tilde{\lambda}_2$, the trajectory $(\tilde{z}(t), \bar{y}(t), \psi(t))$ enters the set $\{V \leq c\} \times \{V_\psi \leq \kappa_2(\epsilon/\mu)^2\}$ in finite time $T_1(\epsilon)$ with $\lim_{\epsilon \to 0} T_1(\epsilon) = 0$.

Step 3. We show that there exists $\tilde{\lambda}_3$ such that for $\lambda \leq \tilde{\lambda}_3$, the system (3.16b)-(3.16d) is exponentially stable from which (3.17) follows.

We show the first step by calculating the derivatives of V and V_ψ on the boundaries $\{V = c\}$ and $\{V_\psi = \kappa_1(\epsilon/\mu)^2\}$, respectively. The saturation is no longer effective when the trajectory is in Λ, from which we have $\Delta = k\eta + \epsilon\gamma k\delta$. By taking the time derivative of V_ψ along (3.16d) we have

$$\epsilon\dot{V}_\psi = -\psi^T\psi + \frac{2\epsilon}{\mu}\psi^T H \begin{bmatrix} \mathbf{0} \\ -LAT\bar{y} + kL\eta + \epsilon\gamma kL\delta \end{bmatrix}$$

With $\lambda \leq 1$, we have

$$\epsilon\dot{V}_\psi \leq -||\psi||^2 + (\epsilon/\mu)q_1||\psi||^2 + (\epsilon/\mu)q_2||\psi||$$

where q_1 and q_2 are some positive constants. For $\epsilon/\mu \leq 1/(2q_1)$ we have

$$\epsilon\dot{V}_\psi \leq -(1/2)||\psi||^2 + (\epsilon/\mu)q_2||\psi||$$

Thus,

$$\epsilon \dot{V}_\psi \leq -(1/4)||\psi||^2, \;\; \forall \; ||\psi|| \geq 4(\epsilon/\mu)q_2$$

Taking $\kappa_1 = 16\lambda_{\max}(H)q_2^2$ ensures that

$$\epsilon \dot{V}_\psi \leq -\frac{1}{4}||\psi||^2, \;\; \forall \; V_\psi \geq \kappa_1(\epsilon/\mu)^2$$

From which we conclude that for sufficiently small λ the set $\{V_\psi \leq \kappa_1(\epsilon/\mu)^2\}$ is positively invariant as $\dot{V}_\psi \leq 0$ on the boundary $V_\psi = \kappa_1(\epsilon/\mu)^2$.

The derivative of V, for all $\psi \in \{V_\psi \leq \kappa_1(\epsilon/\mu)^2\}$, satisfies

$$\begin{aligned}\dot{V} = -\gamma\tilde{z}^T[\tilde{J} + \tilde{J}^T]\tilde{z} + 2\tilde{z}^T R_2\bar{y} - (1/\mu)[\tilde{y}^T(2W + kI)\tilde{y}^T + b\bar{y}_1^2] - (1/\mu)bk\bar{y}_1\bar{\mathcal{L}}_{12}\tilde{y} \\ + 2\gamma\bar{y}^T PR_3\bar{y} + 2\gamma^2\bar{y}^T PR_4\tilde{z} + 2\bar{y}^T PR_5\Delta\end{aligned}$$

Similar to the proof of Lemma 3.2, it can be shown that for sufficiently small μ

$$\dot{V} \leq -b_2||\tilde{z}||^2 - b_3||\bar{y}||^2 + (\epsilon/\mu)q_3||\bar{y}||$$

for some positive constants b_2, b_3, and q_3. From which we have

$$\dot{V} \leq -b_4||\Theta||^2 + (\epsilon/\mu)q_3||\Theta||$$

where $\Theta = \mathrm{col}(||\tilde{z}||, ||\bar{y}||)$ and $b_4 = \min\{b_2, b_3\}$. Thus,

$$\dot{V} \leq -\frac{b_4}{2}||\Theta||^2, \; \forall \; ||\Theta|| \geq \frac{\epsilon}{\mu}(2q_3/b_4)$$

Therefore, $\dot{V}$ is negative on the boundary $\{V = c\}$, for sufficiently small λ. Therefore, there exists $\tilde{\lambda}_1 > 0$, such that for all $\lambda \leq \tilde{\lambda}_1$ the set Λ is positively invariant.

In the second step, because $(\tilde{z}(0), \bar{y}(0))$ lie in the interior of the set $\{V \leq c\}$, and the right-hand-side functions of (3.16b)-(3.16c) are bounded uniformly in ϵ, there exists a time $\tilde{T}_1 > 0$, such that $(\tilde{z}(t), \bar{y}(t)) \in \{V \leq c\}$ for all $t \in [0, \tilde{T}_1]$. For $\psi(0) \notin \{\psi^T H \psi \leq \kappa_1(\epsilon/\mu)^2\}$, it can be seen

$$V_\psi(t) \leq q_4 e^{-q_5 t/\epsilon} ||\psi(0)||^2$$

where $q_4 = \lambda_{\max}(H)$, $q_5 = 1/(4\lambda_{\max}(H))$. Considering $\psi(0) = O(1/\epsilon)$, we have

$$V_\psi(t) \leq (q_6/\epsilon^2) e^{-q_5 t/\epsilon}$$

for some $q_6 > 0$. Since $\epsilon \leq \epsilon/\mu$, for $\lambda \leq 1$, the time taken by $\psi(t)$ to reach the set $\{\psi^T H \psi \leq \kappa_1(\epsilon/\mu)^2\}$ can be estimated by the more conservative time $T_1(\epsilon)$ when $V_\psi = \kappa_1 \epsilon^2$, which is given by $T_1 = (\epsilon/q_5) \ln\left(q_6/(\kappa_1 \epsilon^4)\right)$. By l'Hôpital's rule it can be shown that $\lim_{\epsilon \to 0} T_1(\epsilon) = 0$. Therefore, there exists $\tilde{\lambda}_2 > 0$, such that for all $\lambda \leq \tilde{\lambda}_2$, we can ensure $T_1(\epsilon) < (1/2)\tilde{T}_1$, which implies $(\tilde{z}(t), \bar{y}(t), \psi(t)) \in \{V \leq c\} \times \{V_\psi \leq \kappa_1(\epsilon/\mu)^2\}$ for all $t \geq T_1(\epsilon)$.

In the third step we show the exponential stability of the system (3.16b)-(3.16d), by forming the composite Lyapunov function as $V_c = V + V_\psi$ and analyzing the system inside Λ. For sufficiently small μ the time derivative of V_c along (3.16b)-(3.16d) is given by

$$\dot{V}_c \leq -\Xi^T \begin{bmatrix} b_2 & 0 & 0 \\ 0 & b_3 & -\frac{q_7}{2} - \frac{q_8}{2\mu} \\ 0 & -\frac{q_7}{2} - \frac{q_8}{2\mu} & \frac{1}{\epsilon} - \frac{q_1}{\mu} \end{bmatrix} \Xi$$

where q_7, q_8 are positive constants, and $\Xi = \mathrm{col}(||\tilde{z}||, ||\bar{y}||, ||\psi||)$.

The 2×2 principal minor is positive since b_2 and b_3 are positive. Choose ϵ/μ small enough to make the determinant positive, which makes the above matrix positive definite. Therefore, we can conclude there exists $\tilde{\lambda}_3 > 0$, such that for all $\lambda \leq \tilde{\lambda}_3$,

$$\lim_{t\to\infty} \tilde{z}(t) = 0, \ \lim_{t\to\infty} \bar{y}(t) = 0 \text{ and } \lim_{t\to\infty} \psi(t) = 0. \tag{3.18}$$

Because of the exponential stability of the system (3.16b)-(3.16d), $z_1(t)$ remains bounded and all the agents converge to the consensus value

$$\lim_{t\to\infty} z_1(t) = \text{constant}$$

and by choosing $\lambda^* = \min\{\tilde{\lambda}_1, \tilde{\lambda}_2, \tilde{\lambda}_3, 1\}$ we conclude that (3.17) follows. ■

Theorem 3.3: *Consider that Theorem 3.2 holds and let $x^*(t)$ be the solution of the closed-loop system under state feedback (3.6) with $x^*(0) = x(0)$. Then, given any $\Upsilon > 0$ there exists $\lambda^{**} > 0$ such that for all $\lambda \in (0, \lambda^{**})$*

$$\|x(t) - x^*(t)\| \leq \ \Upsilon \ \ \forall \, t \geq 0, \tag{3.19}$$

Proof : In this Theorem we show the solution $x(t)$ under the output feedback control approaches the solution $x^*(t)$ under the state feedback control which illustrates the performance recovery property of the output feedback controller. We first show this in the transformed coordinates $z = \tilde{P}^{-1}x$, where $z(t) = \mathrm{col}(z_1(t), \tilde{z}(t))$, is the solution of the equations (3.16a) and (3.16b). The system in the transformed coordinates under the state feedback control is given by

$$\dot{z}_1 = 0 \tag{3.20a}$$

$$\dot{\tilde{z}} = -\gamma \tilde{J} \tilde{z} \tag{3.20b}$$

$z_1^*(t)$ and $\tilde{z}^*(t)$ are the solutions of the equations (3.20a) and (3.20b), with initial conditions $\tilde{z}^*(0) = \tilde{z}(0)$ and $z_1^*(0) = z_1(0)$.

The time interval is split into $[0, T_1(\epsilon)]$ and $[T_1(\epsilon), \infty)$ and it is shown that $||z(t) - z^*(t)|| \leq \tilde{\Upsilon}$ holds for each time interval, where $\tilde{\Upsilon} = \Upsilon/(\sqrt{2}||\tilde{P}||)$. This is achieved by showing that $|z_1(t) - z_1^*(t)| \leq \tilde{\Upsilon}$ and $||\tilde{z}(t) - z^*(t)|| \leq \tilde{\Upsilon}$ hold for each time interval. Showing $|z_1(t) - z_1^*(t)| \leq \tilde{\Upsilon}$ is more involved as $z_1(t)$ is in the direction of the zero eigenvalue of $\hat{\mathcal{L}}$.

Since $\tilde{z}(0)$ is in the interior of $\{V \leq c\}$ we have $\|\tilde{z}(t) - \tilde{z}(0)\| \leq \tilde{k}_1 t$ during the interval $[0, T_1(\epsilon)]$, where $\tilde{k}_1$ is a positive constant. Similarly, it can be shown that $\|\tilde{z}^*(t) - \tilde{z}^*(0)\| \leq \tilde{k}_1 t$ during the same time interval. By using $\tilde{z}(0) = \tilde{z}^*(0)$, we have

$$\|\tilde{z}(t) - \tilde{z}^*(t)\| \leq 2\tilde{k}_1 T_1(\epsilon), \ \forall \ t \in [0, T_1(\epsilon)].$$

Since $T_1(\epsilon) \to 0$ as $\epsilon \to 0$, therefore we have

$$\tilde{z}(t) - \tilde{z}^*(t) = O(T_1(\epsilon)), \ \forall \ t \in [0, T_1(\epsilon)]. \tag{3.21}$$

By using continuous dependence of the solutions of differential equations on initial conditions and parameters and the exponential stability of $\dot{\tilde{z}} = -\gamma \tilde{J} \tilde{z}$ we conclude that [91, Theorem

9.1],

$$\tilde{z}(t) - \tilde{z}^*(t) = O(T_1(\epsilon)),\ \forall\ t \geq 0$$

Therefore, for sufficiently small ϵ, we have

$$||\tilde{z}(t) - \tilde{z}^*(t)|| \leq \tilde{\Upsilon},\ \forall\ t \geq 0 \tag{3.22}$$

Next we integrate $\dot{z}_1(t) - \dot{z}_1^*(t)$ and by using $z_1(0) = z_1^*(0)$,

$$z_1(t) - z_1^*(t) = \int_0^t R_1 \bar{y}(\tau) d\tau$$

During the period $[0, T_1(\epsilon)]$, $|R_1\bar{y}(\tau)| \leq \tilde{k}_2$, where $\tilde{k}_2$ is a positive constant independent of ϵ and μ. Since $T_1(\epsilon) \to 0$ as $\epsilon \to 0$, therefore for sufficiently small ϵ we have

$$z_1(t) - z_1^*(t) = O(T_1(\epsilon)), \forall\ t \in [0, T_1(\epsilon)].$$

For $t \geq T_1(\epsilon)$, the system (3.16b)-(3.16d) represents a three-time scale system where ψ is the fast variable and $(\tilde{z}, \bar{y})$ are the slow variables. Following [85, Chapter 2], we perform a change of coordinates $\chi = \psi + D_1\tilde{z} + D_2\bar{y}$, for some matrices $D_1,\ D_2$, which separates the fast variable ψ from the slow ones $(\tilde{z}, \bar{y})$, and $\theta = \bar{y} + S\tilde{z}$, for some matrix S, to separate the intermediate system $\bar{y}$ from the slow one $\tilde{z}$, from which we have

$$\dot{z}_1 = O(\lambda)\tilde{z} + R_1\theta \tag{3.23a}$$

$$\dot{\tilde{z}} = \left[-\gamma\tilde{J} + O(\lambda)\right]\tilde{z} + R_2\theta \tag{3.23b}$$

$$\mu\dot{\theta} = [\tilde{A} + O(\lambda)]\theta + R_6\chi \tag{3.23c}$$

$$\epsilon\dot{\chi} = (A_0 + (\epsilon/\mu)R_7)\chi \tag{3.23d}$$

for some matrices R_6, R_7. For sufficiently small λ, the solution of (3.23c) and (3.23d) for $t \geq T_1(\epsilon)$ is bounded by

$$||\chi(t)|| \leq \tilde{k}_3 e^{-(r_1/\epsilon)(t-T_1(\epsilon))}$$

$$||\theta(t)|| \leq \tilde{k}_4 e^{-(r_2/\mu)(t-T_1(\epsilon))}$$

for $\epsilon << \mu$ and some positive constants r_1, r_2, $\tilde{k}_3$ and $\tilde{k}_4$ independent of λ.

Defining $\phi(t) = \tilde{z}(t) - \tilde{z}^*(t)$ and by differentiating it we have

$$\dot{\phi}(t) = (-\gamma\tilde{J} + O(\lambda))\phi(t) + O(\lambda)\tilde{z}^*(t) + R_2\theta(t).$$

Integrating $\dot{\phi}(t)$ from time $T_1(\epsilon)$ we have

$$\phi(t) = e^{(-\gamma\tilde{J}+O(\lambda))(t-T_1(\epsilon))}\phi(T_1(\epsilon)) + \int_{T_1(\epsilon)}^{t} e^{(-\gamma\tilde{J}+O(\lambda))(t-\tau)}[O(\lambda)\tilde{z}^*(\tau) + R_2\theta(\tau)]d\tau.$$

From (3.21), we have $\phi(T_1(\epsilon)) = O(T_1(\epsilon))$, and therefore it can be shown that

$$\|\phi(t)\| \leq (O(T_1(\epsilon)) + O(\lambda))e^{-r_3(t-T_1(\epsilon))} \tag{3.24}$$

for all $t \geq T_1(\epsilon)$, where r_3 is a positive constant independant of λ. Next integrating $\dot{z}_1(t) - \dot{z}_1^*(t)$ from time $T_1(\epsilon)$ and by substituting $\tilde{z}(t) = \phi(t) + \tilde{z}^*(t)$, we have

$$z_1(t) - z_1^*(t) = [z_1(T_1(\epsilon)) - z_1^*(T_1(\epsilon))] + \int_{T_1(\epsilon)}^{t} [O(\lambda)\phi(\tau) + O(\lambda)\tilde{z}^*(\tau) + R_1\theta(\tau)]\, d\tau.$$

Using $z_1(T_1(\epsilon)) - z_1^*(T_1(\epsilon)) = O(T_1(\epsilon))$, it can be shown that $z_1(t) - z_1^*(t) = O(T_1(\epsilon)) + O(\lambda)$ for all $t \geq T_1(\epsilon)$. Therefore, for all $\lambda \in (0, \lambda^{**})$, we can conclude that

$$|z_1(t) - z_1^*(t)| \leq \tilde{\Upsilon}, \quad \forall\, t \geq 0. \tag{3.25}$$

From which we conclude that $||z(t) - z^*(t)|| \leq \sqrt{2}\tilde{\Upsilon}$ and by using the transformation $x = \tilde{P}z$ we have $x(t) - x^*(t) = \tilde{P}[z(t) - z^*(t)]$. By taking the norm we have

$$||x(t) - x^*(t)|| \leq ||\tilde{P}|| \cdot ||z(t) - z^*(t)|| \leq \sqrt{2}||\tilde{P}||\tilde{\Upsilon}$$

from which (3.19) follows. ■

Theorem 3.2 shows that the agents achieve consensus under the output feedback controller (3.15), while Theorem 3.3 shows $x(t)$ under the output feedback controller approaches the solution $x^*(t)$ under the state feedback controller which illustrates the performance recovery property of the output feedback controller.

3.5 Cyclic Pursuit on Plane

Motivated by robotic coordination problems we take the example of cyclic pursuit [92]. We consider N robots on a plane with positions x_i, for $i = 1, \ldots, N$, and moving according to

$\dot{x}_i = v_i$, where v_i are the velocity commands. The objective of the robots is rendezvous at a common point (while using only onboard sensors). A simple strategy to achieve rendezvous is *cyclic pursuit*: where robot i pursues the next robot $i+1$. In other words, the information available to each robot is given by $\zeta_i = x_{i-1} - x_i$ for $i = 1, \ldots, N$. (Here we consider $x_0 = x_N$). We can arrange the nodes such that the graph for this network of N robots is represented by a circulant directed graph. Fig. 3.1 demonstrates the graph.

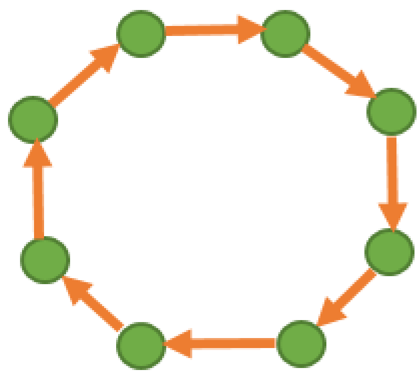

Figure 3.1: A directed circulant graph

We take the number of nodes to be 100. The initial conditions of the agents are chosen to be in the range $[1, 100]$. The circular directed graph is balanced and strongly connected and as a result the convergence rate is given by $\lambda_s(L_s) = 0.0020$, where λ_s is the smallest non-zero eigenvalue of $L_s = (L + L^T)/2$; see [19]. We simulate the system with the PD controller with $\gamma = 3$ and $k = 20$ and the standard controller (3.3) with $k_s = 600$ in order to match the convergence rate of the system under the PD controller. The saturation levels are chosen as $M_i = \pm 170$, for $i = 1, \ldots, 100$. The saturation levels are chosen from simulations to see the maximal values that the state trajectories (3.12) would take when using the state PD controller.

In Fig. 3.2, $\mathrm{x_{hgc}}$ denotes the state under high-gain consensus controller, $\mathrm{x_{pd}}$ denotes the state under PD controller (3.5), $\mathrm{x_{pdo}}$ denotes the state under the output feedback controller

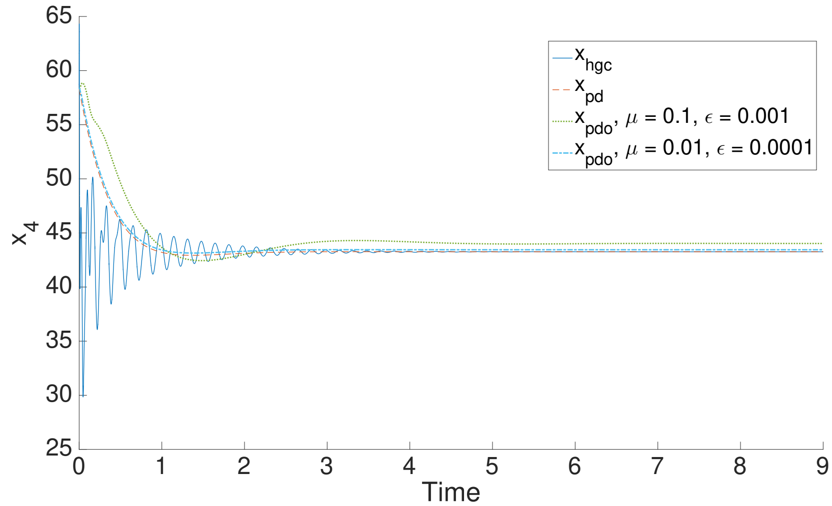

Figure 3.2: Agent 4 state

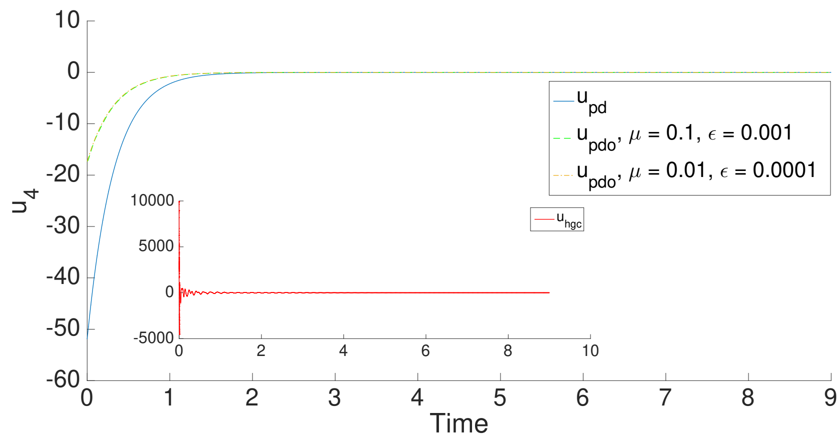

Figure 3.3: Agent 4 control signal

(3.15). We compare the state and control signals of agent 4 for the high-gain consensus controller, the state feedback PD controller, and the output feedback PD controller. From Fig. 3.2, the state under the high-gain consensus controller x_{hgc} oscillates as it approaches the consensus value. The oscillations are due to the presence of the imaginary component in the eigenvalues of L. The state under the state feedback PD controller x_{pd} does not have any oscillations and achieves the same consensus value as in the case of a high-gain consensus controller. The state under the output feedback PD controller x_{pdo} is shown for

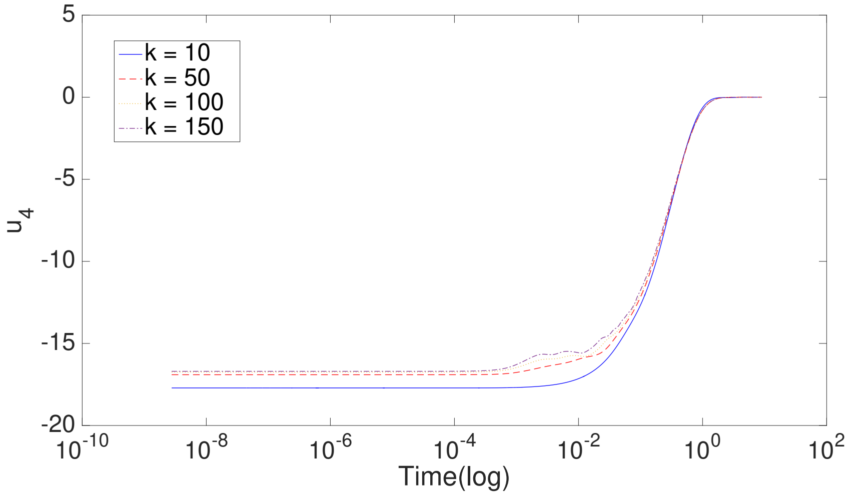

Figure 3.4: Agent 4 control signal with $\mu = 0.1$, $\epsilon = 0.0001$

two different values of ϵ and μ, from Fig. 3.2 it can be seen that as ϵ and μ decrease the trajectory under output feedback approaches, the one under state feedback as predicted by Theorem 3.3 and this trend is representative for all other agent trajectories.

In Fig. 3.3, $\mathrm{u_{hgc}}$ denotes the control signal of the high-gain consensus controller, $\mathrm{u_{pd}}$ denotes the control signal of the PD controller (3.5), $\mathrm{u_{pdo}}$ denotes the control signal of the output feedback controller (3.15). In Fig. 3.3, the control signal of agent 4 under control $\mathrm{u_{hgc}}$ is represented by a subfigure due to the large magnitude difference. As seen in Fig. 3.3 the control signal under the high-gain consensus controller is much higher than the proposed controller for the same convergence rate. Finally, Fig. 3.4 shows the control signal of agent 4 with different values of k. We plot the control signals in the linear-log scale for different values of k to improve the readability of the figure. It can be seen from the figure increasing k does not increase the magnitude of the control signal of agent 4.

3.6 Tree Graphs

In this section, we consider two kinds of self-similar graphs, namely, the Tree-Like Fractal graph and the Vicsek Fractal graph. Self-similar graphs have a prescribed way of increasing the graph size such that the structure of the graph is preserved. Other examples of self-similar graphs include Torus and lattice graphs, where 1-D lattice graphs are line graphs used in the platooning of vehicles [35].

Tree-Like Fractal graphs are generated in an iterative manner, starting from the first generation, which consists of two nodes connected by an edge. Each family of these tree-like fractal graphs is parameterized by a positive integer m. The procedure of creating the graph of generation g+1 starts by replacing each edge with a path of length two in the graph of generation g, thus creating a new node in the process. After that, m new nodes are added to the newly created node; see [93]. Fig. 3.5 represents the first three generations of the Tree-like fractal graphs with $m = 2$.

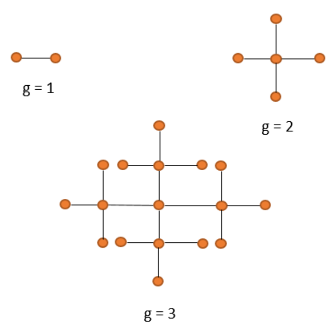

Figure 3.5: Tree-like Fractal graphs

Vicsek fractal graphs are parameterized by a positive integer d. The star graph with $d + 1$ nodes is the first generation (g=1) graph. The graph for the next generation (g+1) is generated from the graph of generation g. A detailed procedure for constructing the graph of generation g+1 from the graph of generation g is given in [93]. Fig. 3.6 represents the first three generations of the Vicsek fractal graphs for $d = 2$. Both graphs have an increasing

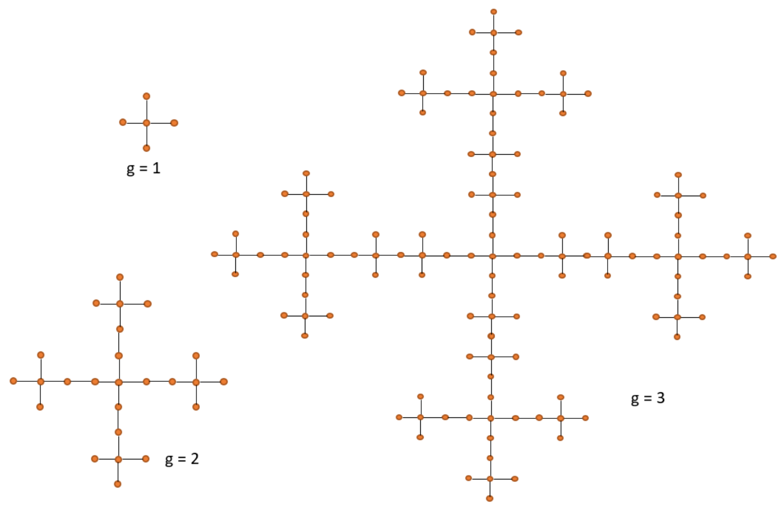

Figure 3.6: Vicsek Fractal graphs

tree diameter (greatest distance between any two nodes in a graph) as the generation of the graph increases. From [94], for a tree with growing diameter the second smallest eigenvalue of the Laplacian is bounded by

$$\lambda_2(L) \leq 2\left(1 - \cos\left(\frac{\pi}{d_g + 1}\right)\right)$$

where d_g represents the diameter of the graph. Therefore $\lambda_2(L)$ decreases with increase in the diameter of the graph.

The following tables illustrate the performance of the proposed controller on Tree-Like Fractal graphs and Vicsek Fractal graphs with different network sizes.

Table 3.1: Laplacian Eigenvalues of Tree-like fractal graphs

N	g	$\lambda_2(L)$	$\lambda_2(\hat{L})$, $k = 20$	$\lambda_2(\hat{L})$, $k = 200$	$\frac{\lambda_2(\hat{L})}{\lambda_2(L)}$, $k = 20$	$\frac{\lambda_2(\hat{L})}{\lambda_2(L)}$, $k = 200$
2	1	2	0.9756	0.9975	0.4878	0.4988
5	2	1	0.9524	0.9950	0.9524	0.9950
17	3	0.2087	0.8067	0.9766	3.8654	4.6794
65	4	0.0314	0.3859	0.8627	12.2898	27.4745

Table 3.1 shows the performance of the proposed controller with two different values of k. As seen from the table as the size of the Tree-Like Fractal graph increases the second smallest eigenvalue of the graph $\lambda_2(L)$ decreases. With increase in network size for higher value of k the ratio between $\lambda_2(\hat{L})$ and $\lambda_2(L)$ significantly increases.

Table 3.2: Laplacian Eigenvalues of Vicsek fractal graphs

N	g	$\lambda_2(L)$	$\lambda_2(\hat{L})$, $k = 60$	$\lambda_2(\hat{L})$, $k = 300$	$\frac{\lambda_2(\hat{L})}{\lambda_2(L)}$, $k = 60$	$\frac{\lambda_2(\hat{L})}{\lambda_2(L)}$, $k = 300$
5	1	1	0.9836	0.9993	0.9836	0.9993
25	2	0.0692	0.8059	0.9540	11.646	13.78
121	3	0.0053	0.2396	0.6117	45.2075	115.4151

Table 3.2 shows the performance of the proposed controller with different size of Vicsek Fractal graph with two different values of k. From the table for $N = 121$, the ratio between $\lambda_2(\hat{L})$ and $\lambda_2(L)$ is significantly higher for $k = 300$ than the other cases.

3.7 Conclusion

In this chapter we proposed a new consensus algorithm which is scalable as with increase in the network size the eigenvalues of the closed-loop Laplacian matrix remain preserved. This has benefits as in certain classes of graphs with increase in network size the convergence rate becomes slow and to achieve fast consensus a large control effort is required.

We simulated the proposed controller on a circular, directed graph with 100 nodes. The magnitude of the proposed controller compared to the high-gain consensus controller for achieving the same convergence rate, was much lower. We also considered two classes of graphs, which show the trend of decrease in the second smallest eigenvalue of the graph Laplacian with an increase in network size. We showed the benefit of using the proposed controller on these networks with different sizes.

Chapter 4

Practical Scalable Synchronization in Leader-Follower Networks

4.1 Introduction

For a network of linear agents, if the performance measure degrades with an increase in network size, then this is because the smallest eigenvalue of the grounded Laplacian matrix approaches zero. We will discuss the effect of this behavior on some standard nonlinear control techniques, which rely on local relative information. Therefore, we will exclude, [55] from our discussion as it uses local output information.

Synchronization was achieved for homogeneous (identical dynamics) second-order nonlinear systems in [95] and [96], using only relative position and velocity feedback. However, the gain of the controller is inversely proportional to the smallest eigenvalue of the grounded Laplacian. As this quantity decreases with an increase in network size, the controller gain becomes very large. In [53] and [97], synchronization was achieved for homogeneous and heterogeneous nonlinear agents, respectively. The feedback gain matrix in these methods depends on the solution of a parametric algebraic Riccati equation (PARE), where the parameter is a lower bound on the real parts of the eigenvalues of the graph Laplacian. Therefore, as the second smallest eigenvalue of the graph Laplacian approaches zero, it implies that the parameter also approaches zero, which in turn makes the controller gain very small. As a result, synchronization is achieved in a very long time.

In [61], practical synchronization is achieved in a network of nonlinear heterogeneous agents by choosing the gain of the diffusive coupling sufficiently large. Other approaches like [98], [99], [100] involve the use of adaptation where the nonlinearity is compensated using neural networks. For undirected graphs, the controller gain in these algorithms is inversely proportional to the smallest eigenvalue of the grounded Laplacian. A similar conclusion can be drawn for the controller gain in [57], where the controller gain is required to be greater than a constant that is inversely proportional to the smallest eigenvalue of the grounded Laplacian.

As discussed above, decrease in the smallest eigenvalue of the grounded Laplacian, has an adverse effect on the controllers of nonlinear systems. Therefore, in this chapter, we design scalable consensus algorithms [101] for leader-follower networks of second-order nonlinear systems. We consider second-order systems as they represent models of real-world systems akin to platooning of vehicles [35], power systems with second-order swing dynamics [65], Euler-Lagrange systems [99], and longitudinal vehicle dynamics [102].

4.2 Problem Setup

4.2.1 Class of Systems

We consider a network of N second-order nonlinear heterogeneous agents given by

$$\dot{x}_i = v_i \tag{4.1a}$$

$$\dot{v}_i = f_i(x_i, v_i) + w_i(t) + b_i u_i, \quad \forall\ i = 1, \ldots, N. \tag{4.1b}$$

where $x_i \in \mathbb{R}$ is the position, $v_i \in \mathbb{R}$ is the velocity, $u_i \in R$ is the control, $f_i(x_i, v_i)$ represents the nonlinearity associated with each system, $w_i(t)$ represents a time-varying disturbance. The system (4.1) represents models of real world systems like power systems [65], and longitudinal vehicle dynamics [102]. We make the following assumptions.

Assumption 4.1: The communication topology is given by a strongly connected weighted directed graph $\mathcal{G}$.

Assumption 4.2: The functions f_i are unknown and continuously differentiable for all $(x, v) \in \mathcal{D}$ where $\mathcal{D}$ is some domain containing the origins.

Assumption 4.3: The disturbances $w_i(t)$ and its derivative $\dot{w}_i(t)$ are unknown and bounded.

Assumption 4.4: The control coefficient b_i is an unknown constant and satisfies $b_i \geq \bar{b}_i > 0$.

4.2.2 Leader

In applications of multi-agent systems like platooning, power systems, etc., the agents are required to follow or synchronize to a desired trajectory. The trajectory is generated by a leader and, to reduce the information flow, it is assumed that only a subset of the agents receives information from the leader. The leader dynamics is defined as

$$\dot{x}_0 = v_0 \tag{4.2a}$$

$$\dot{v}_0 = f_0(x_0, v_0) + u_0(t, x_0, v_0) \tag{4.2b}$$

The leader (4.2) with the control input $u_0(t, x_0, v_0)$ is used to generate trajectories depending on the required objective. We do not require the control of the leader to be known to the agents.

Assumption 4.5: The functions f_0, u_0 are continuously differentiable and the closed-loop trajectories of the leader (x_0, v_0) belongs to a known compact invariant set $\mathcal{W} \subset \mathbb{R}^2$.

Next we discuss the information exchange between the agents which is of the following form:

$$x_{ri} = \sum_{j=1}^{N} a_{ij}(x_j - x_i) + d_i(x_0 - x_i), \tag{4.3a}$$

$$v_{ri} = \sum_{j=1}^{N} a_{ij}(v_j - v_i) + d_i(v_0 - v_i) \tag{4.3b}$$

where $a_{ij} \geq 0$, x_{ri} defines the relative position exchange, v_{ri} defines the relative velocity exchange and $d_i > 0$ is satisfied at least for one agent. We define the synchronization error as

$$e_{xi} = x_i - x_0, \quad e_{vi} = v_i - v_0$$

for all $i = 1, \dots, N$. From which the information exchange can be redefined as

$$x_{ri} = \sum_{j=1}^{N} a_{ij}(e_{xj} - e_{xi}) - d_i e_{xi}, \tag{4.4a}$$

$$v_{ri} = \sum_{j=1}^{N} a_{ij}(e_{vj} - e_{vi}) - d_i e_{vi}, \tag{4.4b}$$

which in matrix form can be written as

$$x_r = -L_G e_x, \quad v_r = -L_G e_v$$

where $L_G = L + D$ is the grounded Laplacian matrix [36], $D = \operatorname{diag}(d_1, \dots, d_N)$, $e_x = \operatorname{col}(e_{x1}, \dots, e_{xN})$ and $e_v = \operatorname{col}(e_{v1}, \dots, e_{vN})$.

The expanded graph is given by $\bar{\mathcal{G}} = (\bar{\mathcal{V}}, \bar{\mathcal{E}}, \bar{\mathcal{A}})$.

Assumption 4.6: There is a directed path from the leader to all the agents in the expanded graph $\bar{\mathcal{G}}$.

Remark 4.1: The above assumption is standard to achieve synchronization in a network of agents with a leader.

Under Assumption 4.1 and 4.6 we have the following properties

(i) L is an $\mathcal{M}$-matrix [6] beacause it can be decomposed into $L = \tilde{d}I - \tilde{\mathcal{A}}$, for some nonnegative matrix $\tilde{\mathcal{A}}$ and $\tilde{d} \geq \rho(\tilde{\mathcal{A}})$, where $\rho(\cdot)$ denotes the spectral radius of a matrix.

(ii) L_G is an $\mathcal{M}$-matrix, since L is an $\mathcal{M}$-matrix and $D = \operatorname{diag}(d_i) \geq 0$.

(iii) L_G is nonsingular and all its eigenvalues have positive real parts [10]. Therefore, L_G is a nonsingular $\mathcal{M}$-matrix.

The objective of this chapter is to design a controller using the information structure (4.4) to achieve

$$\lim_{t \to \infty} e_{xi}(t) = 0, \text{ and } \lim_{t \to \infty} e_{vi}(t) = 0 \tag{4.5}$$

for $i = 1, \ldots, N$.

Remark 4.2: In this chapter we will achieve practical synchronization where the synchronization error can be made arbitrarily small by tuning a control and observer parameter, respectively.

We transform system (4.1) into the error coordinates

$$\dot{e}_{xi} = e_{vi} \tag{4.6a}$$

$$\dot{e}_{vi} = f_i(e_{xi} + x_0, e_{vi} + v_0) + w_i(t) - f_0(x_0, v_0) - u_0(t, x_0, v_0) + b_i u_i \tag{4.6b}$$

for $i = 1, \ldots, N$.

4.3 Controller Design With Full Information

4.3.1 Controller Design

In this section we assume that the relative velocity derivatives are available for feedback and we design the following PD control for each agent, which is given by

$$u_i^s = k_x x_{ri} + k_v v_{ri} + k_d \sigma_i \tag{4.7}$$

where u_i^s denotes the controller designed with full information, k_x, k_v, k_d are positive constants to be chosen later, σ_i is defined as

$$\sigma_i = \dot{v}_{ri} = \sum_{j=1}^{N} a_{ij}(\dot{e}_{vj} - \dot{e}_{vi}) - d_i \dot{e}_{vi},$$

which in matrix form can be written as $\sigma = -L_G \dot{e}_v$, where $\sigma = \mathrm{col}(\sigma_1, \ldots, \sigma_N)$. We assume that σ_i is available for feedback. Substituting for σ_i in (4.7) we have,

$$u_i^s = k_x x_{ri} + k_v v_{ri} + k_d \sum_{j=1}^{N} a_{ij}(\dot{e}_{vj} - \dot{e}_{vi}) - k_d d_i \dot{e}_{vi}$$

The above controller is distributed in nature as it relies only on local information. Next we write the equations in matrix form,

$$(I + k_d L_G B)u^s = k_x x_r + k_v v_r - k_d L_G (f + w) + k_d L_G \mathbf{1}(f_0 + u_0)$$

where $f = \mathrm{col}(f_1, \ldots, f_N)$, $B = \mathrm{diag}(b_1, \ldots, b_N)$, $w = \mathrm{col}(w_1, \ldots, w_N)$ and $u^s = \mathrm{col}(u_1^s, \ldots, u_N^s)$. The terms f, f_0, u_0 and w are written without their arguments for ease of notation.

Lemma 4.1: *Suppose Assumption 4.6 holds, then the matrix $(I + k_d L_G B)$ is nonsingular with eigenvalues having positive real parts.*

Proof: The matrix $(I + k_d L_G B)$ is similar to the matrix $(I + k_d B L_G)$, this follows by pre-multiplying $(I + k_d L_G B)$ by B and then post-multiplying it by B^{-1}, where B is invertible from Assumption 4.4. The matrix BL_G can be thought of as a grounded Laplacian matrix where each row is scaled by b_i. Therefore, it follows that the eigenvalues of BL_G remain on the right half-plane for any positive diagonal matrix B and we have

$$\lambda_i(I + k_d BL_G) = 1 + k_d \lambda_i(BL_G),$$

where $\mathrm{Re}\,(\lambda_i(BL_G)) > 0$, from which we conclude that $(I + k_d L_G B)$ is invertible and its eigenvalues have positive real parts. ■

Choosing $k_d = k$, $k_x = \gamma_1 k$ and $k_v = \gamma_2 k$, where γ_1 and γ_2 are positive constants, we have the control as

$$u^s = -\gamma_1 B^{-1} \hat{L}_G e_x - \gamma_2 B^{-1} \hat{L}_G e_v - B^{-1} \hat{L}_G [f + w - \mathbf{1}(f_0 + u_0)] \tag{4.8}$$

where $\hat{L}_G$ represents the Virtual Grounded Laplacian matrix, defined as

$$\hat{L}_G = \left(\frac{1}{k} I + \bar{L}_G \right)^{-1} \bar{L}_G \tag{4.9}$$

where $\bar{L}_G = BL_G$ is the scaled grounded Laplacian matrix from the proof of Lemma 4.1.

Lemma 4.2: *Let the expanded graph $\bar{\mathcal{G}}$ satisfy Assumption 4.6, then for sufficiently large k,*

$$\mathrm{Re}(\lambda_i(\hat{L}_G)) = 1 - \frac{1}{k} \mathrm{Re} \left(\frac{1}{\lambda_i(\bar{L}_G)} \right) + O\left(\frac{1}{k^2} \right), \tag{4.10a}$$

$$\mathrm{Im}(\lambda_i(\hat{L}_G)) = -\frac{1}{k} \mathrm{Im} \left(\frac{1}{\lambda_i(\bar{L}_G)} \right) + O\left(\frac{1}{k^2} \right), \tag{4.10b}$$

for $i = 1, \ldots, N$, where $\lambda_i(\bar{L}_G)$ and $\lambda_i(\hat{L}_G)$ are the eigenvalues of $\bar{L}_G$ and $\hat{L}_G$, respectively.

The proof of this Lemma can be done by repeating the steps in Theorem 3.1 of chapter 3 and therefore it is omitted.

4.3.2 Closed-loop System Analysis

The system (4.6) with the controller (4.8) becomes

$$\dot{e}_x = e_v \tag{4.11a}$$

$$\dot{e}_v = -\gamma_1 \hat{L}_G e_x - \gamma_2 \hat{L}_G e_v + L_1(f + w) - L_1 \mathbf{1}(f_0 + u_0) \tag{4.11b}$$

where $L_1 = I - \hat{L}_G = (I + k\bar{L}_G)^{-1}$. Next we do a change of coordinates

$$e_x = P\tilde{e}_x, \quad \text{and} \quad e_v = P\tilde{e}_v \tag{4.12}$$

where $\bar{L}_G = PJP^{-1}$, $J = \text{blkdiag}(J_1, J_2, \ldots, J_m)$ is the Jordan block of $\bar{L}_G$ and $m \leq N$ is the number of Jordan blocks. The system in the transformed coordinates becomes

$$\dot{\tilde{e}}_x = \tilde{e}_v \tag{4.13a}$$

$$\dot{\tilde{e}}_v = -\gamma_1 \tilde{J}\tilde{e}_x - \gamma_2 \tilde{J}\tilde{e}_v + L_2(f + w) - L_2 \mathbf{1}(f_0 + u_0) \tag{4.13b}$$

where $L_2 = (I + kJ)^{-1}P^{-1}$, $\tilde{J} = \left(\frac{1}{k}I + J\right)^{-1} J$. The Jordan block $\tilde{J}$ contains eigenvalues with strict positive real parts. For sufficiently large k, we have

$$\tilde{J} = I + O(1/k), \quad \text{and} \quad L_2 = O(1/k).$$

Next we define the Lyapunov function $V_e = e^T W e$, where $W = W^T > 0$ is the solution to the Lyapunov equation $WA + A^T W = -I$, $e = \mathrm{col}(\tilde{e}_x, \tilde{e}_v)$ and A is a Hurwitz matrix given by

$$A = \begin{bmatrix} \mathbf{0} & I \\ -\gamma_1 I & -\gamma_2 I \end{bmatrix}.$$

Theorem 4.1 *Consider the system (4.6) with the controller (4.8). Let* $e(0) \in \Omega$. *where* $\Omega = \{V_e \leq c\}$, *for some* $c > 0$, *such that* $\Omega \subset \mathcal{D}$. *Then, there exists* $k^* > 0$, *such that for all* $k \geq k^*$, *the trajectories of the closed-loop system are bounded for all* $t \geq 0$, *and there exists time* $T > 0$, *such that*

$$x - \mathbf{1}x_0 = O\left(\frac{1}{k}\right), \ \forall\, t \geq T \tag{4.14a}$$

$$v - \mathbf{1}v_0 = O\left(\frac{1}{k}\right), \ \forall\, t \geq T \tag{4.14b}$$

Moreover, the control signal $u^s(t)$ *is bounded uniformly in* k.

Proof: Taking the time-derivative of V_e along (4.13) we have

$$\dot{V}_e \leq -||e||^2 + \frac{a_1}{k}||e||^2 + \frac{a_2}{k}||e||(||f|| + ||w||) + \frac{a_3}{k}||e||(|f_0| + |u_0|)$$

for some positive constants a_1, a_2, a_3. For $k \geq k_1 = 2a_1$, we have

$$\dot{V}_e \leq -\frac{1}{2}||e||^2 + \frac{a_2}{k}||e||(||f|| + ||w||) + \frac{a_3}{k}||e||(|f_0| + |u_0|)$$

Since $f_i(x_i, v_i) = f_i(e_{xi} + x_0, e_{vi} + v_0)$ and the function f_i is continuously differentiable, it follows that for all $e \in \Omega$ and $(x_0, v_0) \in \mathcal{W}$, we have

$$||f|| \leq a_4||e|| + a_5|x_0| + a_6|v_0| \leq a_4||e|| + a_7$$

where a_4, a_5, a_6 and a_7 are positive constants. Moreover, since $w(t)$ is bounded we have

$$\dot{V}_e \leq -(1/2)||e||^2 + (a_8/k)||e||^2 + (a_9/k)||e||$$

for some positive constants a_8 and a_9. For $k \geq k_2 = 4a_8$, we have

$$\dot{V}_e \leq -(1/4)||e||^2 + (a_9/k)||e||$$

From which we have

$$\dot{V}_e \leq -(1/8)||e||^2, \ \forall \ ||e|| \geq (8a_9/k) \tag{4.15}$$

For all $k \geq k_3$ where k_3 is a positive constant, $\dot{V}_e < 0$ on the boundary $V_e = c$ and therefore the set Ω is positively invariant, from which we can conclude that the trajectories of the closed-loop system are bounded for all $t \geq 0$. Finally, by choosing $k^* = \max\{k_1, k_2, k_3\}$, we can conclude that there exists time $T > 0$, such that

$$||e(t)|| = O(1/k), \ \forall \ \ t \geq T$$

Therefore, (4.14) follows from the above expression, which shows that the trajectories of the agents become arbitrarily close to the trajectories of the leader (x_0, v_0).

Next we show that control signal $u^s(t)$ is uniformly bounded in k. From (4.15), using [103, Theorem 4.5] we have

$$||e(t)|| \leq \sqrt{\frac{\lambda_{\max}(W)}{\lambda_{\min}(W)}} \max\left\{||e(0)|| \cdot \exp\left(\frac{-t}{16\lambda_{\max}(W)}\right), \frac{8a_9}{k}\right\} \tag{4.16}$$

The control signal is given by

$$u^s = B^{-1}\hat{L}_G[-\tilde{R}e - f - w + \mathbf{1}(f_0 + u_0)]$$

where $\tilde{R} = [\gamma_1 P \quad \gamma_2 P]$. The norm of $||B^{-1}||$ is given by $||B^{-1}|| = 1/\tilde{b}$, where $\tilde{b} = \min\limits_{1 \leq i \leq N} b_i$ and the norm of $\hat{L}_G$ is bounded uniformly in k as

$$||\hat{L}_G|| \leq ||P|| \cdot ||\tilde{J}|| \cdot ||P^{-1}|| = a_{10} + O(1/k)$$

for some positive constant a_{10} independent of k. Since we have $(x_0(t), v_0(t)) \in \mathcal{W}$ and $w(t)$ is bounded, therefore the norm of the control signal satisfies

$$||u^s(t)|| \leq a_{11}||e|| + a_{12}$$

for some positive constants a_{11} and a_{12}, uniformly independent of k. Using (4.16) in the above inequality we can conclude that the control signal is bounded uniformly in k. ■

4.4 Output Feedback Controller

4.4.1 Observer Design

In the previous section we assumed σ_i is available for feedback, which is not true for practical applications. Therefore, in this section we realize the proposed scalable controller (4.7) by using a reduced-order high-gain observer. The stability analysis using a full-order high-gain observer can be shown only with additional controller dynamics as shown in the previous chapter. Since in this chapter we do not use additional controller dynamics, the stability of the closed-loop system is shown using a reduced-order high-gain observer. However, using reduced-order observers is at the expense of assuming that the initial state of the relative sychronization errors is known. Each agent has measurement of relative state x_{ri} and relative velocity v_{ri} locally. We estimate the relative velocity derivatives by adding a reduced-order high gain observer to each agent in the network to estimate the signal $\sigma_i = \dot{v}_{ri}$. The driving signal to the observer is v_{ri}. The reduced order high-gain observer [90] is constructed as

$$\dot{\phi}_i = -\frac{p}{\epsilon}\left[\phi_i + \frac{p}{\epsilon}v_{ri}\right],\ \hat{\sigma}_i = \phi_i + (p/\epsilon)v_{ri} \tag{4.17}$$

where ϵ, and p are positive constants with $\epsilon << 1$ for $i = 1, \dots, N$. The transfer function of the observer from v_{ri} to $\hat{\sigma}_i$ is $\dfrac{s}{(\epsilon/p)s + 1}$. The output feedback controller is chosen as

$$u_i = \gamma_1 k x_{ri} + \gamma_2 k v_{ri} + k\hat{\sigma}_i \tag{4.18}$$

which in matrix form becomes

$$u = -\gamma_1 k L_G e_x - \gamma_2 k L_G e_v + k\hat{\sigma}$$

where $u = \mathrm{col}(u_1, \ldots, u_N)$ and $\hat{\sigma} = \mathrm{col}(\hat{\sigma}_1, \ldots, \hat{\sigma}_N)$.

4.4.2 Peaking

The estimation error is defined as $\eta_i = \sigma_i - \hat{\sigma}_i$, which satisfies

$$\epsilon\dot{\eta} = -p\eta + \epsilon\dot{\sigma}$$

where $\eta = \mathrm{col}(\eta_1, \ldots, \eta_N)$ and $\dot{\sigma} = -L_G\ddot{e}_v$. After some simplifications the observer error dynamics can be written as

$$\epsilon\dot{\eta} = -p[I + kL_GB]\eta + \epsilon\Delta \tag{4.19}$$

where $\Delta = \Delta(\dot{w}, \dot{f}_0, \dot{u}_0, \dot{f}, e)$. For all $e \in \Omega$, $(x_0(t), v_0(t)) \in \mathcal{W}$ and bounded $\dot{w}$, the term Δ is bounded by a constant independent of ϵ.

The output feedback control is given by $u = -\gamma_1 kL_Ge_x - \gamma_2 kL_Ge_v + k\sigma - k\eta$. Using $\sigma = -L_G\dot{e}_v$, we arrive at

$$u = -\gamma_1 B^{-1}\hat{L}_Ge_x - \gamma_2 B^{-1}\hat{L}_Ge_v - B^{-1}\hat{L}_G[f + w - \mathbf{1}(f_0 + u_0)] - k(I + kL_GB)^{-1}\eta \tag{4.20}$$

Noting that $\eta(0) = -L_G[f(0) + w(0) - \mathbf{1}(f_0(0) + u_0(0))] - L_GBu(0) - \hat{\sigma}(0)$, by substituting $u(0)$, we have

$$\begin{aligned}(I + kL_GB)^{-1}\eta(0) = &-L_G[f(0) + w(0) - \mathbf{1}(f_0(0) + u_0(0))] + \gamma_1 L_G\hat{L}_Ge_x(0) + \gamma_2 L_G\hat{L}_Ge_v(0) \\ &+ L_G\hat{L}_G[f(0) + w(0) - \mathbf{1}(f_0(0) + u_0(0))] - \phi(0) + (p/\epsilon)L_Ge_v(0)\end{aligned}$$

where we have used $I - kL_G B(I + kL_G B)^{-1} = (I + kL_G B)^{-1}$. The term $L_G \hat{L}_G = kL_G B(I + kL_G B)^{-1} L_G = L_G - (I + kL_G B)^{-1} L_G$, from which we have

$$(I + kL_G B)^{-1}\eta(0) = -(I + kL_G B)^{-1} L_G[f(0) + w(0) - \mathbf{1}(f_0(0) + u_0(0))]$$
$$+\gamma_1[L_G - (I + kL_G B)^{-1} L_G]e_x(0) + \gamma_2[L_G - (I + kL_G B)^{-1} L_G]e_v(0) - \phi(0) + (p/\epsilon)L_G e_v(0)$$

Multiplying the above equation by $(I + kL_G B)$, we have

$$\eta(0) = -L_G[f(0) + w(0) - \mathbf{1}(f_0(0) + u_0(0))] + \gamma_1 kL_G BL_G e_x(0) + \gamma_2 kL_G BL_G e_v(0)$$
$$- (I + kL_G B)\phi(0) + (p/\epsilon)(I + kL_G B)L_G e_v(0)$$

Because $\eta(0) = O(1/\epsilon)$, then during the transient period, the observer contains a term of the form $(1/\epsilon)e^{-\bar{a}_1 t/\epsilon}$, for some $\bar{a}_1 > 0$. This term is transmitted to the control as seen in equation (4.20). By choosing $\phi(0) = \gamma_1 L_G e_x(0) + \gamma_2 L_G e_v(0) + (p/\epsilon)L_G e_v(0)$, the initial estimation error becomes

$$\eta(0) = -L_G[f(0) + w(0) - \mathbf{1}(f_0(0) + u_0(0))] - \gamma_1 L_G e_x(0) - \gamma_2 L_G e_v(0),$$

which eliminates peaking and both the estimation error $\eta(t)$ and the control $u(t)$ become bounded uniformly in ϵ and k. Note that the parameters γ_1, γ_2, p, ϵ, and the initial conditions $L_G e_x(0)$ and $L_G e_v(0)$ are locally available to each agent.

4.4.3 Analysis of the closed loop system

The system (4.6) with the controller (4.20) becomes

$$\dot{e}_x = e_v \tag{4.21a}$$

$$\dot{e}_v = -\gamma_1 \hat{L}_G e_x - \gamma_2 \hat{L}_G e_v + L_1(f + w) - L_1 \mathbf{1}(f_0 + u_0) - L_3 \eta \tag{4.21b}$$

where $L_3 = [(1/k)B^{-1} + L_G]^{-1}$. Using the change of coordinates $e_x = P\tilde{e}_x,\ e_v = P\tilde{e}_v$, and $\eta = B^{-1}\tilde{\eta}$, we have

$$\dot{\tilde{e}}_x = \tilde{e}_v \tag{4.22a}$$

$$\dot{\tilde{e}}_v = -\gamma_1 \tilde{J}\tilde{e}_x - \gamma_2 \tilde{J}\tilde{e}_v + L_2(f + w) - L_2 \mathbf{1}(f_0 + u_0) - L_4 \tilde{\eta} \tag{4.22b}$$

$$\epsilon\dot{\tilde{\eta}} = -p[I + k\bar{L}_G]\tilde{\eta} + \epsilon\bar{\Delta} \tag{4.22c}$$

where $L_4 = [(1/k)I + J]^{-1}P^{-1}$ and $\bar{\Delta} = B\Delta$.

Next we recall the following Lemma.

Lemma 4.3, [104], [105]: A square matrix $A_m = [\tilde{a}_{ij}]$, where $\tilde{a}_{ij} \leq 0$ for $i \neq j$, is a nonsingular $\mathcal{M}$-matrix, if and only if one of the following equivalent conditions holds:

(i) There is a positive vector $\tilde{x} > 0$ such that $A_m\tilde{x} > 0$

(ii) There is a positive vector $\tilde{y} > 0$ such that $A_m^T\tilde{y} > 0$

(iii) All eigenvalues of A_m have positive real parts

(iv) A_m is nonsingular and A_m^{-1} is nonnegative

Since $\bar{L}_G$ is a grounded Laplacian matrix with eigenvalues having positive real parts as shown in the proof of Lemma 4.1. It follows that $\bar{L}_G$ is also a nonsingular $\mathcal{M}$-matrix as premultiplying L_G by a diagonal matrix does not change its structure of having outer diagonal nonpositive elements and nonnegative diagonal elements.

The following Theorem constructs a Lyapunov function candidate for the system (4.22c).

Theorem 4.2, [104] : Suppose Assumption 4.6 holds. Let

$$\tilde{x} = \mathrm{col}(\tilde{x}_1, \ldots, \tilde{x}_N) = \bar{L}_G^{-1}\mathbf{1},$$

$$\tilde{y} = \mathrm{col}(\tilde{y}_1, \ldots, \tilde{y}_N) = \bar{L}_G^{-T}\mathbf{1},$$

$$\tilde{P} = \mathrm{diag}(\tilde{p}_i) = \mathrm{diag}(\tilde{y}_i/\tilde{x}_i),$$

$$Q = \tilde{P}\bar{L}_G + \bar{L}_G^T\tilde{P}.$$

Then $\tilde{P} > 0$ and $Q > 0$.

Proof : Since $\bar{L}_G$ is a nonsingular $\mathcal{M}$-matrix, then by Lemma 4.3, $\bar{L}_G^{-1}$ and $\bar{L}_G^{-T}$ are nonnegative matrices with no zero rows. This implies $\tilde{x}, \tilde{y} > 0$ from which $\tilde{P} > 0$. From which we can conclude that Q has outer diagonal nonpositive elements and nonnegative diagnal elements, since $\tilde{P} = \mathrm{diag}(\tilde{p}_i) > 0$. Now

$$\begin{aligned} Q\tilde{x} &= \tilde{P}\bar{L}_G\tilde{x} + \bar{L}_G^T\tilde{P}\tilde{x} \\ &= \tilde{P}\mathbf{1} + \bar{L}_G^T\tilde{y} \\ &= \mathrm{col}(\tilde{p}_1, \ldots, \tilde{p}_N) + \mathbf{1} > 0 \end{aligned}$$

Therefore, from Lemma 4.3 we can conclude Q is a nonsingular $\mathcal{M}$-matrix having eigenvalues with positive real parts. Moreover, it is positive definite since $Q = Q^T$. ■

We construct the Lyapunov function candidate for the system (4.22c) as $V_{\tilde{\eta}} = \tilde{\eta}^T \tilde{P} \tilde{\eta}$.

Theorem 4.3 *Consider the system (4.6) with the output feedback controller (4.18) and the reduced-order high-gain observer (4.17). Let S be a compact set such that $S \subset \Omega$. Let $e(0) \in S$, and $\phi(0)$ be chosen as $\phi(0) = \gamma_1 L_G e_x(0) + (\gamma_2 + (p/\epsilon)) L_G e_v(0))$, then, there exists $\epsilon^* > 0$, such that for every $0 < \epsilon \leq \epsilon^*$, the trajectories of the closed-loop system are bounded for all $t \geq 0$, and there exists time $\tilde{T} > 0$ such that*

$$x - \mathbf{1} x_0 = O\left(\frac{1}{k}\right) + O(\epsilon), \ \forall\, t \geq \tilde{T} \tag{4.23a}$$

$$v - \mathbf{1} v_0 = O\left(\frac{1}{k}\right) + O(\epsilon), \ \forall\, t \geq \tilde{T} \tag{4.23b}$$

Moreover, the control signal $u(t)$ is bounded uniformly in k and ϵ.

Proof : The proof proceeds in three steps:

Step 1. We show that there exists positive constants κ_1 and ϵ_1 such that for $\epsilon_1 \leq \epsilon$ the set $\Upsilon = \{e^T W e \leq c\} \times \{\tilde{\eta}^T \tilde{P} \tilde{\eta} \leq \kappa_1 \epsilon^2\}$ is positively invariant.

Step 2. We show that for $\hat{\sigma}(0) = \gamma_1 L_G e_x(0) + \gamma_2 L_G e_v(0)$ and any $e(0)$ in the interior of $\{e^T W e \leq c\}$, there exists $\epsilon_2 > 0$, such that for $\epsilon \leq \epsilon_2$, the trajectory $(e(t), \tilde{\eta}(t))$ enters the set $\{e^T W e \leq c\} \times \{\tilde{\eta}^T \tilde{P} \tilde{\eta} \leq \kappa_1 \epsilon^2\}$ in finite time $T_1(\epsilon)$ with $\lim_{\epsilon \to 0} T_1(\epsilon) = 0$.

Step 3. We show that there exists ϵ_3 such that for $\epsilon \leq \epsilon_3$, (4.23) holds.

We show the first step by calculating the derivatives of $V_e = e^T W e$, and $V_{\tilde{\eta}} = \tilde{\eta}^T \tilde{P} \tilde{\eta}$ on the boundaries $\{V_e = c\}$, and $\{V_{\tilde{\eta}} = \kappa_1 \epsilon^2\}$, respectively. By taking the time derivative of $V_{\tilde{\eta}}$ along (4.22c) we have

$$\epsilon \dot{V}_{\tilde{\eta}} = -2p\tilde{\eta}^T \tilde{P} \tilde{\eta} - pk\tilde{\eta}^T Q \tilde{\eta} + 2\epsilon \tilde{\eta}^T \tilde{P} \bar{\Delta}$$

For all $(x_0(t), v_0(t)) \in \mathcal{W}$, $e(t) \in \Omega$ and bounded $\dot{w}$, we have $||\bar{\Delta}|| \leq l_1$, where l_1 is a positive constant independent of ϵ. From which we have,

$$\epsilon\dot{V}_{\tilde{\eta}} \leq -p[2\lambda_{\min}(\tilde{P}) + k\lambda_{\min}(Q)]||\tilde{\eta}||^2 + \epsilon l_2||\tilde{\eta}||$$

where $l_2 = 2l_1||\tilde{P}||$. Thus,

$$\epsilon\dot{V}_{\tilde{\eta}} \leq -\alpha||\tilde{\eta}||^2, \ \forall \ ||\tilde{\eta}|| \geq \epsilon l_3$$

where $\alpha = -(p/2)[2\lambda_{\min}(\tilde{P}) + k\lambda_{\min}(Q)]$ and $l_3 = l_2/\alpha$. Taking $\kappa_1 = l_3^2\lambda_{\max}(\tilde{P})$ ensures that

$$\epsilon\dot{V}_{\tilde{\eta}} \leq -\alpha||\tilde{\eta}||^2, \ \ \forall \ V_{\tilde{\eta}} \geq \kappa_1\epsilon^2$$

From which we can conclude that $\dot{V}_{\tilde{\eta}} \leq 0$ on the boundary $V_{\tilde{\eta}} = \kappa_1\epsilon^2$.

The derivative of $V_e = e^TWe$ satisfies

$$\dot{V}_e \leq -||e||^2 + \frac{l_4}{k}||e||^2 + \frac{l_5}{k}||e||(||f|| + ||w||) + \frac{l_6}{k}||e||(|f_0| + |u_0|) + l_7||e|| \cdot ||\tilde{\eta}||$$

for some positive constants l_4, l_5, l_6 and l_7. For all $(x_0(t), v_0(t)) \in \mathcal{W}$, $e(t) \in \Omega$, bounded $w(t)$, $\dot{w}(t)$ and $\tilde{\eta} \in \{V_{\tilde{\eta}} \leq \kappa_1\epsilon^2\}$, we have

$$\dot{V}_e \leq -||e||^2 + \frac{l_8}{k}||e||^2 + \frac{l_9}{k}||e|| + \epsilon l_{10}||e||$$

where l_8, l_9 and l_{10} are positive constants. For $k \geq \tilde{k}_1 = 2l_8$, we have

$$\dot{V}_e \leq -(1/2)||e||^2 + \frac{l_9}{k}||e|| + \epsilon l_{10}||e||$$

From which we have,

$$\dot{V}_e \le -(1/4)||e||^2, \ \ \forall \ ||e|| \ge 4(l_9/k + \epsilon l_{10})$$

Therefore, for all $k \ge \tilde{k}_2 > 0$ and $\epsilon \le \epsilon_1 > 0$, $\dot{V}_e$ is negative on the boundary $\{V_e = c\}$ and the set $\{e^T W e \le c\} \times \{\tilde{\eta}^T \tilde{P} \tilde{\eta} \le \kappa_1 \epsilon^2\}$ is positively invariant.

In the second step, because $e(0)$ lies in the interior of the set $\{e^T W e \le c\}$, and the right-hand-side function of (4.22a)-(4.22b) is bounded uniformly in ϵ, there exists a time $\tilde{T}_1 > 0$, such that $e(t) \in \{e^T W e \le c\}$ for all $t \in [0, \tilde{T}_1]$. During this time period, we have $\tilde{\eta}(0) \notin \{\tilde{\eta}^T \tilde{P} \tilde{\eta} \le \kappa_1 \epsilon^2\}$, it can be seen that

$$V_{\tilde{\eta}}(t) \le l_{11} e^{-l_{12} t/\epsilon} ||\tilde{\eta}(0)||^2$$

where $l_{11} = \lambda_{\max}(\tilde{P})$, $l_{12} = \alpha/(\lambda_{\max}(\tilde{P}))$. From the choice of initial condition of $\phi(0) = -\gamma_1 x_r(0) - \gamma_2 v_r(0) - (p/\epsilon) v_r(0)$, we have $\tilde{\eta}(0) = B\eta(0) = B[\sigma(0) - \hat{\sigma}(0)]$, which is given by

$$\tilde{\eta}(0) = -BL_G[f(0) + w(0) - \mathbf{1}(f_0(0) + u_0(0))] - \gamma_1 BL_G e_x(0) - \gamma_2 BL_G e_v(0)$$

For all $(x_0(t), v_0(t)) \in \mathcal{W}$, $e(t) \in \Omega$, bounded $w(t)$, we can conclude that $\tilde{\eta}(0) = O(1)$, and we have

$$V_{\tilde{\eta}}(t) \le l_{13} e^{-l_{12} t/\epsilon}$$

for some $l_{13} > 0$. The time taken by $\tilde{\eta}(t)$ to reach the set $\{\tilde{\eta} \tilde{P} \tilde{\eta} \le \kappa_1 \epsilon^2\}$ is given by $\tilde{T}_2 = (\epsilon/l_{12}) \ln \left(l_{13}/(\kappa_1 \epsilon^2) \right)$. By l'Hôpital's rule it can be shown that $\lim_{\epsilon \to 0} \tilde{T}_2(\epsilon) = 0$. Therefore, there exists $\epsilon_2 > 0$, such that for all $\epsilon \le \epsilon_2$, we can ensure $\tilde{T}_2(\epsilon) < (1/2)\tilde{T}_1$, which implies

$(e(t), \tilde{\eta}(t)) \in \{V_e \leq c\} \times \{V_{\tilde{\eta}} \leq \kappa_1 \epsilon^2\}$ for all $t \geq \tilde{T}_2(\epsilon)$. Therefore, by choosing $k^{**} = \max\{\tilde{k}_1, \tilde{k}_2\}$ and $\epsilon^* = \min\{\epsilon_1, \epsilon_2\}$, we conclude that all the trajectories of the closed-loop system are bounded for all $t \geq 0$ and there exists time $\tilde{T} > 0$, such that

$$x - \mathbf{1}x_0 = O\left(\frac{1}{k}\right) + O\left(\epsilon\right), \quad \text{and } v - \mathbf{1}v_0 = O\left(\frac{1}{k}\right) + O\left(\epsilon\right)$$

for all $t \geq \tilde{T}$.

Next we show that the control signal $u(t)$ is bounded uniformly in k. From (4.20), after time $t \geq \tilde{T}_2(\epsilon)$, the control signal is given by

$$u = B^{-1}\hat{L}_G[-\gamma_1 e_x - \gamma_2 e_v - f - w + \mathbf{1}(f_0 + u_0)] + O(\epsilon)$$

Therefore, following the same steps as in Theorem 4.1 it can be shown that $||u(t)||$ for all $t \geq \tilde{T}_2(\epsilon)$ is uniformly bounded in k. During the time period $t \in [0, \tilde{T}_2(\epsilon)]$ since $e(t) \in \{e^T W e \leq c\}$, $(x_0(t), v_0(t)) \in \mathcal{W}$, $w(t)$ is bounded, and $\dot{V}_{\tilde{\eta}} \leq -(\alpha/(\epsilon\lambda_{\max}(\tilde{P})))V_{\tilde{\eta}}$. Therefore, the norm of $\tilde{\eta}$ is given by

$$||\tilde{\eta}(t)|| \leq \sqrt{\frac{\lambda_{\max}(\tilde{P})}{\lambda_{\min}(\tilde{P})}}||\tilde{\eta}(0)||\exp\left(\frac{-\alpha t}{2\epsilon\lambda_{\max}(\tilde{P})}\right), \forall\ t \in [0, \tilde{T}_2(\epsilon)]$$

Since $\tilde{\eta}(0) = O(1)$, it implies $\tilde{\eta}(t)$ is bounded independent of ϵ for all $t \in [0, \tilde{T}_2(\epsilon)]$. As shown in Theorem 4.1 since $||\hat{L}_G||$ is uniformly bounded in k and $L_3 = O(1)$, it follows that $||u(t)||$ is uniformly bounded in k during the time period $t \in [0, \tilde{T}_2(\epsilon)]$. From which we conclude that the control signal $u(t)$ is uniformly bounded in k for all $t \geq 0$. ∎

Theorem 4.4 *Consider that Theorem 4.3 holds and let $\bar{e}(t)$ and $e(t)$ be the trajectories of the closed-loop systems (4.13) and (4.21), respectively with $\bar{e}(0) = e(0)$. Then, given any*

$\Xi > 0$, there exists $k^{***} > 0$, and for each $k \in [k^{***}, \infty)$, $\epsilon^{**} = \epsilon^{**}(k)$ exists such that for each $k \in [k^{***}, \infty)$ and $\epsilon \in (0, \epsilon^{**}(k)]$,

$$||e(t) - \bar{e}(t)|| \leq \Xi, \quad \forall\ t \geq 0 \tag{4.24}$$

Proof: The proof is done in three steps where we first show (4.24) during the time period $[\hat{T}_2, \infty)$, where $\hat{T}_2 > 0$ is some finite time followed by $[0, \hat{T}_1(\epsilon)]$ and then during $[\hat{T}_1(\epsilon), \hat{T}_2]$. From Theorem 4.3, given any $\Xi > 0$, there exists $k \geq \hat{k}_1 > 0$ and $\hat{\epsilon}_1 = \epsilon_1(k) > 0$ such that for each $k \in [\hat{k}_1, \infty)$ and $\epsilon \in (0, \hat{\epsilon}_1(k)]$

$$||e(t)|| \leq \Xi/2, \quad ||\bar{e}(t)|| \leq \Xi/2,\ \forall\ t \geq \hat{T}_2$$

Therefore, using $||e(t) - \bar{e}(t)|| \leq ||e(t)|| + ||\bar{e}(t)||$ it follows that

$$||e(t) - \bar{e}(t)|| \leq \Xi,\ \forall\ t \geq \hat{T}_2$$

Next we show (4.24) during the time period $[0, \hat{T}_1(\epsilon)]$. From Theorems 4.1 and 4.3, we know that $e(t) \in \Omega$ and $\bar{e}(t) \in \Omega$ during the time period $[0, \hat{T}_1(\epsilon)]$. Therefore, the right-hand-side of (4.13a)-(4.13b) and (4.21a)-(4.21b) is bounded by a constant independent of ϵ. By using $e(0) = \bar{e}(0)$ we have

$$||e(t) - \bar{e}(t)|| \leq 2b\hat{T}_1(\epsilon),$$

for all $t \in [0, \hat{T}_1(\epsilon)]$, where $\lim_{\epsilon \to 0} \hat{T}_1(\epsilon) = 0$ and b is a positive constant. Therefore, there exists

$k \geq \hat{k}_2 > 0$ and $\hat{\epsilon}_2 = \hat{\epsilon}_2(k) > 0$ such that for each $k \in [\hat{k}_2, \infty)$ and $\epsilon \in (0, \hat{\epsilon}_2(k)]$, we have

$$||e(t) - \bar{e}(t)|| \leq \Xi, \ \forall \ t \in [0, \hat{T}_1(\epsilon)]$$

Over the time interval $[\hat{T}_2(\epsilon), \hat{T}_2]$, equations (4.21a)-(4.21b) under output feedback is $O(\epsilon)$ perturbation from the corresponding model (4.13a)-(4.13b). Therefore, it follows from the continuous dependence of solutions of differential equation on initial conditions and parameters [91, Theorem 3.5] that

$$||e(t) - \bar{e}(t)|| \leq \Xi, \ \forall \ t \in [\hat{T}_2(\epsilon), \hat{T}_2]$$

Therefore, (4.24) follows by choosing $k^{***} = \max\{\hat{k}_1, \hat{k}_2\}$ and $\epsilon^{**} = \min\{\hat{\epsilon}_1, \hat{\epsilon}_2\}$. ∎

4.5 Examples

4.5.1 IEEE 300-Bus System

In this example we consider the synchronization problem on a network of oscillators on the IEEE-300 Bus system. Fig. 4.1 which is modified from [106] represents the network. The edge weights are taken to be 1 or 0 depending on whether an edge exists or not between two nodes. The leader node 0 is connected to node with highest degree which is node 268. The smallest eigenvalue of the grounded Laplacian is given by $\lambda_{\min}(L_G) = 0.0010$. Therefore, standard nonlinear control approaches will require a very high controller gain to achieve synchronization.

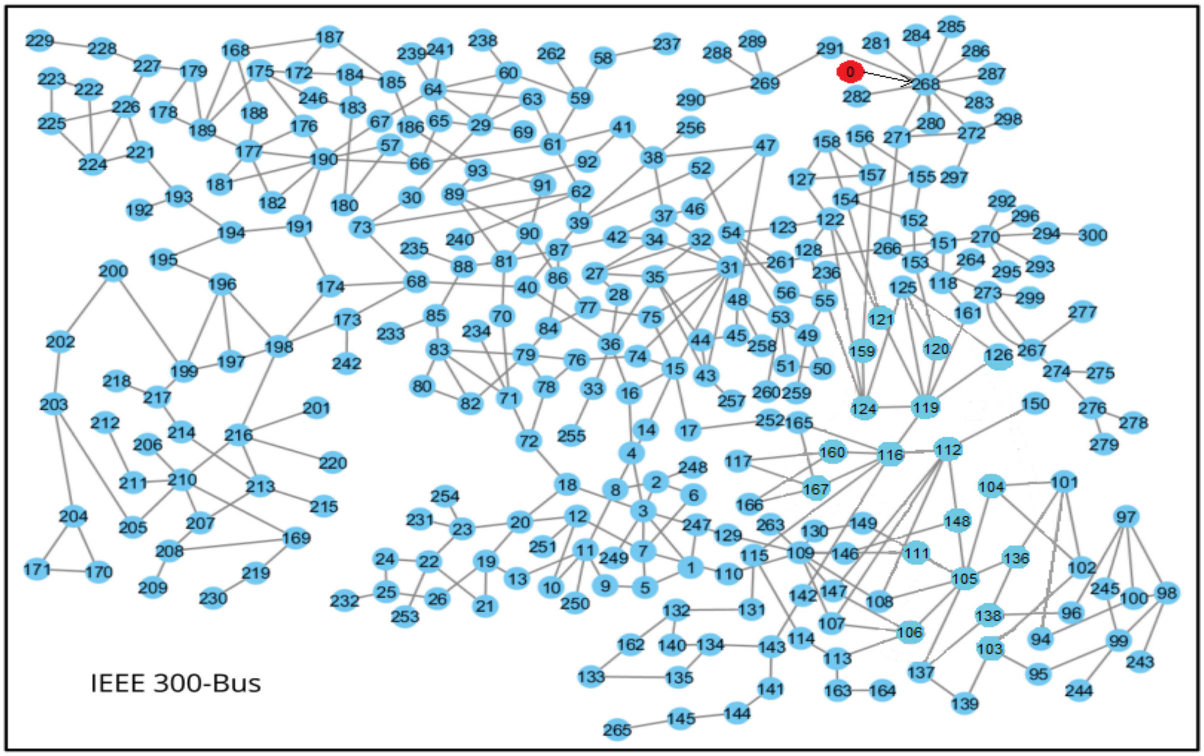

Figure 4.1: Diagram of node connections for the IEEE 300-Bus System

The oscillator dynamics is given by

$$\dot{x}_i = v_i \tag{4.25a}$$

$$\dot{v}_i = -x_i + g_i(1 - x_i^2)v_i + \tilde{g}_i u_i \tag{4.25b}$$

where g_i and $\tilde{g}_i$ are constants. The constants are chosen to lie in the range $g_i \in [-5.5, 16.5]$, $\tilde{g}_i \in [1, 3]$. The leader dynamics is given by

$$\dot{x}_0 = v_0, \quad \dot{v}_0 = -x_0 - x_0^2 v_0$$

The initial conditions of the leader are chosen as $x_0(0) = 2, v_0(0) = -2$ and the initial conditions of the other oscillators are chosen to lie in the range $x_i \in [-1, 1]$, $v_i \in [-1, 1]$.

The controller parameters are chosen as $\gamma_1 = 20$, $\gamma_2 = 20$, $k = 300$, $p = 1$, $\epsilon = 0.01$.

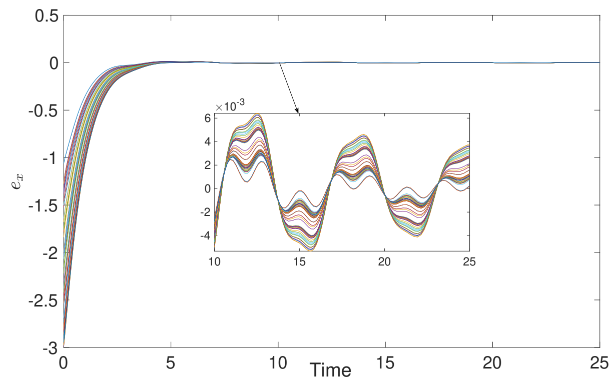

Figure 4.2: State one synchronization error $e_x = x - x_0$

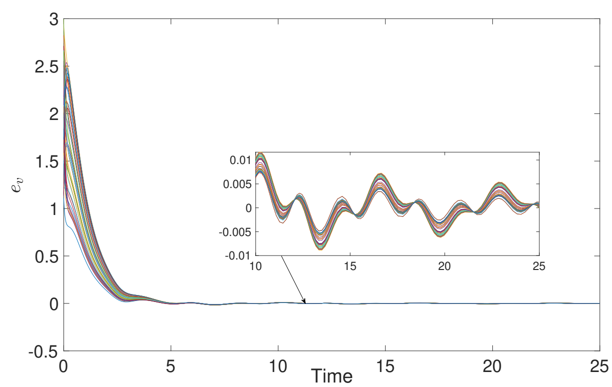

Figure 4.3: State two synchronization error $e_v = v - v_0$

Fig. 4.2 and Fig. 4.3 illustrate the synchronization error of the first state and second state for the first 50 oscillators. From the figures it can be seen that the steady-state synchronization error is very small.

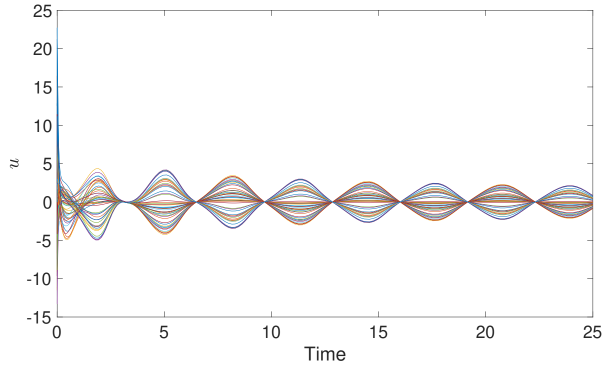

Figure 4.4: Control signal of the oscillators

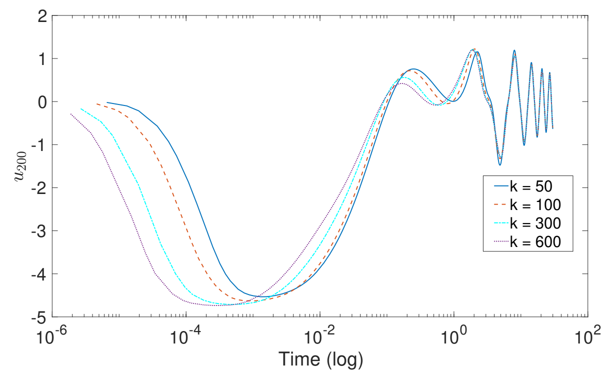

Figure 4.5: Log-Linear plot of the contol signal for different value of k

Fig. 4.4 represents the control signal of the first 50 oscillators. It can be seen from figure that the control signal is bounded independent of the value of k. In order to better illustrate the uniform boundedness of the control signal with respect to k, we use log-linear plot for the control signal of the 200th oscillator for different values of k. From Fig. 4.5 it can be seen that the control signal does not increase as the value of k increases.

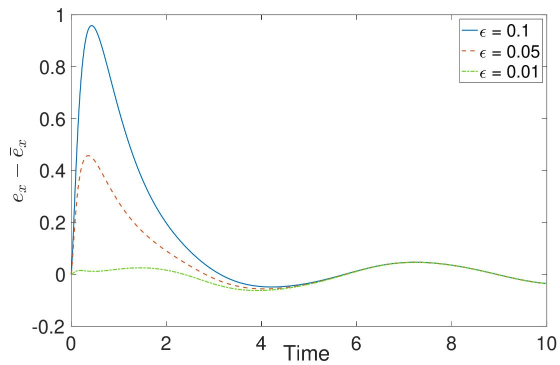

Figure 4.6: Performance recovery with $k = 300$

Finally, Fig. 4.6 shows the results of Theorem 4.4, where the trajectory e_x under the output feedback controller approaches the trajectory $\bar{e}_x$ under the controller with full information (4.7) as the value of ϵ decreases. The trajectories e_x and $\bar{e}_x$ are shown for the 100th oscillator.

4.5.2 Platooning of Vehicles

We consider a platoon of vehicles which are described by their longitudinal dynamics given by [102]:

$$\dot{\tilde{x}}_i = v_i \tag{4.26a}$$

$$m_i \dot{v}_i = -\tilde{a}_i v_i^2 - \tilde{b}_i m_i g \cos\theta - m_i g \sin\theta + d_i(t) + u_i \tag{4.26b}$$

where $\tilde{x}_i = x_i - x_i^{0d}$, x_i^{0d} denotes the desired distance of vehicle i from the leader, (x_i, v_i) denotes the position and velocity of the i^{th} vehicle, m_i denotes the mass of vehicle i, $\tilde{a}_i$ is the drag factor, $\tilde{b}_i$ is the rolling resistance coefficient, θ is the slope of the road, and $d_i(t) = a_m^i \sin(2\pi f_i t)$ denotes a time-varying disturbance acting on the vehicles, u_i is the control input. All the units are in SI system. We consider that the desired inter-vehicle distance between two adjacent vehicles is 50m and therefore x_i^{0d} is chosen as $x_i^{0d} = 50i$. The system parameters are chosen as $m_i \in [1545, 1550]$, $\tilde{a}_i \in [1, 2]$, $\tilde{b} = [0.01, 0.04]$, $\theta = 0.049$, $f_i \in [0.1, 0.9]$, $g = 9.8$ and $a_m^i \in [1, 6]$.

The leader decides the synchronizing velocity of the platoon of vehicles and its dynamics is given by

$$\dot{x}_0 = v_0, \quad \dot{v}_0 = 0$$

Note that although x_0 is unbounded, the Theorems of this chapter still apply because in system (4.26), x_i does not appear in the second equation. A more general class of second-order system will be treated in the next chapter. Moreove, we will provide a rigorous analysis of the closed-loop system.

The leader sends its information to the first vehicle. The initial condition of the leader is chosen as $x_0(0) = 0, v_0(0) = 25$. We assume that the followers start at the desired inter-vehicle distance and speed, which implies $\tilde{x}_i(0) = 0$ and $v_i(0) = 25$ for $i = 1, \ldots, 100$. The minimum eigenvalue of the grounded Laplacian is given by $\lambda_{\min}(L_G) = 0.002$. The controller parameters chosen are $\gamma_1 = 40$, $\gamma_2 = 40$, $k = 600$, $p = 1$, $\epsilon = 0.001$.

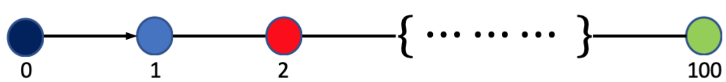

Figure 4.7: Line graph representing platoon of vehicles

Fig. 4.7 illustrates the network topology. In the figure node 0 is the leader, while nodes $1, \ldots, 100$ are the followers.

Fig. 4.8 shows the position error of vehicle ten ($\tilde{x}_{10}$), which is the difference between the position of vehicle ten and the desired distance of vehicle ten from the leader. As seen from the figure, the position error is small, and it approaches steady-state. Fig. 4.9 shows

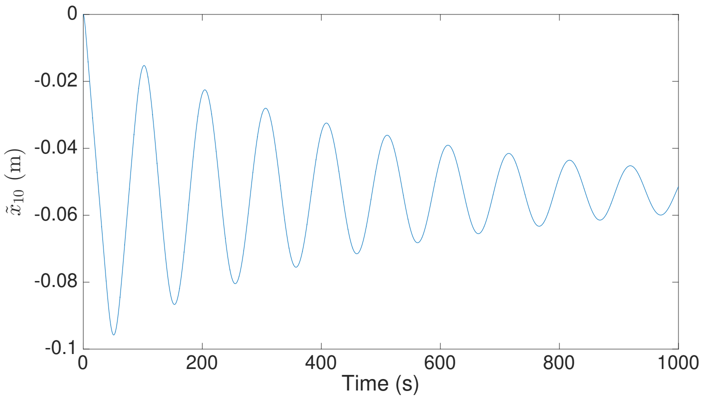

Figure 4.8: Position error of vehicle ten, $\tilde{x}_{10} = x_{10} - x_{10}^{0d}$

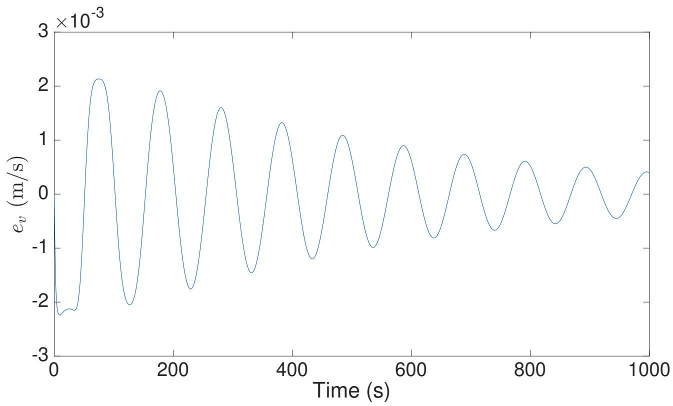

Figure 4.9: Velocity error of vehicle ten, $\tilde{e}_{v10} = v_{10} - v_0$

the velocity synchronization error of vehicle ten. It can be seen from the figure that the steady-state velocity synchronization error is small.

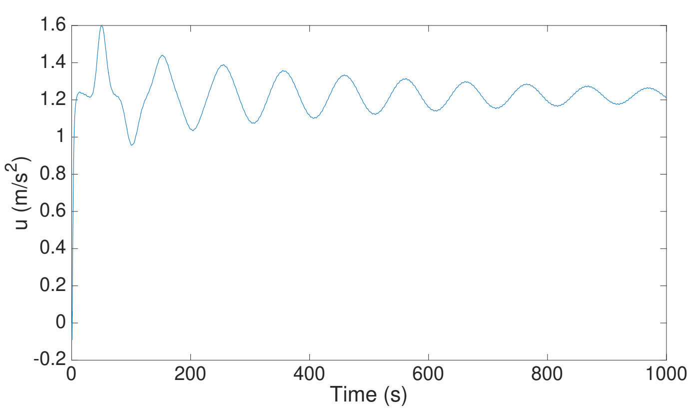

Figure 4.10: Control signal of vehicle ten

Fig. 4.10 shows the control signal of vehicle ten. The fluctuation in the control signal is because it compensates for the time-varying disturbance $d_i(t)$.

Remark 4.3: The string stability or network coherence [35] in a platoon of vehicles is also an important performance measure. In this chapter we do not study coherence in a platoon of vehicles. However, scalable coherence in a platoon of vehicles represented by second-order linear systems has been studied in [107]. It is shown the $\mathcal{H}_2$-norm from the disturbance input to the difference between the output of a vehicle to the average output of all the vehicles in the network is scalable with respect to the network size.

4.6 Conclusion

In this chapter, we proposed a distributed scalable controller for the practical synchronization of second-order nonlinear heterogeneous systems using high-gain observers. The synchronization error can be made arbitrarily small by tuning a controller and observer parameter, respectively. The tuning of these parameters does not affect the magnitude of the control signal as we show that it is uniformly bounded in these parameters. The system performance remains almost invariant as the smallest eigenvalue of the grounded Laplacian approaches zero, as the controller gain can be chosen sufficiently large without affecting the magnitude of the control signal. This is unlike the case for standard nonlinear controller approaches where the magnitude of the controller signal is inversely proportional to the smallest eigenvalue of the grounded Laplacian. We also showed the performance recovery property of the output feedback controller. In other words, the trajectories under output feedback can be made arbitrarily close to the trajectory under the controller using relative velocity derivative information by tuning the controller and observer parameters, respectively. The performance of the controller was shown for two large-scale nonlinear systems motivated by practical applications.

Chapter 5

Practical Synchronization in Networks of Nonlinear Heterogenous Agents under Reduced Information

5.1 Introduction

More recently, the research in multi-agent systems is geared towards the synchronization of agents with complex individual dynamics and reduced information exchange. In this chapter, we consider the practical state synchronization problem in a network of nonlinear heterogeneous agents exchanging only relative output information. The class of systems studied in the previous chapter is a special case of the one considered in this chapter. But unlike the previous chapter, we do not focus on scalable synchronization but instead on synchronization under reduced information exchange. The controller design approach used in this chapter is different from the previous one, and it also uses less information. An extended high-gain observer is a primary tool used in this chapter to achieve synchronization. The use of extended high-gain observers for attaining synchronization is challenging as it is not clear how to use it for the original problem formulation described in Isidori et al. [55]. Therefore, the first step before applying the tool requires the original problem to be transformed into the relative coordinates. In the relative coordinates, the synchronization problem is converted into a stabilization problem of N nonlinear systems. It is then that we use the extended high-gain observer based on the relative output exchange to estimate the uncertain terms, and then using feedback control, we cancel them. In other words, we compensate for the heterogeneous dynamics of each agent using extended high-gain observer and feedback control.

The proposed approach shapes the transient performance of the closed-loop system and guarantees a steady-state error that can be made arbitrarily small [108] by tuning the observer parameter. This is achieved by first designing the state feedback controller with full information to shape the transient response of the closed-loop system. The transient response under output feedback is shaped by the performance recovery property which is achieved by bringing the trajectories under output feedback arbitrarily close to the trajectories under state feedback for sufficiently small observer parameter.

5.2 Problem Formulation

We consider a network of N non-identical uncertain heterogeneous nonlinear agents having the same relative degree r, which exchange information through a communication graph $\mathcal{G}$. We assume that there is a leader which can communicate with a subset of the agents in the network. The objective is to synchronize the trajectories of the agents to the trajectory of the leader. The controller structure is decentralized in nature and therefore the local controller of each agent depends only on the relative information exchanged with its neighbors.

The dynamics of the agents are defined as

$$\dot{\eta}_i = f_i(\eta_i, \xi_i) \tag{5.1a}$$

$$\dot{\xi}_i = A\xi_i + B\left[b_i(\eta_i, \xi_i)u_i + \phi_i(t, \eta_i, \xi_i)\right] \tag{5.1b}$$

$$y_i = C\xi_i \tag{5.1c}$$

for $i = 1, \ldots, N$, where $\eta_i \in \mathbb{R}^{n_i - r}$ is the internal state, n_i denotes the dimension of each agent, r is the relative degree of the agent, $\xi_i \in \mathbb{R}^r$ is the external state and the matrices $A \in \mathbb{R}^{r\times r}$, $B \in \mathbb{R}^{r\times 1}$ and $C \in \mathbb{R}^{1\times r}$ are defined as

$$A = \begin{bmatrix} 0 & 1 & 0 & \ldots & 0 \\ 0 & 0 & 1 & \ldots & 0 \\ \vdots & \vdots & \ddots & \ddots & \vdots \\ 0 & 0 & \ldots & 0 & 1 \\ 0 & 0 & \ldots & \ldots & 0 \end{bmatrix}, \; B = \begin{bmatrix} 0 \\ 0 \\ \vdots \\ 0 \\ 1 \end{bmatrix},$$

$$C = \begin{bmatrix} 1 & 0 & \ldots & 0 & 0 \end{bmatrix}.$$

The agents are minimum-phase which implies that the origin of $\dot{\eta}_i = f_i(\eta_i, 0)$ is asymptotically stable.

Assumption 5.1: There exists continuously differentiable functions $V_i(\eta_i)$, class $\mathcal{K}$ functions Ψ_i, Γ_i and X_i such that

$$\Psi_i(||\eta_i||) \leq V_i(\eta_i) \leq \Gamma_i(||\eta_i||)$$

$$\frac{\partial V_i}{\partial \eta_i} f_i(\eta_i, \xi_i) \leq 0, \quad ||\eta_i|| \geq X_i(||\xi_i||)$$

for all $(\eta_i, \xi_i) \in S_i \subset \mathbb{R}^{n_i}$ where S_i is a domain that contains the origin.

Assumption 5.1 implies that the internal dynamics of the agents are regionally input-to-state stable.

Assumption 5.2: The functions b_i and ϕ_i are continuously differentiable with locally Lipschitz derivatives and the function f_i is locally Lipschitz.

Assumption 5.3: There exists $\tilde{b}_i$ such that

$$b_i(\eta_i, \xi_i) > \tilde{b}_i > 0, \quad \forall\ (\eta_i, \xi_i) \in S_i$$

The agents class defined in (5.1) covers a wide variety of practical systems used for engineering applications.

5.2.1 Leader

The agents are required ro synchronize to a desired trajectory. The desired trajectory can be generated by a leader or exosystem and, to reduce the information flow, it is assumed that only a subset of the agents receives information from the leader. The leader dynamics is defined as

$$\dot{\xi}_0 = A_0 \xi_0 + B\nu(t, \xi_0) \tag{5.2a}$$

$$y_0 = C\xi_0 \tag{5.2b}$$

where $\xi_0 \in \mathbb{R}^r$ and $y_0 \in \mathbb{R}$. In this problem we are interested in the synchronization between the external state of the agents ξ and the state of the leader ξ_0 and therefore the leader is not required to have internal dynamics. The leader (5.2) with the control input $\nu(t, \xi_0)$ covers both the class of linear and nonlinear dynamics. The control $\nu(t, \xi_0)$ is not required to be known to the agents in the network and is chosen such that the following assumption holds.

Assumption 5.4: The closed-loop trajectories of the leader $\xi_0(t)$ belongs to a known compact invariant set $W \subset \mathbb{R}^r$.

Remark 5.1: If the control $\nu(t, \xi_0) = 0$ or $\nu(t, \xi_0) = -\tilde{K}\xi_0$, then (5.2) corresponds to a leader with linear dynamics and then for Assumption 5.4 to hold the eigenvalues of A_0 or $(A_0 - B\tilde{K})$ should lie in the closed left-half complex plane with distinct eigenvalues on the imaginary axis.

We require the matrix A_0 defined in (5.2) to have the following structure

$$A_0 = A + \tilde{A} \tag{5.3}$$

where

$$\tilde{A} = \begin{bmatrix} 0 & 0 & \dots & \dots & 0 \\ 0 & 0 & \dots & \dots & 0 \\ \vdots & & & & \vdots \\ 0 & \dots & \dots & 0 & 0 \\ a_0 & \dots & \dots & a_{r_2} & a_{r-1} \end{bmatrix}_{r \times r}$$

We define the expanded graph as $\bar{\mathcal{G}} = (\bar{\mathcal{V}}, \bar{\mathcal{E}}, \bar{\mathcal{A}})$, where $\bar{\mathcal{V}} = \{v_0, v_1, v_2, \dots, v_N\}$, $\bar{\mathcal{E}} \subseteq \bar{\mathcal{V}} \times \bar{\mathcal{V}}$ and $\bar{\mathcal{A}}$ contains the weights of the edges from the leader to the other agents.

Assumption 5.5: There is a directed path from the leader to all the other nodes in the expanded graph $\bar{\mathcal{G}}$.

The above assumption is standard for achieving synchronization in a network of agents with a leader. We assume that the agents do not have access to their own state or output. The information available to the agents is a linear combination of its own output relative to its neighbors. The information structure is written as

$$\chi_i = \sum_{j=1}^{N} a_{ij}(y_j - y_i) + d_i(y_0 - y_i) \tag{5.4}$$

where $a_{ij} \geq 0$ are the edge coefficients of the communication graph $\mathcal{G}$, $d_i > 0$ if agent i receives information from the leader otherwise $d_i = 0$. The leader does not receive any information from the agents in the network. In applications like deep space [43] and underwater, it is difficult for the agent to measure its own output or state as GPS is not available, and it is more likely that the agent can measure relative information between itself and those of its neighbors. The physical meaning of the coefficients in the weighted sum could represent the scaling in measuring the relative outputs of the agents. For engineering applications like swarm robotics, installing sensors for each robot so that it can measure its own state or output may become costly. On the other hand, it is cheaper to install sensors in agents that can measure relative states or outputs for example in low-cost swarm robots like Kilobots [109]. The main goal is to find a distributed control law using only the relative information structure (5.4) such that synchronization between the external state of the agents ξ and the state of the leader ξ_0 is achieved which implies that

$$\lim_{t \to \infty} [\xi_i(t) - \xi_0(t)] = 0$$

for $i = 1, 2, \ldots, N$.

5.3 Relative Dynamics

In this section we define the relative dynamics among the agents in the network and hence transform system (5.1). We first define the relative states as

$$\rho^i = \sum_{j=1}^{N} a_{ij}(\xi_j - \xi_i) + d_i(\xi_0 - \xi_i) \tag{5.5}$$

$i = 1, 2, \ldots, N$. Defining $\rho = \mathrm{col}(\rho^1, \ldots, \rho^N)$, $\xi = \mathrm{col}(\xi_1, \ldots, \xi_N)$ we have

$$\rho = -(L_G \otimes I_r)\xi + (D \otimes I_r)(\mathbf{1} \otimes \xi_0)$$

where $L_G = L + D$, $D = \mathrm{diag}(d_1, \ldots, d_N)$, I_r represents an identity matrix of dimension $r \times r$ and $\mathbf{1}$ represents column of all ones. From Assumption 5.5 the matrix L_G is nonsingular. Using the Kronecker product properties we have

$$\rho = -(L_G \otimes I_r)\xi + (d \otimes \xi_0) \tag{5.6}$$

where $d = D\mathbf{1} = \mathrm{col}(d_1, \ldots, d_N)$. The ξ_i dynamics of all the agents in the network can be written in the following compact form

$$\dot{\xi} = (I_N \otimes A)\xi + (I_N \otimes B)\tilde{B}(\eta, \xi)u + (I_N \otimes B)\phi(t, \eta, \xi) \tag{5.7}$$

where $\eta = \mathrm{col}(\eta_1, \ldots, \eta_N)$, $\tilde{B}(\eta, \xi) = \mathrm{diag}(b_1(.), \ldots, b_N(.))$, $u = \mathrm{col}(u_1, \ldots, u_N)$ and $\phi = \mathrm{col}(\phi_1, \ldots, \phi_N)$. Taking the time derivative of (5.6) yields

$$\dot{\rho} = -(L_G \otimes I_r)\dot{\xi} + (d \otimes \dot{\xi}_0)$$

$$= \{L_G \otimes I_r\}\{(I_N \otimes A)\xi + (I_N \otimes B)\tilde{B}(\eta, \xi)u + \phi(t, \eta, \xi)\} + (d \otimes \dot{\xi}_0)$$

From (5.6) we have

$$\xi = (L_G \otimes I_r)^{-1}\{-\rho + (d \otimes \xi_0)\}$$

$$= (L_G^{-1} \otimes I_r)\{-\rho + (d \otimes \xi_0)\}$$

$$\dot{\rho} = (I_N \otimes A)\rho - (d \otimes A\xi_0) - (L_G \otimes B)\phi(t, \eta, \rho, \xi_0) - (L_G \otimes B)\tilde{B}(\eta, \rho, \xi_0)u$$
$$+ (d \otimes (A_0\xi_0 + B\nu(t, \xi_0)))$$

Using (5.3) we have

$$\dot{\rho} = (I_N \otimes A)\rho + (I_N \otimes B)\left[d\mathbf{1}^T\left(\tilde{A}\xi_0 + B\nu(t, \xi_0)\right)\right]$$
$$- (I_N \otimes B)\, L_G \left[\phi(t, \eta, \rho, \xi_0) + \tilde{B}(\eta, \rho, \xi_0)u\right] \quad (5.8)$$

Therefore, the system dynamics in the new coordinates becomes

$$\dot{\eta}_i = f_i(\eta_i, \delta_i(\rho, \xi_0)) \tag{5.9a}$$

$$\dot{\rho}^i = A\rho^i + B\left[-\left(\sum_{j=1}^{N} a_{ij} + d_i\right) b_i u_i + \Delta_u^i + \Delta_\phi^i + \Delta_0^i\right] \tag{5.9b}$$

$$\chi_i = C\rho^i \tag{5.9c}$$

where $\delta = \text{col}(\delta_1, \ldots, \delta_N) = \left\{L_G^{-1} \otimes I_r\right\}[(d \otimes \xi_0) - \rho]$, $\Delta_u^i = \sum_{j=1}^{N} a_{ij} b_j u_j$ represents the control inputs of the neighbors of the agent, $\Delta_\phi^i = \sum_{j=1}^{N} a_{ij}\phi_j - \left(\sum_{j=1}^{N} a_{ij} + d_i\right)\phi_i$ represents the uncertain heterogeneous nonlinearities of the agent and its neighbors and $\Delta_0^i = d_i \mathbf{1}^T \left(\tilde{A}\xi_0 + B\nu(t, \xi_0)\right)$ represents the leader states and control. The terms ϕ_i, and b_i are written without their arguments, their complete forms are $\phi_i = \phi_i(t, \eta_i, \delta_i(\rho, \xi_0))$, and $b_i = b_i(\eta_i, \delta_i(\rho, \xi_0))$.

From the definition of δ we have

$$\begin{aligned}
\delta &= \left(L_G^{-1} d \otimes \xi_0\right) - \left(L_G^{-1} \otimes I_r\right)\rho \\
&= \left(L_G^{-1} D\mathbf{1} \otimes \xi_0\right) - \left(L_G^{-1} \otimes I_r\right)\rho \\
&= \left(L_G^{-1} L_G \mathbf{1} \otimes \xi_0\right) - \left(L_G^{-1} \otimes I_r\right)\rho
\end{aligned}$$

where the term $D\mathbf{1}$ is written as $L_G\mathbf{1}$ since the Laplacian L satisfies the property $L\mathbf{1} = 0$. Therefore

$$\delta = \mathbf{1} \otimes \xi_0 - \left(L_G^{-1} \otimes I_r\right)\rho$$

Taking the norm we have

$$||\delta|| \leq \sqrt{N}||\xi_0|| + \kappa||\rho||$$

where $\kappa = ||L_G^{-1} \otimes I_r||$.

The internal dynamics (5.9a) in the new coordinates now satisfies

$$\frac{\partial V_i}{\partial \eta_i} f_i(\eta_i, \delta_i(\rho, \xi_0)) \leq 0, \quad ||\eta_i|| \geq X_i(\kappa||\rho|| + \sqrt{N}||\xi_0||)$$

for all $(\eta, \rho, \xi_0) \in S \times W$ where $S = S_1 \times S_2 \times \ldots S_N$. Therefore, the internal dynamics in the new coordinates still has the regionally input-to-state stable property.

5.4 Synchronization under full information

In this section we assume that each agent has full knowledge of the system states (η, ρ, ξ_0), leader control ν, functions Δ_u^i, Δ_ϕ^i and Δ_0^i. The system (5.8) can be treated as a multi-input multi-output system where the coefficient of the control is given by

$$G(\eta, \rho, \xi_0) = L_G \tilde{B}(\eta, \rho, \xi_0).$$

In order to make the representation compact we drop the argument of G. A centralized feedback linearizing controller is given by

$$u = G^{-1}\left\{-L_G\phi(t, \eta, \rho, \xi_0) + d\mathbf{1}^T\left(\tilde{A}\xi_0 + B\nu(t, \xi_0)\right)\right\} + G^{-1}(I_N \otimes K)\rho \qquad (5.10)$$

where K is designed such that the matrix $(A - BK)$ is Hurwitz.

Theorem 5.1: *Consider the closed-loop system formed of the system (5.9) with the controller*

(5.10). Suppose Assumptions 5.1-5.5 are satisfied. Then

$$\lim_{t\to\infty} [\xi_i(t) - \xi_0(t)] = 0, \quad \textit{for} \;\; i = 1, 2, \ldots, N. \tag{5.11}$$

Proof: In the new coordinates we need to solve the stabilization problem of N nonlinear systems represented by (5.9) in order to achieve state synchronization in the original coordinates. The closed loop system of the plant (5.9) with the controller (5.10) is given by

$$\dot{\rho} = \{I_N \otimes (A - BK)\}\, \rho \tag{5.12}$$

From (5.6) we have

$$\left(L_G^{-1} \otimes I_r\right) \rho = -\xi + \left(L_G^{-1} \otimes I_r\right) (D\mathbf{1} \otimes \xi_0)$$

which can be simpfied into

$$\left(L_G^{-1} \otimes I_r\right) \rho = -\xi + \mathbf{1} \otimes \xi_0$$

From (5.12) we have exponential stability of ρ which implies (5.11) using the above equation. Therefore, the stabilization of N nonlinear systems (5.9) results in

$$\lim_{t\to\infty} [\xi(t) - \mathbf{1} \otimes \xi_0(t)] = 0 \tag{5.13}$$

which implies that all the states of the agents synchronize to the state of the leader. ∎

We define a Lyapunov function as $V_\rho(\rho) = \rho^T (I_N \otimes P)\, \rho$ where $P = P^T > 0$ is the solution of the Lyapunov equation $P(A - BK) + (A - BK)^T P = -Q$ for some $Q = Q^T > 0$. Let

$c > 0$ be chosen such that $\{V_\rho(\rho) \leq c\} \subset S \times W$. Next we define the compact set

$$\Omega = \{V_1(\eta_1) \leq c_1\} \times \ldots \times \{V_N(\eta_N) \leq c_N\} \times \{V_\rho \leq c\}$$

where $c_i \geq \Gamma_i(X_i(\gamma(c)))$ such that the set $\{V_i(\eta_i) \leq c_i\}$ is compact and contained in S_i and $\gamma(c)$ is defined as

$$\gamma(c) = \max_{\rho \in \{V_\rho \leq c\}, \xi_0 \in W} (\kappa||\rho|| + \sqrt{N}||\xi_0||)$$

Since c_i should be chosen such that the set $\{V_i(\eta_i) \leq c_i\}$ is contained in S_i, this may put a restriction on the choice of c.

The compact set Ω is positively invariant with respect to the system

$$\dot{\eta}_i = f_i(\eta_i, \delta_i(\rho, \xi_0)), \quad \dot{\rho} = \{I_N \otimes (A - BK)\}\rho \tag{5.14}$$

for $i = 1, 2, \ldots, N$ because on the boundary $\{V_i = c_i\}$

$$\begin{aligned} \Gamma_i(||\eta_i||) \geq c_i \geq \Gamma_i(X_i(\gamma(c))) &\implies ||\eta_i|| \geq X_i(\gamma(c)) \\ &\implies ||\eta_i|| \geq X_i(\kappa||\rho|| + \sqrt{N}||\xi_0||) \implies \dot{V}_i \leq 0 \end{aligned}$$

and on the boundary $\{V_\rho = c\}$, $\dot{V}_\rho < 0$.

Remark 5.2: Under Assumptions 5.1-5.5, the synchronization achieved will be regional. However, if all the assumptions hold globally, i.e. $S_i = \mathbb{R}^{n_i}$ and $\dot{\eta}_i = f_i(\eta_i, \xi_i)$ is input-to-state stable, then the constants $c_1, \ldots, c_N$ and c, can be chosen arbitrarily large, and any compact set of $\mathbb{R}^{n_1 - r} \times \ldots \times \mathbb{R}^{n_N - r} \times \mathbb{R}^{Nr}$ can be put in the interior of $\Omega = \{V_1(\eta_1) \leq c_1\} \times \ldots \times \{V_N(\eta_N) \leq c_N\} \times \{V_\rho \leq c\}$. Then, the synchronization achieved for this case will be semi-global.

5.5 Synchronization under output feedback

The control design of the previous section is not realizable as the agents only have the knowledge of the relative outputs (5.4). The terms Δ_u^i, Δ_ϕ^i, Δ_0^i in (5.9b) are unknown and therefore are treated as disturbance inputs. In this section we use extended high-gain observers to estimate the unknown terms and cancel them using feedback control. The extended high-gain observer is built for each agent locally and then the local controllers are designed to stabilize the network of N nonlinear systems (5.9b) in order to achieve state synchronization.

We assume that we have no knowledge of the functions $\phi_i(t, \eta_i, \delta_i(\rho, \xi_0))$. Let g_i be positive constants, then the $\dot{\rho}_r^i$ equation can be written as

$$\dot{\rho}_r^i = \sigma^i - g_i u_i$$

where $\sigma^i = \Delta_\phi^i + \Delta_0^i + \Delta_G^i u$ and $\Delta_G^i = -[G_i - \hat{G}_i]$, where G_i and $\hat{G}_i$ are the ith rows of G and $\hat{G}$ respectively where $\hat{G}$ is defined as $\hat{G} = \mathrm{diag}(g_1, g_2, \ldots, g_N)$. Since we assume that an agent has no information about the control input of its neighbors, this constrains $\hat{G}$ to be diagonal matrix.

Defining $\sigma = \mathrm{col}(\sigma^1, \ldots, \sigma^N)$, we have

$$\sigma = -L_G \phi(t, \eta, \rho, \xi_0) + d\mathbf{1}^T \left(\tilde{A}\xi_0 + B\nu(t, \xi_0)\right) - \left[G - \hat{G}\right] u$$

We augment σ^i as an additional state to the chain of integrators (5.9b) for each agent, therefore a high-gain observer for the extended system of the agent is taken as

$$\dot{\hat{\rho}}_k^i = \hat{\rho}_{k+1}^i + \frac{\alpha_k}{\varepsilon^k}(\rho_1^i - \hat{\rho}_1^i), \qquad \text{for } 1 \leq k \leq r-1, \tag{5.15a}$$

$$\dot{\hat{\rho}}_r^i = \hat{\sigma}^i - g_i u_i + \frac{\alpha_r}{\varepsilon^r}(\rho_1^i - \hat{\rho}_1^i), \tag{5.15b}$$

$$\dot{\hat{\sigma}}^i = \frac{\alpha_{r+1}}{\varepsilon^{r+1}}(\rho_1^i - \hat{\rho}_1^i), \tag{5.15c}$$

for $i = 1, 2, \ldots, N$, where α_1 to α_{r+1} are chosen such that the roots of the polynomial

$$s^{r+1} + \alpha_1 s^r + \ldots + \alpha_{r+1} \tag{5.16}$$

are real and negative and $\varepsilon > 0$ is a small parameter. The output feedback control is chosen as

$$u_i = \left\{ \frac{\hat{\sigma}^i + K\hat{\rho}^i}{g_i} \right\} = \psi_i(\hat{\rho}^i, \hat{\sigma}^i). \tag{5.17}$$

A characteristic of using high-gain observers is the peaking phenomenon, which occurs when $\hat{\rho}^i(0) \neq \rho^i(0)$ and the estimates become $O(1/\varepsilon^{r-1})$ and when these estimates are used in feedback control they may destabilize the closed-loop system [90]. Denote the ith component of

$$G^{-1}\left\{-L_G\phi + d\mathbf{1}^T\left(\tilde{A}\xi_0 + B\nu\right) + (I_N \otimes K)\rho\right\}$$

by $T_i(\eta, \rho, \xi_0)$ and let

$$M_i > \max_{(\eta,\rho)\in\Omega, \xi_0 \in W} |T_i(\eta, \rho, \xi_0)| \tag{5.18}$$

The control is saturated outside the compact set $\Omega \times W$ in order to protect the system from the peaking effect of the observer. We saturate the expression of u_i (5.18) at $\pm M_i$ using the saturation function sat(.) which gives the output feedback controller

$$u_i = M_i \text{ sat}\left(\frac{\psi_i(\hat{\rho}^i, \hat{\sigma}^i)}{M_i}\right) \tag{5.19}$$

Theorem 5.2: *Consider the closed-loop system formed of the plant (5.9), the observer (5.15) and the controller (5.19) for i=1,2,...,N. Suppose that Assumptions 5.1-5.5 are satisfied,*

$$\max_{|e_i|\leq 1}\left\{\max_{(\eta,\rho)\in\Omega,\xi_0\in W}\left\|[G(\eta,\rho,\xi_0)-\hat{G}]E\hat{G}^{-1}\right\|\right\} < 1, \tag{5.20}$$

where $E = \text{diag}(e_1, \ldots, e_N)$*, the initial states of the observers* $(\hat{\rho}^i(0), \hat{\sigma}^i(0))$ *belong to a compact subset of* $\mathbb{R}^{r+1}$*, and the initial states of the plant* $(\eta_i(0), \rho^i(0))$ *belong to a compact set in the interior of* Ω *for* $i = 1, 2, \ldots, N$*. Then*

- *there exists* $\varepsilon_1^* > 0$ *such that for every* $0 < \varepsilon \leq \varepsilon_1^*$*, the trajectories of the closed-loop system are bounded for all* $t \geq 0$*;*
- *given any* $\mu > 0$*, there exists* $\varepsilon_2^* > 0$*, dependent on* μ*, such that for every* $0 < \varepsilon \leq \varepsilon_2^*$

$$||\rho(t) - \rho_{tr}(t)|| \leq \mu \quad \forall \quad t \geq 0, \tag{5.21}$$

  where ρ_{tr} *is the solution of the system (5.12) with* $\rho_{tr}(0) = \rho(0)$*;*

- *given any* $\mu > 0$*, there exist* $\varepsilon_3^* > 0$ *and* $T_1 > 0$*, both dependent on* μ*, such that for every* $0 < \varepsilon \leq \varepsilon_3^*$*,*

$$||\rho(t)|| \leq \mu, \quad \forall\ t \geq T_1 \tag{5.22}$$

Remark 5.3: The first bullet shows that for sufficiently small ϵ, the trajectories of the closed-loop system are bounded. The second bullet shows the performance recovery property of the output feedback controller, as the trajectories under output feedback $\rho(t)$ can be made arbitrarily close to the trajectories of the target system $\rho_{tr}(t)$, for sufficiently small ϵ. Finally, the third bullet shows that the output feedback controller achieves practical state synchronization, as the ultimate bound on $||\rho(t)||$, can be made arbitrarily small, by choosing ϵ small.

Remark 5.4: From the change of coordinates (5.6), we have

$$\xi - \mathbf{1} \otimes \xi_0 = -\left(L_G^{-1} \otimes I_r\right) \rho$$

Taking the norm on both sides we have

$$||\xi - \mathbf{1} \otimes \xi_0|| \leq \kappa ||\rho||$$

where κ is defined earlier in section 5.3. Therefore, if the desired synchronization error is required to be $\tilde{\mu}$, then by choosing $\mu \leq \tilde{\mu}/\kappa$, from the third bullet we have

$$||\xi - \mathbf{1} \otimes \xi_0|| \leq \tilde{\mu}, \quad \forall\, t \geq T_1$$

which implies we achieve practical state synchronization in the original coordinates.

Proof: We define the change of variables

$$\zeta_k^i = (\rho_k^i - \hat{\rho}_k^i)/\varepsilon^{r+1-k}, \text{ for } 1 \leq k \leq r, \tag{5.23a}$$

$$\zeta_{r+1}^i = \Delta_\phi^i + \Delta_0^i + \Delta_G^i \psi_s(\rho, \hat{\sigma}) - \hat{\sigma}^i \tag{5.23b}$$

where

$$\psi_s = \text{col}\left(M_1 g_\varepsilon\left(\frac{\psi_1(\rho^1, \hat{\sigma}^1)}{M_1}\right), \dots, M_N g_\varepsilon\left(\frac{\psi_N(\rho^N, \hat{\sigma}^N)}{M_N}\right)\right)$$

and g_ε is on odd function defined by

$$g_\varepsilon(y) = \begin{cases} y & \text{for } \ 0 \leq y < 1, \\ y + \dfrac{y-1}{\varepsilon} - \dfrac{0.5(y^2-1)}{\varepsilon} & \text{for } 1 \leq y \leq 1+\varepsilon, \\ 1 + 0.5\varepsilon & \text{for } y \geq 1+\varepsilon. \end{cases}$$

The function g_ε is nondecreasing, continuously differentiable with a locally Lipschitz derivative, bounded uniformly in ε for any bounded interval of ε and satisfies $|g_\varepsilon^{'}(y)| \leq 1$ and $|g_\varepsilon(y) - \text{sat}(y)| \leq \varepsilon/2$ for all $y \in \mathbb{R}$.

The observer error dynamics are

$$\varepsilon\dot{\zeta}_k^i = -\alpha_k\zeta_1^i + \zeta_{k+1}^i \quad \text{for } \ 1 \leq k \leq r-1 \tag{5.24a}$$

$$\varepsilon\dot{\zeta}_r^i = -\alpha_r\zeta_1^i + \zeta_{r+1}^i + \Upsilon^i(\eta, \rho, \hat{\rho}, \hat{\sigma}, \varepsilon) \tag{5.24b}$$

$$\varepsilon\dot{\zeta}_{r+1}^i = -\alpha_{r+1}\zeta_1^i + \alpha_{r+1}\Delta_G^i F\hat{G}^{-1}(I_N \otimes C)\zeta + \varepsilon\Pi^i \tag{5.24c}$$

where

$$\Upsilon^i = -\Delta_G^i \left[\psi_s(\rho, \hat{\sigma}) - \psi_{\text{sat}}(\hat{\rho}, \hat{\sigma})\right],$$

$$\Pi^i = \dot{\Delta}_\phi^i + \dot{\Delta}_0^i + \Delta_G^i F \psi_\rho^{'} + \dot{\Delta}_G^i \psi_s(\rho, \hat{\sigma}),$$

$$\psi_{\text{sat}} = \text{col}\left(M_1 \text{sat}\left(\frac{\psi_1(\hat{\rho}^1, \hat{\sigma}^1)}{M_1}\right), \ldots, M_N \text{sat}\left(\frac{\psi_N(\hat{\rho}^N, \hat{\sigma}^N)}{M_N}\right)\right),$$

$$F = \text{diag}(g_\epsilon^{'}(\psi_1(\cdot)), \ldots, g_\epsilon^{'}(\psi_N(\cdot))),$$

$$\psi_\rho^{'} = \text{col}\left(\frac{\partial \psi_1}{\partial \rho^1}\dot{\rho}^1, \ldots, \frac{\partial \psi_N}{\partial \rho^N}\dot{\rho}^N\right),$$

and $\zeta^i = \text{col}(\zeta_1^i, \ldots, \zeta_{r+1}^i)$ where $\zeta = \text{col}(\zeta^1, \ldots, \zeta^N)$.

From (5.24c), the term Π^i on the right hand side of $\varepsilon\dot{\zeta}_{r+1}^i$ is a continuous function of $(\eta, \rho, \zeta, \xi_0, \dot{\xi}_0, \nu, \dot{\nu}, \varepsilon)$. Since g_ε is continuously differentiable with locally Lipschitz derivatives and globally bounded using (5.23a) and from the definition of g_ε it can be shown that Υ^i/ε is a locally Lipschitz function [83].

The local observer error dynamics is given by

$$\varepsilon\dot{\zeta}^i = \Lambda\zeta^i + \alpha_{r+1}\bar{B}_1\Delta_G^i F \hat{G}^{-1}(I_N \otimes C)\zeta + \varepsilon\left[\bar{B}_1\Pi^i + \bar{B}_2\Upsilon^i/\varepsilon\right] \tag{5.25}$$

where

$$\Lambda = \begin{bmatrix} -\alpha_1 & 1 & 0 & \ldots & 0 \\ -\alpha_2 & 0 & 1 & \ldots & 0 \\ \vdots & \vdots & \ddots & \ddots & \vdots \\ -\alpha_r & 0 & \ldots & 0 & 1 \\ -\alpha_{r+1} & 0 & \ldots & \ldots & 0 \end{bmatrix}, \bar{B}_1 = \begin{bmatrix} 0 \\ B \end{bmatrix}, \bar{B}_2 = \begin{bmatrix} B \\ 0 \end{bmatrix}.$$

The observer error dynamics of the network is given by

$$\varepsilon\dot{\zeta} = (I_N \otimes \Lambda)\zeta - \alpha_{r+1}(I_N \otimes \bar{B}_1)\Delta_\zeta(I_N \otimes C)\zeta + \varepsilon\left[(I_N \otimes \bar{B}_2)\Upsilon + (I_N \otimes \bar{B}_1)\Pi\right] \quad (5.26)$$

where $\Pi = \mathrm{col}(\Pi^1, \ldots, \Pi^N)$, $\Upsilon = \mathrm{col}(\Upsilon^1, \ldots, \Upsilon^N)$ and can be expressed as

$$\begin{aligned}
\Upsilon &= \frac{1}{\varepsilon}\left[(G - \hat{G})\left(\psi_s(\rho, \hat{\sigma}) - \psi_{\mathrm{sat}}(\hat{\rho}, \hat{\sigma})\right)\right], \\
\Pi &= -(G - \hat{G})F\psi_\rho' + \dot{\Delta}_0 + \dot{\Delta}_\phi - (\dot{G} - \dot{\hat{G}})\psi_s(\rho, \hat{\sigma}), \\
\dot{\Delta}_0 &= \mathrm{col}(\dot{\Delta}_0^1, \ldots, \dot{\Delta}_0^N), \quad \dot{\Delta}_\phi = \mathrm{col}(\dot{\Delta}_\phi^1, \ldots, \dot{\Delta}_\phi^N) \ \text{ and} \\
\Delta_\zeta &= (G - \hat{G})F\hat{G}^{-1}.
\end{aligned}$$

The functions Υ, Π and Δ_ζ are locally Lipschitz in their arguments and bounded from above by $k_a + k_b||\zeta||$, where k_a and k_b are positive constants independent of ε. The matrix Λ is Hurwitz by design, the fast dynamics of the observer (5.26) is the same as seen in high-gain observer theory [84] except for the term $\alpha_{r+1}(I_N \otimes \bar{B}_1)\Delta_\zeta(I_N \otimes C)\zeta$. The system (5.26) without $O(\varepsilon)$ terms on the right hand side is given by

$$\varepsilon\dot{\zeta} = (I_N \otimes \Lambda)\zeta - \alpha_{r+1}(I_N \otimes \bar{B}_1)\Delta_\zeta(I_N \otimes C)\zeta. \quad (5.27)$$

Equation (5.27) can be represented by a negative feedback connection of the transfer function

$$\Theta(\varepsilon s) = \left(\frac{\alpha_{r+1}}{(\varepsilon s)^{r+1} + \alpha_1(\varepsilon s)^r + \ldots + \alpha_{r+1}}\right) I_N$$

and the time-varying gain Δ_ζ. Since we consider that the observer poles are real, we have

$||\Theta||_\infty = 1$. It can be shown that the origin of the system (5.27) is globally exponentially stable using (5.20) by applying the circle criterion [83].

The change of variables (5.23b) is well defined if

$$\frac{\partial \zeta_{r+1}}{d\hat{\sigma}} = -I_N + \Delta_\zeta$$

is nonsingular for $(\eta, \rho) \in \Omega$ and $\xi_0 \in W$, where $\zeta_{r+1} = \text{col}(\zeta_{r+1}^1, \ldots, \zeta_{r+1}^N)$, and $\hat{\sigma} = \text{col}(\hat{\sigma}^1, \ldots, \hat{\sigma}^N)$, which is the case because $\|\Delta_\zeta\| < 1$.

Applying a loop transformation to (5.27) and using the Kalman-Yakubovich-Poppov lemma [103, Lemma 5.3] we can obtain a quadratic Lyapunov function $W(\zeta) = \zeta^T (I_N \otimes Y)\zeta$ whose derivative with respect to (5.27) is bounded from above by $-(\lambda/\varepsilon)W(\zeta)$ for some positive constant λ, independent of ε. Using $W(\zeta)$ as a Lyapunov function candidate for (5.27), we can show that all the state variables are bounded. We show that for any $\tilde{c}_1 > 0$, the set $\Sigma = \Omega \times \{W(\zeta) \leq \tilde{c}_1 \varepsilon^2\}$ is positively invariant.

Since the initial conditions $(\eta(0), \rho(0))$ are defined in the interior of the set Ω and due to the global boundedness of the control u_i there exists a finite time $T^* > 0$ independent of ε such that the trajectories of the system (5.9) do not leave the compact set Ω for all $t \in [0, T^*]$. Initially the scaled estimation error $\zeta(0)$ could be outside the set $\{W(\zeta) \leq \tilde{c}_1 \varepsilon^2\}$. But from the time-derivative of $W(\zeta)$ it can be shown that $\zeta(t)$ enters the set $\{W \leq \epsilon^2 \tilde{c}_1\}$ in finite time $T(\epsilon)$, where $\lim\limits_{\epsilon \to 0} T(\epsilon) = 0$. By choosing ϵ small enough we can ensure that $T(\epsilon) < T^*$. While the system trajectory $(\eta, \rho, \zeta) \in \Sigma$, we have $\zeta_{r+1}(t) = O(\varepsilon)$ and $\rho(t) - \hat{\rho}(t) = O(\varepsilon)$. Therefore,

$$\psi(\hat{\rho}, \hat{\sigma}) = \psi(\rho, \hat{\sigma}) + O(\varepsilon)$$

$$\hat{\sigma} = -L_G \phi(t, \eta, \rho, \xi_0) + d\mathbf{1}^T (\tilde{A}\xi_0 + B\nu(t, \xi_0)) - (G - \hat{G})\psi_s(\rho, \hat{\sigma}) + O(\varepsilon)$$

Therefore, up to an $O(\varepsilon)$ error, the control $\psi(\rho, \hat{\sigma})$ satisfies

$$\psi(\rho, \hat{\sigma}) = \hat{G}^{-1}\{\hat{\sigma} + (I_N \otimes K)\rho\}$$

$$= \hat{G}^{-1}\{-L_G\phi(t, \eta, \rho, \xi_0) + d\mathbf{1}^T(\tilde{A}\xi_0 + B\nu(t, \xi_0)) - (G - \hat{G})\psi_s(\rho, \hat{\sigma}) + (I_N \otimes K)\rho\}$$

$$\psi + \hat{G}^{-1}(G - \hat{G})\psi_s(\rho, \hat{\sigma}) = \hat{G}^{-1}\{-L_G\phi(t, \eta, \rho, \xi_0) + d\mathbf{1}^T(\tilde{A}\xi_0 + B\nu(t, \xi_0)) + (I_N \otimes K)\rho\}$$

Next we define the map $\mathcal{F}\ : \mathbb{R}^N \to \mathbb{R}^N$ as

$$\mathcal{F}(s) = s + \hat{G}^{-1}(G - \hat{G})\psi_s(s)$$

The map $\mathcal{F}$ is proper which implies $|\mathcal{F}(s)| \to \infty$ as $|s| \to \infty$. This follows from the definition of ψ_s and from the fact that G is bounded. Using Hadamard's Theorem [110], if the Jacobian of $\mathcal{F}(s)$ is nonsingular in $\mathbb{R}^N$, then the map $\mathcal{F}$ is *one-to-one* and *onto* which implies that the map has globally defined inverse. The Jacobian of $\mathcal{F}(s)$ is defined as

$$\frac{\partial \mathcal{F}}{\partial s} = I_N + \hat{G}^{-1}(G - \hat{G}^{-1})F \tag{5.28}$$

Rearranging the terms we have

$$\frac{\partial \mathcal{F}}{\partial s} = \hat{G}^{-1}\left(I_N + (G - \hat{G}^{-1})F\hat{G}^{-1}\right)\hat{G} = \hat{G}^{-1}\left(I_N + \Delta_\zeta\right)\hat{G}$$

The Jacobian (5.28) is nonsingular because $\|\Delta_\zeta\| < 1$. Therefore, the mapping $\mathcal{F}$ is globally invertible and by direct substitution it can be seen that the unique solution is

$$\psi = G^{-1}\left\{-L_G\phi(t,\eta,\rho,\xi_0) + d\mathbf{1}^T\left(\tilde{A}\xi_0 + B\nu(t,\xi_0)\right)\right\} + G^{-1}(I_N \otimes K)\rho$$

Hence,

$$\psi(\hat{\rho},\hat{\sigma}) = G^{-1}\left\{-L_G\phi(t,\eta,\rho,\xi_0) + d\mathbf{1}^T\left(\tilde{A}\xi_0 + B\nu(t,\xi_0)\right)\right\} + G^{-1}(I_N \otimes K)\rho + O(\varepsilon).$$

The saturation levels M_i are chosen greater than T_i, and therefore for sufficiently small ε, $\psi(\hat{\rho},\hat{\sigma})$ will be in the linear region of the saturation function and therefore the closed-loop system is represented by

$$\dot{\eta}_i = f_i(\eta_i, \delta_i(\rho,\xi_0)) \quad \text{for} \quad 1 \le i \le N \tag{5.29a}$$

$$\dot{\rho} = \{I_N \otimes (A - BK)\}\rho + O(\varepsilon) \tag{5.29b}$$

$$\varepsilon\dot{\zeta} = (I_N \otimes \Lambda)\zeta - \alpha_{r+1}(I_N \otimes \bar{B}_1)\Delta_\zeta(I_N \otimes C)\zeta + O(\varepsilon) \tag{5.29c}$$

From the equations (5.29), it can be easily argued that the set $\Omega \times \{W(\zeta) \le \epsilon^2\tilde{c}_1\}$ is positively invariant for sufficiently small ϵ, which establishes boundedness of all state variables. Since $\rho(t)$ satisfies (5.29b) for $t \ge T(\varepsilon)$, $\dot{\rho}$, $\dot{\rho}_{tr}$ are bounded uniformly in ε and $\rho(0) = \rho_{tr}(0)$, therefore it follows that

$$\rho(t) - \rho_{tr}(t) = O(T(\varepsilon)), \quad \text{for} \quad 0 \le t \le T(\varepsilon) \tag{5.30}$$

Hence, $\rho(T(\varepsilon)) - \rho_{tr}(T(\varepsilon)) = O(T(\varepsilon))$. Using (5.30), (5.12), (5.29b), continuous dependence of the solutions of differential equations on initial conditions and parameters [91, Theorem

9.1], and exponential stability of $\dot{\rho} = \{I_N \otimes (A - BK)\}\rho$, we conclude that

$$\rho(t) - \rho_{tr}(t) = O(\varepsilon) + O(T(\varepsilon)), \quad \forall \;\; t \geq T(\varepsilon) \tag{5.31}$$

Therefore from (5.30) and (5.31) we conclude that

$$\rho(t) - \rho_{tr}(t) = O(\varepsilon) + O(T(\varepsilon)), \quad \forall \;\; t \geq 0 \tag{5.32}$$

and therefore given any $\mu > 0$ there exists $\epsilon_2^* > 0$ such that for all $\varepsilon \in (0, \epsilon_2^*]$ (5.21) is satisfied.

Because $\lim_{t\to\infty} \rho_{tr}(t) = 0$, given any $\mu > 0$ there is a finite time $T_1 > 0$ such that $||\rho_{tr}(t)|| \leq \mu/2$ for all $t \geq T_1$. From (5.30) there exists $\epsilon_3^* > 0$ such that for all $\varepsilon \in (0, \epsilon_3^*]$, $||\rho(t) - \rho_{tr}(t)|| \leq \mu/2$ for all $t \geq T_1$. Hence

$$||\rho(t)|| = ||\rho(t) - \rho_{tr}(t) + \rho_{tr}(t)|| \leq ||\rho(t) - \rho_{tr}(t)|| + ||\rho_{tr}(t)||$$

$$||\rho(t)|| \leq \mu \quad \forall \; t \geq T_1,$$

which proves (5.22). ■

We consider three special cases for which condition (5.20) holds. In all cases, we take $\hat{G} = g_m I$ with $g_m > 0$. Therefore,

$$\|(G - \hat{G})E\hat{G}^{-1}\| = \|(G - \hat{G})\hat{G}^{-1}E\| \leq \left\| I - \frac{1}{g_m} G \right\|$$

as $||E|| \leq 1$.

Case I: The graph $\mathcal{G}$ is undirected with control coefficients $b_i = 1$ for $i = 1, \ldots, N$. In this case $G = L_G$ is symmetric and positive definite. The condition (5.20) is satisfied by taking

$$g_m > \frac{1}{2}\lambda_{\max}(L_G)$$

Proof of Case I: In this case,

$$\left\| I - \frac{1}{g_m}G \right\| \leq \max_{1 \leq i \leq N} \left| 1 - \frac{\lambda_i(L_G)}{g_m} \right|$$

Choosing $g_m > \dfrac{\lambda_{\max}(L_G)}{2}$

$$\begin{aligned}
&\implies 0 < \frac{\lambda_i(L_G)}{g_m} < 2, \\
&\implies -1 < 1 - \frac{\lambda_i(L_G)}{g_m} < 1, \\
&\implies \left| 1 - \frac{\lambda_i(L_G)}{g_m} \right| < 1.
\end{aligned}$$

Therefore, we can conclude $\left\| I - \dfrac{1}{g_m}G \right\| < 1$.

Case II: $G = L_G$, where L_G is a normal matrix and the control coefficients $b_i = 1$ for $i = 1, \ldots, N$. We take

$$g_m > \max_{1 \leq i \leq N} \frac{\alpha_i^2 + \beta_i^2}{2\alpha_i}$$

where $\alpha_i + j\beta_i$, for $i = 1, \ldots, N$, are the eigenvalues of L_G. The set of graphs where the matrix L_G is normal includes undirected graphs but is more general as the eigenvalues can be complex [111], [112].

Proof of Case II: Since the matrix L_G is a normal matrix, it is unitarily diagonalizable

$$L_G = Z\tilde{\Lambda}Z^*$$

where Z is a unitary matrix and $\tilde{\Lambda} = \text{diag}(\tilde{\lambda}_1, \ldots, \tilde{\lambda}_N)$ is a diagonal matrix where the diagonal elements are the eigenvalues of L_G. Therefore

$$\left\| I_N - \frac{L_G}{g_m} \right\| = \left\| I_N - \frac{Z\tilde{\Lambda}Z^*}{g_m} \right\| = \left\| ZZ^* - \frac{Z\tilde{\Lambda}Z^*}{g_m} \right\|$$

$$\left\| Z \left(I_N - \frac{\tilde{\Lambda}}{g_m} \right) Z^* \right\| \leq ||Z|| \left\| I_N - \frac{\tilde{\Lambda}}{g_m} \right\| ||Z^*||$$

where $||Z|| = ||Z^*|| = 1$ and

$$\left\| I_N - \frac{\tilde{\Lambda}}{g_m} \right\| \leq \max_{1 \leq i \leq N} \sqrt{(1 - \alpha_i/g_m)^2 + (\beta_i/g_m)^2}$$

where α_i and β_i are the real and imaginary parts of the eigenvalues of L_G. The eigenvalues of the matrix L_G are in the open right half plane which implies that $\alpha_i > 0$. Therefore for $\left\| I - \frac{1}{g_m} G \right\| < 1$ to hold

$$\max_{1 \leq i \leq N} (1 - \alpha_i/g_m)^2 + (\beta_i/g_m)^2 < 1$$

and therefore g_m should satisfy

$$g_m > \max_{1 \leq i \leq N} \frac{\alpha_i^2 + \beta_i^2}{2\alpha_i}$$

Case III: $G(\eta, \xi)$ satisfies

$$G(\eta, \xi) + G^T(\eta, \xi) \geq \beta_1 I \quad \text{and} \quad ||G(\eta, \xi)|| \leq \beta_2$$

for some positive constants β_1 and β_2, for all $(\eta_i, \xi_i) \in S_i$, for $i = 1, \ldots, N$. The condition (5.20) is satisfied by taking $g_m > \beta_2^2/\beta_1$. A special case arises when $G(\eta, \xi)$ is symmetric and satisfies

$$0 < \tilde{g}_1 I \leq G(\eta, \xi) \leq \tilde{g}_2 I$$

Proof of Case III:

$$\begin{aligned}
\left\| I_N - \frac{1}{g_m} G \right\| &= \max_{||y||=1} \left\| \left[I_N - \frac{1}{g_m} G \right] y \right\| \\
&= \max_{||y||=1} \sqrt{y^T \left[I_N - \frac{1}{g_m} G \right]^T \left[I_N - \frac{1}{g_m} G \right] y} \\
&= \max_{||y||=1} \sqrt{y^T \left\{ I_N - \frac{1}{g_m} [G + G^T] + \frac{1}{g_m^2} G^T G \right\} y} \\
&\leq \max_{||y||=1} \sqrt{y^T y - \frac{\beta_1}{g_m} y^T y + \frac{\beta_2^2}{g_m^2} y^T y} \\
&= \max_{||y||=1} \sqrt{\left(1 - \frac{\beta_1}{g_m} + \frac{\beta_2^2}{g_m^2} \right) y^T y}
\end{aligned}$$

Choosing $g_m > \beta_2^2/\beta_1$, there is $0 < \tilde{k} < 1$ such that

$$\left(1 - \frac{\beta_1}{g_m} + \frac{\beta_2^2}{g_m^2} \right) \leq \tilde{k}$$

Hence

$$\left\| I_N - \frac{1}{g_m} G \right\| \leq \sqrt{\tilde{k}} < 1$$

5.6 Example

We illustrate our method by applying to an example that was treated in [55]. In [55] the network consisted of three subsystems where each subsystem comprised of an agent and an exosystem. Each exosystem exchanged information with neighboring exosystems and with the agent in its subsystem. We consider that there is only one exosystem in the network, which is connected to agent 1 and, instead of the exosystems, the agents exchange information with their neighbors. The agents are labeled as $1, 2, 3$, while the exosystem is labeled as 0. The communication topology is taken to be the same as in [55]. In this case the L and D matrix become

$$L = \begin{bmatrix} 1 & 0 & -1 \\ -1 & 1 & 0 \\ 0 & -1 & 1 \end{bmatrix}, \quad D = \begin{bmatrix} 1 & 0 & 0 \\ 0 & 0 & 0 \\ 0 & 0 & 0 \end{bmatrix}$$

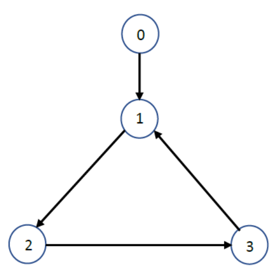

Figure 5.1: Network interconnection between the agents

Fig. 5.1 illustrates the connections between the leader and the agents. The exosystem is taken as the leader and its dynamics are defined as

$$\dot{\xi}_{01} = \xi_{02} \tag{5.33a}$$

$$\dot{\xi}_{02} = 2(1-\xi_{01}^2)\xi_{02} - \xi_{01} \tag{5.33b}$$

$$y_0 = \xi_{01} \tag{5.33c}$$

It can be seen that the leader is a Van der Pol oscillator and the compact set W consists of the limit cycle of the oscillator and its interior [103]. The set W is globally uniformly attractive with respect to the dynamics (5.33). The agent dynamics are defined as

$$\dot{\xi}_{i1} = \xi_{i2} \tag{5.34a}$$

$$\dot{\xi}_{i2} = \phi_i(\mu_i, \xi_i) + u_i, \quad 1 \leq i \leq 3 \tag{5.34b}$$

$$y_i = \xi_{i1} \tag{5.34c}$$

where $\phi_1 = -\mu_1\xi_{11}$, $\phi_2 = \mu_2(1-\xi_{21}^2)\xi_{22} - \xi_{21}$ and $\phi_3 = -\mu_3\xi_{31} + \xi_{31}^3$. The relative states are defined as

$$\rho_1 = (\xi_3 - \xi_1) + (\xi_0 - \xi_1),\ \rho_2 = (\xi_1 - \xi_2),\ \rho_3 = (\xi_2 - \xi_3) \tag{5.35}$$

Defining $\rho = \mathrm{col}(\rho_1, \rho_2, \rho_3)$ we have

$$\rho = -(L_G \otimes I_2)\xi + (d \otimes \xi_0) \tag{5.36}$$

where $\xi = \mathrm{col}(\xi_1, \xi_2, \xi_3)$ and $d = \mathrm{col}(d_1, d_2, d_3) = \mathrm{col}(1, 0, 0)$. Differentiating (5.36) we have

$$\dot{\rho} = (I_3 \otimes A)\rho + (I_3 \otimes B)\left[d\mathbf{1}^T B\nu(\xi_0) - G\phi(\xi) + Gu\right] \tag{5.37}$$

where $G = L_G$, $\phi = \mathrm{col}(\phi_1, \phi_2, \phi_3)$ and $\nu = 2(1 - \xi_{01}^2)\xi_{02} - \xi_{01}$. The local dynamics are defined as

$$\begin{aligned}
\dot{\rho}_i &= A\rho_i - B\left\{\left(\sum_{j=1}^{3} a_{ij} + d_i\right)u_i - \sum_{j=1}^{3} a_{ij}u_j - \left(\sum_{j=1}^{3} a_{ij} + d_i\right)\phi_i - \sum_{j=1}^{3} a_{ij}\phi_j\right\} \\
&\qquad + B(d_i\mathbf{1}^T B\nu(\xi_0)) \\
\chi_i &= C\rho_i
\end{aligned}$$

The extended high-gain observer is constructed as

$$\dot{\hat{\rho}}_{i1} = \hat{\rho}_{i2} + \frac{\alpha_1}{\varepsilon}(\rho_{i1} - \hat{\rho}_{i1}), \tag{5.38a}$$

$$\dot{\hat{\rho}}_{i2} = \hat{\sigma}_i - g_m u_i + \frac{\alpha_2}{\varepsilon^2}(\rho_{i1} - \hat{\rho}_{i1}), \tag{5.38b}$$

$$\dot{\hat{\sigma}}_i = \frac{\alpha_3}{\varepsilon^3}(\rho_{i1} - \hat{\rho}_{i1}). \tag{5.38c}$$

with $\alpha_1 = \alpha_2 = 3$ and $\alpha_3 = 1$, which assigns all three roots of the polynomial

$$s^3 + \alpha_1 s^2 + \alpha_2 s + \alpha_3 \tag{5.39}$$

at -1, and $\varepsilon > 0$ is a small parameter. The output feedback control is chosen as

$$u_i = M_i \mathrm{sat}\left(\frac{\hat{\sigma}_i + K\hat{\rho}_i}{g_m M_i}\right), \quad i = 1, 2, 3. \tag{5.40}$$

where $K = [18 \quad 9]$ and the estimates $(\hat{\rho}_i, \hat{\sigma}_i)$ are provided by extended high-gain observer and M_i is the saturation level of control. For simulation, the initial condition of the agents were chosen as $\xi_0 = (1,1)$, $\xi_1 = (2.4, 2.7)$, $\xi_2 = (2.6, 3.2)$, $\xi_3 = (3.2, 3.8)$ and saturation levels were chosen as $M_1 = \pm 35$, $M_2 = \pm 50$ and $M_3 = \pm 100$. The saturation levels were chosen from simulation of the closed-loop system under the state feedback controller to see the maximum value of the control signals. For this example the matrix $G = L + D$ satisfies case III with $\beta_1 = 0.43$ and $\beta_2 = 2.46$ so that $\beta_2^2/\beta_1 = 14.07$ and therefore g_m is chosen as $g_m = 15$.

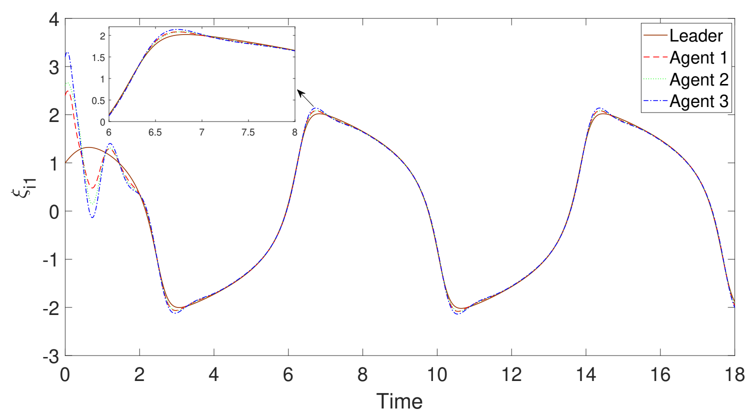

(a) $\xi_{i,1}$ for i=1,2,3.

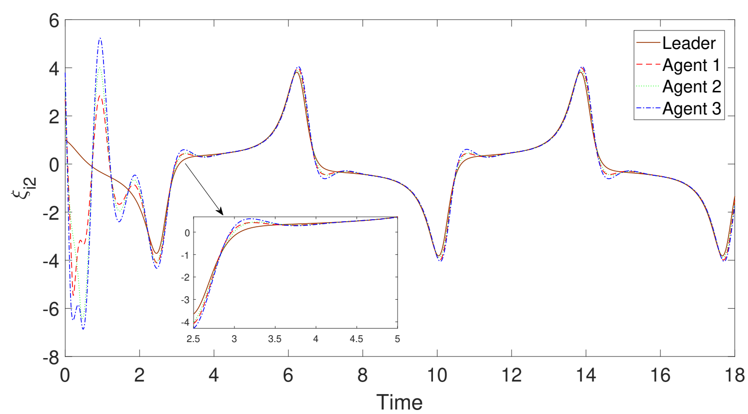

(b) $\xi_{i,2}$ for i=1,2,3.

Figure 5.2: States of the agents under the proposed controller with $\epsilon = 0.001$

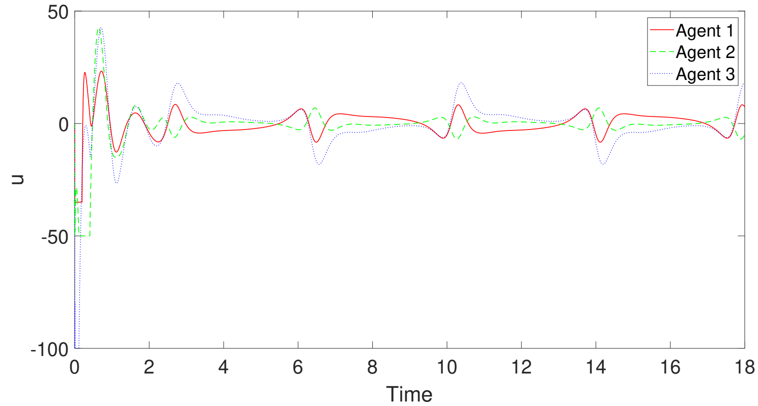

Figure 5.3: Control of the agents with $\epsilon = 0.001$

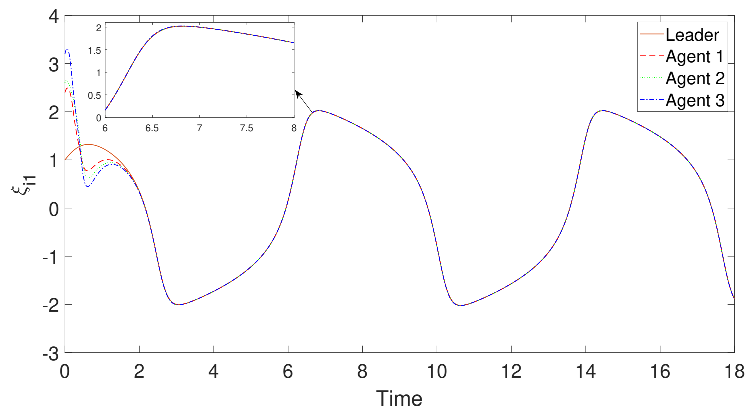

(a) $\xi_{i,1}$ for i=1,2,3.

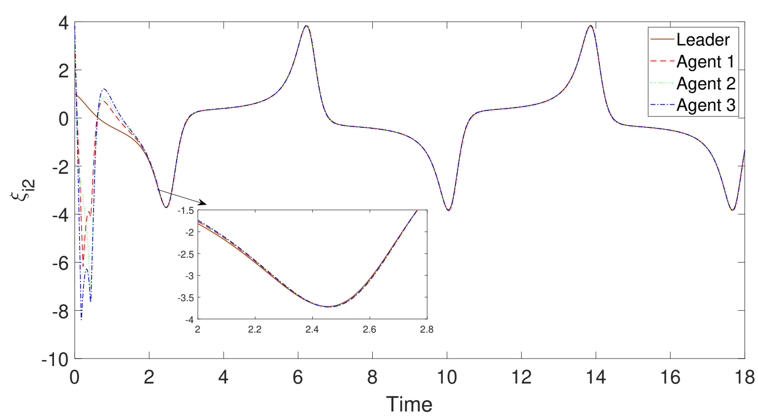

(b) $\xi_{i,2}$ for i=1,2,3.

Figure 5.4: States of the agents under the proposed controller with $\epsilon = 0.0001$

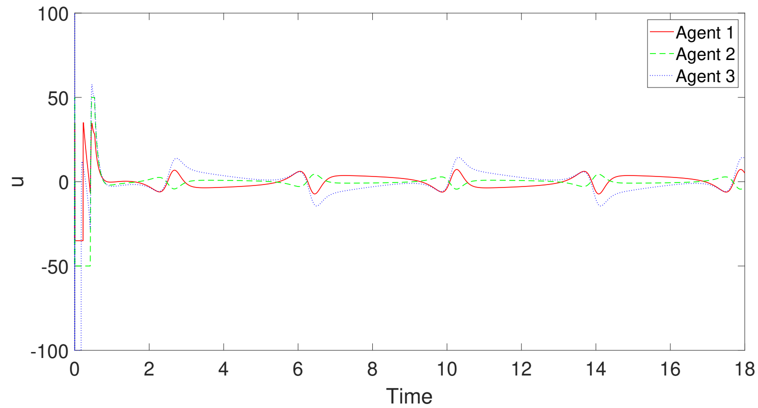

Figure 5.5: Control of the agents with $\epsilon = 0.0001$

Fig 5.2. and Fig. 5.4 show that after the transient period the states of the agents track the states of the exosystem and the synchronization error is small for sufficiently small value of ϵ. Fig 5.3. and Fig 5.5. show the control of the agents and it can be seen that the control saturates during the peaking period of the observer. As seen from Fig 5.2. and Fig 5.4. that as ϵ decreases the synchronization error also decreases.

5.7 Case with Some Unbounded Leader States

The designed state and output feedback controllers developed in section 5.4 and 5.5 deal with the case when the leader state is bounded. In applications like formation control of mobile robots [66] and frequency control of power systems [113] some of the leaders state need be unbounded. Therefore in this section we deal with a special case where the systems have relative degree two ($r = 2$) and the second-order equation of the leader has unbounded first component of the state. The systems take the form

$$\dot{\xi}_{i1} = \xi_{i2} \tag{5.41a}$$

$$\dot{\xi}_{i2} = \bar{b}_i(\xi_{i2})u_i + \bar{\phi}_i(\xi_{i2}) + h_i\left(\sum_{j=1}^{N} m_{ij}(\xi_i - \xi_j)\right) \tag{5.41b}$$

$$y_i = C\xi_i \tag{5.41c}$$

where $h_i : \mathbb{R}^2 \to \mathbb{R}$ is continuously differentiable and $m_{ij} = 0$ if there no coupling between agent i and j. The system (5.41) is a special case of (5.1) where there is no zero dynamics, $r = 2$, and the functions $\bar{b}_i$ and $\bar{\phi}_i$ depend only on the second component of ξ_i. On the other hand, (5.41) allows for a coupling term between the agents that depends only on the differences $\xi_i - \xi_j$. Examples of systems that appear in the form (5.41) are phase oscillators [114], power systems [72], [113] and double integrator models of mobile robots [66], [115]. The leader dynamics are defined as

$$\dot{\xi}_{01} = \xi_{02} \tag{5.42a}$$

$$\dot{\xi}_{02} = 0 \tag{5.42b}$$

which implies that ξ_{02} is bounded and ξ_{01} is unbounded. The information structure (5.4) can be rewritten as

$$\chi_i = \sum_{j=1}^{N} a_{ij}\{(\xi_{j1} - \xi_{01}) - (\xi_{i1} - \xi_{01})\} + d_i(\xi_{01} - \xi_{i1})$$

Next we define the relative states as

$$\vartheta^i = \sum_{j=1}^{N} a_{ij}(\tilde{\xi}_j - \tilde{\xi}_i) - d_i\tilde{\xi}_i \tag{5.43}$$

where $\tilde{\xi}_i = \mathrm{col}(\xi_{i1} - \xi_{01}, \xi_{i2} - \xi_{02})$ defines the synchronization error. Equation (5.43) in matrix form can be written as

$$\vartheta = -\{L_G \otimes I_2\}\tilde{\xi} \tag{5.44}$$

where $\tilde{\xi} = \mathrm{col}(\tilde{\xi}_1, \ldots, \tilde{\xi}_N)$, $\vartheta = \mathrm{col}(\vartheta^1, \ldots, \vartheta^N)$, I_2 represents an identity matrix of dimension 2. The synchronization error dynamics of the network is given by

$$\dot{\tilde{\xi}} = (I_N \otimes A)\tilde{\xi} + (I_N \otimes B)\left[\bar{B}(\tilde{\xi}, \xi_{02})u + \bar{\phi}(\tilde{\xi}, \xi_{02}) + H(\tilde{\xi})\right] \tag{5.45}$$

where $\bar{B} = \mathrm{diag}(\bar{b}_1(\tilde{\xi}_{12} + \xi_{02}), \ldots, \bar{b}_N(\tilde{\xi}_{N2} + \xi_{02}))$, $\bar{\phi} = \mathrm{col}(\bar{\phi}_1(\tilde{\xi}_{12} + \xi_{02}), \ldots, \bar{\phi}_N(\tilde{\xi}_{N2} + \xi_{02}))$ and $H = \mathrm{col}(h_1\left(\sum_{j=1}^{N} m_{1j}(\tilde{\xi}_1 - \tilde{\xi}_j)\right), \ldots, h_N\left(\sum_{j=1}^{N} m_{Nj}(\tilde{\xi}_N - \tilde{\xi}_j)\right))$.

The relative dynamics is given by

$$\dot{\vartheta} = (I_N \otimes A)\vartheta - (I_N \otimes B)[L_G\bar{B}(\vartheta, \xi_{02})u + L_G\bar{\phi}(\vartheta, \xi_{02}) + L_G H(\vartheta)] \tag{5.46a}$$

$$\chi = (I_N \otimes C)\vartheta \tag{5.46b}$$

where $\chi = \mathrm{col}(\chi_1, \ldots, \chi_N)$ and $\tilde{\xi} = -\left[L_G^{-1} \otimes\ I_2\right]\vartheta$. It can be seen that equation (5.46) does not depend on the unbounded state of the leader ξ_{01}. The control coefficient for system (5.46) is given by

$$\bar{G} = L_G\bar{B}(\vartheta, \xi_{02}).$$

5.7.1 State feedback Controller

The state feedback controller that achieves synchronization will be of the form

$$u = -\bar{G}^{-1} L_G \{\bar{\phi}(\vartheta, \xi_{02}) + H(\vartheta)\} + \bar{G}^{-1}(I_N \otimes K)\vartheta \tag{5.47}$$

Theorem 5.3: *Consider the closed-loop system formed of the system (5.46) with the controller (5.47). Then*

$$\lim_{t\to\infty} [\xi_{i1}(t) - \xi_{01}(t)] = 0, \quad \lim_{t\to\infty} [\xi_{i2}(t) - \xi_{02}(t)] = 0 \ \text{ for } \ i = 1, 2, \ldots, N. \tag{5.48}$$

Proof: The closed loop system is given by

$$\dot{\vartheta} = \{I_N \otimes (A - BK)\}\, \vartheta \tag{5.49}$$

which implies that ϑ exponentially converges to zero. And from (5.44) we can conclude that $\lim_{t\to\infty} \tilde{\xi}(t) = 0$ from which (5.48) follows. ■

We define a Lyapunov function as $V_\vartheta(\vartheta) = \vartheta^T (I_N \otimes P)\, \vartheta$. Let $a > 0$ be chosen such that $\Omega_a = \{V_\vartheta(\vartheta) \leq a\}$ is a compact positively invariant set with respect to the dynamical system (5.49).

5.7.2 Output feedback Controller

The $\dot{\vartheta}_2$ equation for (5.46) can be written as

$$\dot{\vartheta}_2 = \Xi - \hat{G}u$$

where $\vartheta_2 = \text{col}(\vartheta_2^1, \ldots, \vartheta_2^N)$, and $\Xi = \text{col}(\Xi_1, \ldots, \Xi_N)$ is defined as

$$\Xi = -L_G\bar{\phi}(\vartheta, \xi_{02}) - L_G H(\vartheta) - \left[\bar{G} - \hat{G}\right] u$$

The extended high-gain observer is given by

$$\dot{\hat{\vartheta}}_1^i = \hat{\vartheta}_2^i + \frac{\alpha_1}{\varepsilon}(\vartheta_1^i - \hat{\vartheta}_1^i) \tag{5.50a}$$

$$\dot{\hat{\vartheta}}_2^i = \hat{\Xi}^i - g_i u_i + \frac{\alpha_2}{\varepsilon^2}(\vartheta_1^i - \hat{\vartheta}_1^i) \tag{5.50b}$$

$$\dot{\hat{\Xi}}^i = \frac{\alpha_3}{\varepsilon^3}(\vartheta_1^i - \hat{\vartheta}_1^i) \tag{5.50c}$$

for $i = 1, 2, \ldots, N$, where α_1 to α_3 are chosen such that the roots of the polynomial

$$s^3 + \alpha_1 s^2 + \alpha_2 s + \alpha_3 \tag{5.51}$$

are real and negative and $\varepsilon > 0$ is a small parameter. The output feedback control is chosen as

$$u_i = \left\{ \frac{\hat{\Xi}^i + K\hat{\vartheta}^i}{g_i} \right\} \triangleq \bar{\psi}_i(\hat{\vartheta}^i, \hat{\Xi}^i). \tag{5.52}$$

The control is saturated outside the compact set $\Omega_a \times \Omega_s$ where Ω_s is the set of the synchronization trajectories ξ_{02}. Denote the ith component of

$$-\bar{G}^{-1}L_G\{\bar{\phi}(\vartheta, \xi_{02}) + H(\vartheta)\} + \bar{G}^{-1}(I_N \otimes K)\vartheta$$

by $\bar{T}_i(\vartheta, \xi_{02})$ and let

$$\bar{M}_i > \max_{\vartheta \in \Omega_a, \xi_{02} \in \Omega_s} \left|\bar{T}_i(\vartheta, \xi_{02})\right| \tag{5.53}$$

We saturate the expression of u_i (5.53) at $\pm\bar{M}_i$ using the saturation function sat(.), which gives the output feedback controller

$$u_i = \bar{M}_i \text{ sat}\left(\frac{\bar{\psi}_i(\hat{\vartheta}^i, \hat{\Xi}^i)}{\bar{M}_i}\right) \tag{5.54}$$

where the estimates $(\hat{\vartheta}^i, \hat{\Xi}^i)$ are provided by extended high-gain observers and $\bar{M}_i$ is the saturation level of control.

Theorem 5.4: *Consider the closed-loop system formed of the system (5.46), observer (5.50) and the controller (5.54). Suppose*

$$\max_{|r_i|\leq 1}\left\{\max_{\vartheta\in\Omega_a,\xi_{02}\in\Omega_s}\left\|[G(\vartheta,\xi_{02}) - \hat{G}]R\hat{G}^{-1}\right\|\right\} < 1, \tag{5.55}$$

where $R = \text{diag}(r_1, \ldots, r_N)$, *the initial states of the observers* $(\hat{\vartheta}_1^i(0), \hat{\vartheta}_2^i(0), \hat{\Xi}^i(0))$ *for i=1,2,...,N belong to a compact subset of* $\mathbb{R}^3$, *and the initial states of the plant* $\vartheta(0)$ *belong to a compact set in the interior of* Ω_a. *Then there exists* $\varepsilon^* > 0$ *such that for every* $0 < \varepsilon \leq \varepsilon^*$, *the trajectories of the closed-loop system are bounded for all* $t \geq 0$ *and there is* $\bar{T} > 0$ *such that*

$$|\xi_{i1}(t) - \xi_{01}(t)| = O(\epsilon) \quad \forall\ t \geq \bar{T} \tag{5.56a}$$

$$|\xi_{i2}(t) - \xi_{02}(t)| = O(\epsilon) \quad \forall\ t \geq \bar{T} \tag{5.56b}$$

for i=1,2,...,N.

Proof: We define the change of variables

$$\varphi_1^i = (\vartheta_1^i - \hat{\vartheta}_1^i)/\varepsilon^2, \tag{5.57a}$$

$$\varphi_2^i = (\vartheta_2^i - \hat{\vartheta}_2^i)/\varepsilon, \tag{5.57b}$$

$$\varphi_3^i = \Delta_d^i - (\bar{G}_i - \hat{G}_i)\bar{\psi}_s(\vartheta, \hat{\Xi}) - \hat{\Xi}^i \tag{5.57c}$$

where $\bar{G}_i$ and $\hat{G}_i$ are the ith rows of $\hat{G}$ and $\hat{G}$ respectively, Δ_d represents the nonlinear couplings of the agents neighbors,

$$\bar{\psi}_s = \mathrm{col}\left(\bar{M}_1 g_\varepsilon\left(\frac{\bar{\psi}_1(\vartheta^1, \hat{\Xi}^1)}{\bar{M}_1}\right), \ldots, \bar{M}_N g_\varepsilon\left(\frac{\bar{\psi}_N(\vartheta^N, \hat{\Xi}^N)}{\bar{M}_N}\right)\right)$$

Following similar steps as in the section 5.5 the observer error dynamics of the network are given by

$$\varepsilon\dot{\varphi} = (I_N \otimes \Lambda)\varphi - \alpha_3(I_N \otimes \bar{B}_1)\Delta_\varphi(I_N \otimes C)\varphi + \varepsilon\left[(I_N \otimes \bar{B}_2)\bar{\Upsilon} + (I_N \otimes \bar{B}_1)\bar{\Pi}\right] \tag{5.58}$$

$$\Lambda = \begin{bmatrix} -\alpha_1 & 1 & 0 \\ -\alpha_2 & 0 & 1 \\ -\alpha_3 & 0 & 0 \end{bmatrix}, \;\; \bar{\Upsilon} = \frac{1}{\varepsilon}\left[(\bar{G} - \hat{G})\left(\bar{\psi}_s(\vartheta, \hat{\Xi}) - \bar{\psi}_{\mathrm{sat}}(\hat{\vartheta}, \hat{\Xi})\right)\right]$$

$$\bar{\psi}_{\mathrm{sat}} = \mathrm{col}\left(\bar{M}_1 \mathrm{sat}\left(\frac{\bar{\psi}_1(\hat{\vartheta}^1, \hat{\Xi}^1)}{\bar{M}_1}\right), \ldots, \bar{M}_N \mathrm{sat}\left(\frac{\bar{\psi}_N(\hat{\vartheta}^N, \hat{\Xi}^N)}{\bar{M}_N}\right)\right),$$
$$\bar{\Pi} = \mathrm{col}(\bar{\Pi}^1, \ldots, \bar{\Pi}^N),\;\; \bar{\Pi}^i = \bar{\Pi}^i(\dot{\Delta}_d, \vartheta, \Xi),\;\; \Delta_\varphi = (\bar{G} - \hat{G})\bar{F}\hat{G}^{-1},$$

$$\bar{F} = \mathrm{diag}(g_\epsilon'(\bar{\psi}_1(\cdot)), \ldots, g_\epsilon'(\bar{\psi}_N(\cdot))),\; \varphi^i = \mathrm{col}(\varphi_1^i, \varphi_2^i, \varphi_3^i),\; \varphi = \mathrm{col}(\varphi^1, \ldots, \varphi^N).$$

Similarly, the system (5.58) without $O(\varepsilon)$ terms on the right hand side is given by

$$\varepsilon\dot{\varphi} = (I_N \otimes \Lambda)\varphi - \alpha_3(I_N \otimes \bar{B}_1)\Delta_\varphi(I_N \otimes C)\varphi. \tag{5.59}$$

Equation (5.59) can be represented by a negative feedback connection of the transfer function

$$\Theta(\varepsilon s) = \left(\frac{\alpha_3}{(\varepsilon s)^3 + \alpha_1(\varepsilon s)^2 + \alpha_2(\varepsilon s) + \alpha_3}\right) I_N$$

and the time-varying gain Δ_φ. Similar to the proof of Theorem 5.2, the origin of (5.59) is globally exponentially stable using (5.55) by applying the circle criterion [83].

Using the same steps as in the proof of Theorem 5.2 it can be shown that after a finite time $\bar{T} > 0$, the closed-loop system is given by

$$\dot{\vartheta} = \{I_N \otimes (A - BK)\}\vartheta + O(\varepsilon) \tag{5.60a}$$

$$\varepsilon\dot{\varphi} = (I_N \otimes \Lambda)\varphi - \alpha_3(I_N \otimes \bar{B}_1)\Delta_\varphi(I_N \otimes C)\varphi + O(\varepsilon) \tag{5.60b}$$

from which (5.56) follows. ■

Remark 5.5: Similar to Theorem 5.2, we can consider three special cases where inequality (5.55) is satisfied. The first two cases are exactly the same as the general case, since they depend on the communication topology which is considered the same for both the cases. The third case will be different as it depends on $\bar{G}(\nu, \xi_{02})$ and therefore the inequalities will be satisfied by constants different than the general case.

Remark 5.6: The performance recovery property can also be shown by following the same steps as in the last part of the proof of Theorem 5.2.

5.8 Frequency Control of Power Systems

We consider the frequency control of power systems when only relative phase measurement is available. Each synchronous generator is equipped with an encoder to measure the angular position of the rotor, which is the phase of the generator [116]. The generators can exchange their phase measurements with their neighbors. The frequency measurement is not available, which might be due to the lack of speed sensor. In [117], it is illustrated that the lack of a speed sensor reduces the system cost and can enhance the reliability of the generator. We consider a network of generators interconnected by transmission lines. The objective is to achieve frequency control where the frequencies of the buses synchronize to a reference frequency. For this system the per unit nonlinear swing equation is given by [65]

$$\tilde{m}_i \dot{\omega}_i + \tilde{d}_i \omega_i = -\sum_{j=1}^{N} k_{ij} \sin(\theta_i - \theta_j) + p_i^m + u_i \tag{5.61}$$

where θ_i is the phase angle of bus i, $\tilde{m}_i = 2H/\omega_s$, H is the inertia constant defined as $H = m_i \omega_s^2/(2S)$, S is the MVA rating of the generator, m_i and $\tilde{d}_i$ are the inertia and damping coefficients respectively, ω_s is the synchronizing frequency, ω is the frequency, p_i^m is the electrical power load at bus i and u_i is the mechanical input power. The coefficient k_{ij} is nonnegative and is given by $k_{ij} = |V_i||V_j|b_{ij}$ where $|V_i|$ is the absolute value of the voltage of bus i and b_{ij} is the susceptance of the line (i, j). Next we define a change in the time scale by $\tau = t/\tilde{m}_i$ from which we get the modified equation as

$$\frac{d\omega_i}{d\tau} = -\tilde{d}_i \omega_i - \sum_{j=1}^{N} k_{ij} \sin(\theta_i - \theta_j) + p_i^m + u_i \tag{5.62}$$

In state space form the swing equation is defined as

$$\dot{\theta}_i = \omega_i \tag{5.63a}$$

$$\dot{\omega}_i = -\tilde{d}_i\omega_i - \sum_{j=1}^{N} k_{ij}\sin(\theta_i - \theta_j) + p_i^m + u_i \tag{5.63b}$$

where $(\dot{\cdot})$ denotes the derivative w.r.t τ. The leader dynamics is defined as

$$\dot{\theta}_0 = \omega_0 \tag{5.64a}$$

$$\dot{\omega}_0 = 0 \tag{5.64b}$$

This definition implies that ω_0 is bounded and θ_0 is unbounded and therefore the problem formulation is the same as discussed in section 5.7. The information structure can be written as

$$\chi_i = \sum_{j=1}^{N} a_{ij}(\theta_j - \theta_i) + d_i(\theta_0 - \theta_i) \tag{5.65}$$

where $a_{ij} = \beta k_{ij}$, β is a positive constant, $d_i > 0$ if agent i receives information from the leader otherwise $d_i = 0$. The terms k_{ij} might be large and therefore they are scaled by β. The synchronization error dynamics of the network is given by

$$\begin{aligned}\dot{\xi} = (I_n \otimes A)\xi + (I_N \otimes B)\left[-\tilde{D}(I_N \otimes \bar{C})\xi - \tilde{D}(\mathbf{1} \otimes \bar{C}\xi_0)\right] \\ + (I_N \otimes B)\left[P_m + u - \mathcal{B}\Gamma_L \sin(\mathcal{B}^T(I_N \otimes C)\xi\right]\end{aligned} \tag{5.66}$$

where $\xi = \text{col}(\xi_1, \ldots, \xi_N)$, $\xi_i = \text{col}(\theta_i - \theta_0, \omega_i - \omega_0)$, $\bar{C} = [0 \quad 1]$, $\tilde{D} = \text{diag}(\tilde{d}_1, \ldots, \tilde{d}_N)$, $P_m = \text{col}(p_m^1, \ldots, p_m^N)$, $u = \text{col}(u_1, \ldots, u_N)$, Γ_L is a diagonal matrix whose diagonal elements represents the edges weights of the graph $\mathcal{G}$ and $\mathcal{B}$ is the graph incidence matrix [17] which is related to the Laplacian by $L = \mathcal{B}\Gamma_L\mathcal{B}^T$. The design of the output feedback controller can be done by following the same steps as in section 5.7 first by designing the extended high-gain observer (5.50) and then designing the control (5.54). The extended high-gain observer estimates the nonlinear couplings and disturbances and then by using feedback control compensates for them in the closed-loop system.

The exosystem (5.64) with the initial condition $\omega_0(0) = 100\pi$ will guarantee that the frequencies of the buses track the reference frequency of 50 Hz. The constants were chosen as $\beta = 1/(|V|^2)$ where $V_i = V$ for $i = 1, 2, \ldots, N$ and $D = \text{diag}(0, 0, 3, \ldots, 0)$, $d = \text{col}(0, 0, 3, \ldots, 0)$. The fact that $d_3 = 3$ implies that bus 3 receives information about the reference phase and frequency from the exosystem (5.64). The proposed controller is tested on the IEEE 30 bus test system [118]. The line admittances were extracted from [118] and the line voltages were assumed to be 11 kV for all buses. The mass and damping coefficients are given by $m_i = 10^5$ kgm^2, $\tilde{d}_i = 1\text{s}^{-1}$, $\omega_s = 100\pi$ rad/s, $S = 100$ MVA. For simulation the initial condition of the exosystem (5.64) was chosen as $(\theta_0, \omega_0) = (0, 100\pi)$ and the initial condition of the system (5.63) was chosen to be in the range $\theta_i \in [0, \pi]$, $\omega_i \in (290, 314.15)$ for $i = 1, 2, \ldots, N$ and the controller parameters were chosen as $K = [9 \;\; 6]$. The observer parameters were chosen as $\alpha_1 = 3$, $\alpha_2 = 3$, $\alpha_3 = 1$, $\epsilon = 0.0001$ and the saturation levels were taken as $M_i = 436$ for $i = 1, \ldots, 30$. The saturation levels were chosen from simulation of the closed-loop system under the state feedback controller to see the maximum value of the control signal. In power systems the graph is undirected because the generators are connected by physical links, which makes the coupling bidirectional. Since the graph is undirected it implies that the matrix G is symmetric and positive definite and therefore satisfies case I with $\frac{1}{2}\lambda_{\max}(L_G) = 52.4$. Therefore, g_m was chosen as $g_m = 54$. The power

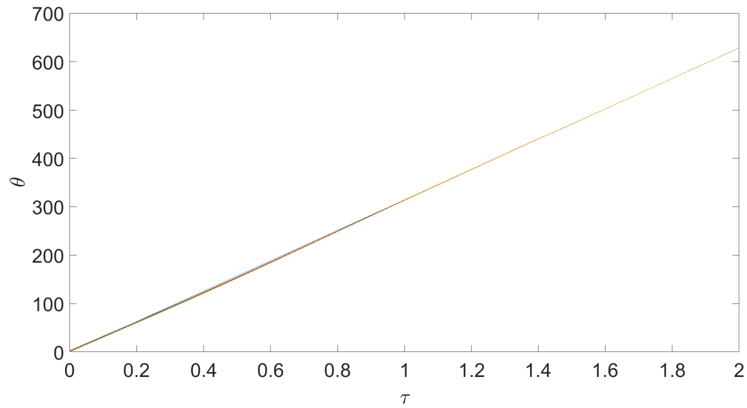

Figure 5.6: Phase of the buses

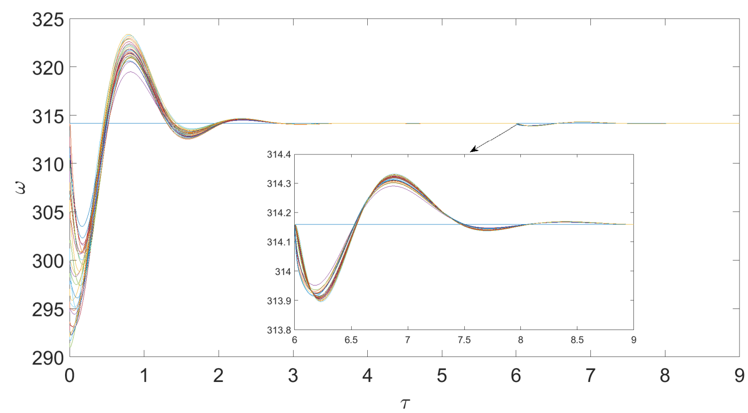

Figure 5.7: Frequency of the buses

system was initially not in the operational equilibrium and therefore as seen from Fig. 5.6 and Fig. 5.7 the phase and frequency synchronize to the trajectory of the exosystem (5.64). The power load at buses 2, 3 and 7 was increased by 30 per unit at $\tau = 6$, which results in the immediate desynchronization of the frequencies. After the desynchronization the phases and frequencies under the distributed controller again synchronize towards the phase and frequency of the exosystem (5.64). Fig. 5.8 shows the per unit control signal at each of the buses.

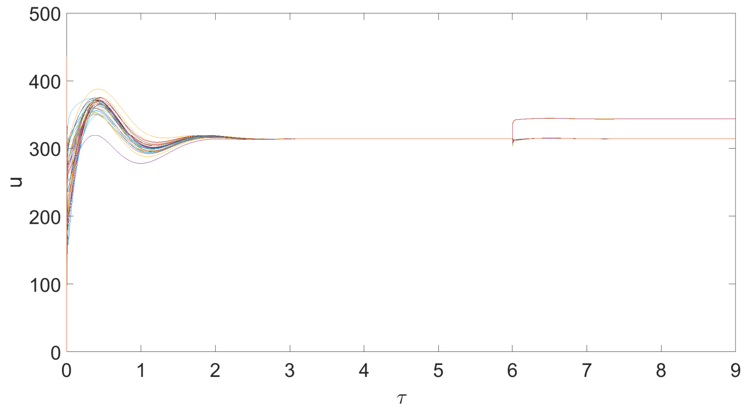

Figure 5.8: Control

5.9 Conclusion

In this chapter, we presented a new distributed control design for practical synchronization in a network of nonlinear heterogeneous agents. A state transformation was done to transform the system into relative dynamics where the agents are coupled. The problem then changes into a stabilization problem for the network of agents. Extended high-gain observers were used to estimate the nonlinear coupling terms and then cancel them by feedback control.

The proposed distributed controller requires only relative output measurement from its neighbors, which is a less restrictive information requirement from a practical standpoint. The efficacy of the controller was tested on the example from [55] and on the IEEE 30 bus system [118] for the frequency control of power systems.

Chapter 6

Power Systems Frequency Synchronization

6.1 Introduction

In this chapter, we study the frequency control of power systems when the frequency measurement is available. The main reason behind assuming the availability of the frequency measurement is that the controller designed in this chapter does not use feedback linearization to cancel the power system dynamics compared to the previous chapter. The designed controller compensates for the time-varying power demand and does not cancel the rich power system dynamics.

The existing approaches to achieve frequency synchronization assume the unknown power demand to be constant. However, increasing use of renewable energy sources causes the power demand to fluctuate at the same timescale as the power system dynamics and therefore approximating the power demand by a constant value becomes unrealistic [74]. In this chapter we design a dynamic consensus based extended high-gain observer algorithm [119] that achieves practical frequency synchronization in the presence of unknown time-varying power demand.

6.1.1 System Model

We consider a lossless, connected and network-reduced power system with N generators modeled by the following swing equation [65]

$$\dot{\theta} = \tilde{\omega} - \omega_{ref} \tag{6.1a}$$

$$M\dot{\tilde{\omega}} = -D(\tilde{\omega} - \omega_{ref}) - P(t) - \nabla U(\theta) + u \tag{6.1b}$$

where $\theta = \mathrm{col}(\theta_1, \dots, \theta_N)$ are the generator rotor angles, $\tilde{\omega} = \mathrm{col}(\tilde{\omega}_1, \dots, \tilde{\omega}_N)$ are the velocities of the generator rotors with respect to a fixed reference frame [65], ω_{ref} is the synchronous frequency which is typically 120π for a 60 Hz system, $M = \mathrm{diag}(m_1, \dots, m_N)$ represents the inertia matrix with $m_i > 0$, $D = \mathrm{diag}(d_1, \dots, d_N)$ represents the droop coefficient matrix with $d_i > 0$, $P(t) = \mathrm{col}(P_1(t), \dots, P_n(t))$ represents the time-varying vector of unknown power demand, $\nabla U(\theta) \in \mathbb{R}^N$ represents the power flow and $u = \mathrm{col}(u_1, \dots, u_N)$ is the control input. All quantities are normalized following the per unit representation of the power system models [65]. The time-varying power demand can be decomposed into

$$P(t) = \bar{P} + \tilde{P}(t) \tag{6.2}$$

where $\bar{P}$ and $\tilde{P}(t)$ represent the unknown constant and time-varying components of the power-demand.

The power system network can be viewed as an undirected graph $\mathcal{G} = (\mathcal{V}, \mathcal{E})$, where the nodes, $\mathcal{V}$, represent the number of generators and the edges, $\mathcal{E}$, represent the power transmission lines connecting the generators. We introduce the potential function given by

$$U(\theta) = -\frac{1}{2}\sum_{i,j=1}^{N} B_{ij}V_iV_j\cos(\theta_i - \theta_j)$$

where $B_{ij} = B_{ji} \geq 0$ is the susceptance of the line connecting generators i and j with constant terminal voltage magnitudes $V_i, V_j > 0$. The i^{th} component of the gradient of the potential function is

$$(\nabla U(\theta))_i = \sum_{j=1}^{N} B_{ij}V_iV_j\sin(\theta_i - \theta_j) \tag{6.3}$$

$\nabla U(\theta)$ satisfies a zero net power flow balance given by $\mathbf{1}^T\nabla U(\theta) = 0$. The terms $U(\theta)$ and $\nabla U(\theta)$ can be compactly written as

$$U(\theta) = -\mathbf{1}^T\Gamma\mathbf{cos}(\mathcal{B}^T\theta), \quad \nabla U(\theta) = \mathcal{B}\Gamma\mathbf{sin}(\mathcal{B}^T\theta)$$

where $\mathcal{B} \in \mathbb{R}^{N\times m}$ is the incidence matrix of the power system network, with N generators and m transmission lines, $\mathbf{cos}(\cdot) = \mathrm{col}(\cos(\cdot), \ldots, \cos(\cdot))$, $\mathbf{sin}(\cdot) = \mathrm{col}(\sin(\cdot), \ldots, \sin(\cdot))$, $\Gamma \in \mathbb{R}^{m\times m}$ is a diagonal matrix which encodes the susceptance B_k of the power lines and the voltage amplitudes V_i, V_j at each edge as $[\Gamma]_{kk} = B_kV_iV_j$, for each edge $k = (i, j) \in \mathcal{E}$ and $B_k = B_{ij}$.

For ease of analysis we apply a change of coordinates as $\omega = \tilde{\omega} - \omega_{ref}$, which represents the frequency deviation and $\delta = \Pi\theta = \left(I - \frac{1}{N}\mathbf{1}\mathbf{1}^T\right)\theta$, which is inspired by the center-of-inertia coordinates, see [68], [65]. From which we have $\mathcal{B}^T\delta = \mathcal{B}^T\Pi\theta = \mathcal{B}^T\theta - \frac{1}{N}\mathcal{B}^T\mathbf{1}\mathbf{1}^T\theta = \mathcal{B}^T\theta$, since $\mathcal{B}^T\mathbf{1} = 0$. By a slight abuse of notation we refer to the potential function of δ by the same symbol U. Therefore, the system in the new coordinate becomes

$$\dot{\delta} = \Pi\omega \tag{6.4a}$$

$$M\dot{\omega} = -D\omega - P(t) - \nabla U(\delta) + u \tag{6.4b}$$

where $\nabla U(\delta) = \mathcal{B}\Gamma\mathbf{sin}(\mathcal{B}^T\delta)$.

6.2 Control Objective

The control objective is to achieve frequency synchronization, i.e., to regulate the frequency deviation ω to zero while achieving proportional power sharing among the generators. We characterize the steady-state solution (δ^*, ω^*) of (6.4), with steady-state control $u(t) = u^*(t)$, where ω^* is a constant that belongs to $\ker(\Pi)$, which implies that ω^* is a constant vector with all the elements being the same. The constant steady-state solution satisfies

$$0 = \Pi\omega^* \tag{6.5a}$$

$$0 = -D\omega^* - P(t) - \nabla U(\delta^*) + u^*(t) \tag{6.5b}$$

Lemma 6.1, [74] : *If there exists $(\delta^*, \omega^*) \in Im\ \Pi \times \mathbb{R}^N$, such that (6.5) holds, then $\omega^* = \omega_s\mathbf{1}$, with*

$$\omega_s = \frac{\mathbf{1}^T(u^*(t) - P(t))}{\mathbf{1}^T D\mathbf{1}} \tag{6.6}$$

Remark 6.1: From, equation (6.5), we can observe that the left-hand-side is constant while the right-hand-side contains a time-varying quantity $P(t)$. This equation can only be satisfied when $P(t)$ satisfies a certain condition which will be defined later in this section.

From equation (6.6), it is clear that in order to regulate the frequency deviation ω to zero, there are infinitely many choices for $u^*(t)$ to satisfy $\mathbf{1}^T(u^*(t) - P(t)) = 0$. This also implies that the controller u^* is time-varying. Therefore, we split the control into constant and time-varying parts as

$$u^*(t) = \bar{u}^* + \tilde{u}^*(t)$$

where $\bar{u}^*$ and $\tilde{u}^*(t)$ should satisfy $\mathbf{1}^T(\bar{u}^* - \bar{P}) = 0$ and $\mathbf{1}^T(\tilde{u}^*(t) - \tilde{P}(t)) = 0$. This freedom in the choice of $\bar{u}^*$ leads to the design of controllers that are optimal with respect to a certain cost function. The controllers are designed based on the concept of optimal power dispatch given a constant power demand, where the cost is dependent only on the amount of power produced at each generator. A solution to the optimal dispatch problem is given by [74]

$$\bar{u}^*_{opt} = Q^{-1}\frac{\mathbf{1}\mathbf{1}^T\bar{P}}{\mathbf{1}^TQ^{-1}\mathbf{1}} \tag{6.7}$$

where $Q = \text{diag}(Q_1, \ldots, Q_n)$ is the marginal cost matrix. From (6.7), it is clear that the power generated at each node i, is inversely proportional to its marginal cost Q_i and optimal steady-state controller is chosen as $\bar{u}^* = \bar{u}^*_{opt}$. However, in order to achieve frequency synchronization, we need to satisfy $\mathbf{1}^T(u^*(t) - P(t)) = 0$, and therefore $u^*(t)$ is

$$u^*(t) = Q^{-1}\frac{\mathbf{1}\mathbf{1}^TP(t)}{\mathbf{1}^TQ^{-1}\mathbf{1}} = \bar{u}^* + \tilde{u}^*(t) \tag{6.8}$$

where $\tilde{u}^*(t) = Q^{-1}\dfrac{\mathbf{1}\mathbf{1}^T\tilde{P}(t)}{\mathbf{1}^TQ^{-1}\mathbf{1}}$, represents the time-varying part of the steady-state controller. Equation (6.5b) can now be satisfied with $u^*(t) = \bar{u}^* + \tilde{u}^*(t)$ and $\omega^* = 0$, from which

$$\mathcal{B}\Gamma\mathbf{sin}(\mathcal{B}^T\delta^*) = \left(Q^{-1}\frac{\mathbf{1}\mathbf{1}^T}{\mathbf{1}^TQ^{-1}\mathbf{1}} - I\right)P(t) \tag{6.9}$$

From, equation (6.9), we can observe that left-hand-side is constant while the right-hand-side contains a time-varying quantity $\tilde{P}(t)$; therefore we require $\tilde{P}(t)$ to belong to $\ker\left(Q^{-1}\dfrac{\mathbf{1}\mathbf{1}^T}{\mathbf{1}^T Q^{-1}\mathbf{1}} - I\right)$.

It is shown in [74], that $\mathcal{R}(Q^{-1}\mathbf{1})$ is included in $\ker\left(Q^{-1}\dfrac{\mathbf{1}\mathbf{1}^T}{\mathbf{1}^T Q^{-1}\mathbf{1}} - I\right)$. Therefore, we make the following assumption.

Assumption 6.1, [74], [76]: The time-varying part of the power demand satisfies

$$\tilde{P}(t) = Q^{-1}\mathbf{1}\tilde{p}(t) \tag{6.10}$$

where $\tilde{p}(t)$ is some bounded unknown time-varying function with bounded derivative. Assumption 6.1 guarantees the existence of the steady-state solution (6.5), despite the presence of the time-varying quantity $P(t)$. From Assumption 6.1, equation (6.9) is simplified as

$$\mathcal{B}\Gamma\mathbf{sin}(\mathcal{B}^T\delta^*) = \left(Q^{-1}\frac{\mathbf{1}\mathbf{1}^T}{\mathbf{1}^T Q^{-1}\mathbf{1}} - I\right)\bar{P} \tag{6.11}$$

Next we make a feasibility assumption.

Assumption 6.2, [74]: *For a given constant $\bar{P}$, there exists $\delta^* \in Im\ \Pi$, such that equation (6.11) has a solution.*

Assumptions 6.1 and 6.2 guarantees the existence of a constant steady-state solution (6.5), despite the presence of the time-varying quantity $P(t)$.

Assumption 6.3, [68] : The synchronous solution (6.5) is such that $\mathcal{B}^T\delta^* \in \Theta := \left(-\frac{\pi}{2} + \rho, \frac{\pi}{2} - \rho\right)^m$, for a constant $\rho \in \left(0, \frac{\pi}{2}\right)$.

The assumption on δ^*, is standard in stability analysis of power systems [68], and is usually called the security constraint [71].

Remark 6.2: Assumptions 6.1, 6.2 and 6.3 are made in order to guarantee the existence of the synchronous solution (6.5). These assumptions are standard in the power systems literature [68], [73], [74], [76].

6.3 Controller Design Under known Time-Varying Power Demand

6.3.1 Communication Topology

We will proceed with a two-step approach for the design of the controller, where in the first step, the controller will be designed assuming that the power demand is known. In the second step, we will use observers to remove the requirement of knowing the power demand. In this section we discuss the first step.

Assumption 6.4: *There exists a balanced, directed, strongly connected communication topology to allow the exchange of information among the controllers.*

The communication graph is represented by $\tilde{\mathcal{G}} = (\mathcal{V}, \tilde{\mathcal{E}}, \tilde{\mathcal{A}})$ and the graph Laplacian is denoted by L. In general, the communication graph can be different from the graph represented by the power transmission lines i.e., $(\tilde{\mathcal{E}}, \tilde{\mathcal{A}})$ can be different from $(\mathcal{E}, \mathcal{A})$. The generators are coupled physically through the graph $\mathcal{G}$, which evolve in a slow time-scale, while the dynamic controllers exchange information through the graph $\tilde{\mathcal{G}}$ and evolve in a fast time-scale.

6.3.2 Dynamic Average Consensus

To achieve a steady-state controller of the form (6.8), a natural intuitive idea is that if each controller knows its local power demand P_i, then it can communicate its local P_i to its neighbors. Such a strategy would require an all-to-all communication graph so that each controller can calculate the sum of the total power demand. However, such design would be quite restrictive because an all-to-all communication topology (complete graph) is a costly communication requirement. In this section, for the design of the controller, we will assume that each generator has knowledge about its own power demand. Next, to alleviate the requirement of a complete graph, we will apply ideas from dynamic average consensus [120].

The dynamic average consensus algorithm states that if each node i has access to a time-varying reference signal $r_i(t)$, then using a distributed consensus algorithm it is possible that each node is able to track the average of the reference signals given by $\sum_{j=1}^{N} r_i(t)/N$. The dynamic average consensus algorithm is given by [120]:

$$\dot{z}_i = -\sum_{j=1}^{N} a_{ij}(z_i(t) - z_j(t)) + \dot{r}_i(t), \quad \forall\ i \in \{1, \ldots, N\} \tag{6.12}$$

with the initial condition $z_i(0) = r_i(0)$. In order to obviate the requirement of the derivative of the reference signal, we do a change of coordinates [120], $z_i = r_i(t) - p_i$, from which we get

$$\dot{p}_i = \sum_{j=1}^{N} a_{ij}(z_i(t) - z_j(t)), \quad p_i(0) = 0 \tag{6.13}$$

The applications and a tutorial of the dynamic average consensus algorithm can be found in [120]. We choose the reference signal $r_i(t)$ at each generator to be σ_i, which is given by

$$\sigma_i = -(\nabla U(\delta))_i - P_i(t), \quad \forall\ i = 1, \ldots, N.$$

or in vector form $\sigma = -\nabla U(\delta)) - P(t)$. For the controller design we consider that each generator has access to the signal σ_i. The signal σ_i is treated as the known time-varying reference signal as in the case of the dynamic consensus algorithm.

The distributed dynamic average consensus algorithm is given by

$$\mu\dot{p} = -Lp + L\sigma = Ly \tag{6.14}$$

where μ is a small positive consant, $p \in \mathbb{R}^N$ is the state of the dynamic consensus algorithm and $y = \sigma - p$.

Remark 6.3 : In the literature the dynamic consensus algorithm is not coupled with any other dynamics. In the current problem it will be coupled with the power system dynamics as the controller will depend on the state p. Therefore, we require p to be faster than the power system dynamics and we achieve it by introducing the parameter μ.

6.3.3 Analysis of the Closed-loop System

We define the dynamic consensus tracking error as

$$e = y - \frac{\mathbf{1}^T\sigma\mathbf{1}}{N} = \sigma - p - \frac{\mathbf{1}^T\sigma\mathbf{1}}{N} = \left[I - \frac{\mathbf{1}\mathbf{1}^T}{N}\right]\sigma - p = \Pi\sigma - p$$

Differentiating the above equation and using $L\mathbf{1} = 0$ we have,

$$\mu\dot{e} = -Le + \mu\Pi\dot{\sigma} \tag{6.15}$$

We define the change of coordinates as $\tilde{e} = T^T e$ where $T = \left[\frac{1}{\sqrt{N}}\mathbf{1} \;\; R\right]$ in which $R^T R = I, R^T\mathbf{1} = 0$. Hence, $T^T T = TT^T = I$. By the change of coordinates we have

$$\mu\dot{\tilde{e}} = -(T^T LT)\tilde{e} + \mu T^T\Pi\dot{\sigma}$$

$$T^T L T = \begin{bmatrix} 0 & 0 \\ 0 & R^T L R \end{bmatrix}, \quad T^T \Pi = \begin{bmatrix} \frac{1}{\sqrt{N}} \mathbf{1}^T \\ R^T \end{bmatrix} \left[I - \frac{\mathbf{1}\mathbf{1}^T}{N} \right] = \begin{bmatrix} 0 \\ R^T \end{bmatrix}$$

The system (6.15) is transformed to

$$\dot{\tilde{e}}_1 = 0 \tag{6.16a}$$

$$\mu \dot{s} = -\tilde{L} s + \mu R^T \dot{\sigma} \tag{6.16b}$$

where $s = \mathrm{col}(\tilde{e}_2, \ldots, \tilde{e}_N)$, $\tilde{L} = R^T L R$ and the eigenvalues of $\tilde{L}$ are the nonzero eigenvalues of L.

The initial condition of the dynamic consensus state $p(t)$ is taken as $p(0) = 0$, from which the initial condition of $\tilde{e}_1(0)$ is given by

$$\tilde{e}_1(0) = \frac{\mathbf{1}^T e(0)}{\sqrt{N}} = \frac{\mathbf{1}^T [\Pi \sigma(0)]}{\sqrt{N}} = \frac{\mathbf{1}^T \Pi \sigma(0)}{\sqrt{N}} = 0$$

where we have used $\mathbf{1}^T \Pi = 0$. Therefore, we conclude that

$$\tilde{e}_1(t) \equiv 0, \quad \forall\ t \geq 0$$

Assumption 6.5: The controller at each generator has access to the quantity $Q_i^{-1}/\mathbf{1}^T Q^{-1} \mathbf{1}$.

Remark 6.4: Assumption 6.5 requires a central authority which will communicate the quantity $Q_i^{-1}/\mathbf{1}^T Q^{-1} \mathbf{1}$ to the generators. This communication occurs only when the system is initialized or when there is a change in the cost matrix Q. This assumption is not restrictive because the optimal dispatch problem is solved centrally offline in order to obtain the optimal controller (6.8) and then the cost Q_i is made available to the generators. Therefore, the information $Q_i^{-1}/\mathbf{1}^T Q^{-1}\mathbf{1}$ can be made available to the controllers after the optimal dispatch problem is solved centrally.

The controller is chosen as

$$u = -F_1(\sigma - p) \tag{6.17}$$

where $F_1 = (N/(\mathbf{1}^T Q^{-1}\mathbf{1}))Q^{-1}$. Substituting $y = e + (\mathbf{1}^T \sigma \mathbf{1})/N$ and after some simplifications we have

$$u(t) = u^*(t) - F_1 e$$

The error e can be written as $e = \dfrac{1}{\sqrt{N}}\tilde{e}_1 + Rs = Rs$, since $\tilde{e}_1 = 0$, from which the control becomes

$$u(t) = u^*(t) - F_1 Rs \tag{6.18}$$

and the closed-loop system is given by

$$\dot{\delta} = \Pi\omega \tag{6.19a}$$

$$M\dot{\omega} = -D\omega - \nabla U(\delta) - P(t) + u^*(t) - F_1 Rs \tag{6.19b}$$

$$\mu\dot{s} = -\tilde{L}s - \mu R^T \nabla^2 U(\delta)\omega - \mu R^T Q^{-1}\mathbf{1}\dot{\tilde{p}}(t) \tag{6.19c}$$

The closed-loop system (6.19) does not have an equilibrium point due to the presence of the time-varying component $\dot{\tilde{p}}(t)$ in equation (6.19c), therefore we proceed with a singular perturbation framework. The reduced-order model of (6.19), obtained by setting $\mu = 0$, is

$$\dot{\delta} = \Pi\omega \tag{6.20a}$$

$$M\dot{\omega} = -D\omega - \nabla U(\delta) - P(t) + u^*(t) \tag{6.20b}$$

and the boundary-layer-model, obtained by choosing $t = \mu\tau$ and setting $\mu = 0$, is

$$\frac{ds}{d\tau} = -\tilde{L}s \tag{6.21}$$

Theorem 6.1: *Consider the closed-loop system (6.19) obtained from the power system model (6.4), the dynamic consensus algorithm (6.14) and the controller (6.17). Let $(\bar{\delta}(t), \bar{\omega}(t))$ and $(\delta(t), \omega(t))$ be the trajectories of the reduced-order model (6.20) and the closed-loop system (6.19), respectively, with $(\delta(0), \omega(0)) = (\bar{\delta}(0), \bar{\omega}(0))$. Then, there exists $\mu^* > 0$ such that for all $\mu \in (0, \mu^*)$,*

$$\delta(t) - \bar{\delta}(t) = O(\mu), \quad \omega(t) - \bar{\omega}(t) = O(\mu), \quad \forall\ t \geq 0 \tag{6.22}$$

Proof : The reduced-order model (6.20) has a synchronous solution $(\delta^*, 0)$, which follows from Assumptions 6.1 and 6.2. We first show the exponential stability of the reduced-order system by using the following Lyapunov function from [73],

$$V(\delta, \delta^*, \omega) = U(\delta) - U(\delta^*) - \nabla U(\delta^*)^T(\delta - \delta^*) + \frac{1}{2}\omega^T M\omega + h(\nabla U(\delta) - \nabla U(\delta^*))^T M\omega$$

where h is a small positive constant. It can be shown from [73, Lemma 2] that

$$\gamma_1||\delta - \delta^*||^2 \leq ||\nabla U(\delta) - \nabla U(\delta^*)||^2 \leq \gamma_2||\delta - \delta^*||^2 \tag{6.23}$$

where γ_1 and γ_2 are positive constants and

$$c_{\min}||x||^2 \leq V(\delta, \delta^*, \omega) \leq c_{\max}||x||^2 \tag{6.24}$$

where $x = \mathrm{col}(\delta - \delta^*, \omega)$, $c_{\max}$ is a positive constant and $c_{\min}$ is positive for sufficiently small h and therefore V is a Lyapunov function candidate. Taking the time derivative of V, along the reduced-order model (6.20), and substituting $P(t) = -\nabla U(\delta^*) + u^*(t)$ from the steady-state of (6.20b), we have

$$\dot{V} = -\omega^T D\omega - h(\nabla U(\delta) - \nabla U(\delta^*))^T(\nabla U(\delta) - \nabla U(\delta^*)) - h(\nabla U(\delta) - \nabla U(\delta^*))^T D\omega + h\omega^T H(\delta)\omega$$

where $H(\delta) = (M\nabla^2 U(\delta) + \nabla^2 U(\delta)M)/2$ which is obtained by using $\nabla^2 U(\delta)\Pi = \nabla^2 U(\delta)$ since $\nabla^2 U(\delta)\mathbf{1} = 0$. Since $\nabla^2 U(\delta)$ is bounded for any δ, we have $||H(\delta)|| \leq k_1$ where k_1 is a positive constant. From which we have

$$\dot{V} \leq -\begin{bmatrix} ||\nabla U(\delta) - \nabla U(\delta^*)|| \\ ||\omega|| \end{bmatrix}^T \Upsilon \begin{bmatrix} ||\nabla U(\delta) - \nabla U(\delta^*)|| \\ ||\omega|| \end{bmatrix}$$

where

$$\Upsilon = \begin{bmatrix} h & -\dfrac{h\lambda_{\max}(D)}{2} \\ -\dfrac{h\lambda_{\max}(D)}{2} & \lambda_{\min}(D) - hk_1 \end{bmatrix}$$

By choosing h sufficiently small we can make the determinant of Υ positive thereby making Υ a positive definite matrix. Let $\chi = \mathrm{col}(||\nabla U(\delta) - \nabla U(\delta^*)||, ||\omega||)$. Since Υ is positive definite, we have $\dot{V} \leq -k_2||\chi||^2$, for some positive constant k_2. From (6.23), $||\chi||^2 \geq k_3||x||^2$, where $k_3 = \min(1, \gamma_1)$. Hence

$$\dot{V} \leq -k_2 k_3||x||^2 \leq -k_4||x||^2$$

where $k_4 = k_2 k_3$. Therefore, we can conclude that (6.20) is exponentially stable.

The boundary-layer system is exponentially stable and a Lyapunov function candidate for (6.21) is given by $V_s = s^T G s$, where $G = G^T > 0$, is the solution to the Lyapunov equation

$G\tilde{L} + \tilde{L}^T G = I$. The time-derivative of V_s along (6.21) is given by $\dot{V}_s = -||s||^2$.

The time-derivative of V and V_s by taking into account the coupling between the systems (6.19b) and (6.19c) is given by,

$$\dot{V} \leq -\frac{k_5}{2}V - \frac{k_5}{2}\sqrt{V}\left[\sqrt{V} - \frac{2k_6}{k_5}\sqrt{V_s}\right] \tag{6.25a}$$

$$\dot{V}_s \leq -\frac{k_7}{2\mu}V_s - \frac{k_7}{2\mu}\sqrt{V}_s\left[\sqrt{V}_s - \frac{2\mu k_8}{k_7}\sqrt{V} - \frac{2\mu k_9}{k_7}\right] \tag{6.25b}$$

where $k_5 = k_4/c_{\max}$, $k_6 = ||F_1 R||(1 + h\sqrt{\gamma_2})/\sqrt{c_{\min} \cdot \lambda_{\min}(G)}$, $k_7 = 1/\lambda_{\max}(G)$, $k_8 = 2l||GR^T||/\sqrt{c_{\min} \cdot \lambda_{\min}(G)}$, $k_9 = 2p_m||GR^T Q^{-1}\mathbf{1}||/\sqrt{\lambda_{\min}(G)}$, $||\dot{\tilde{p}}(t)|| \leq p_m$, and $||\nabla^2 U(\delta)|| \leq l$, for some positive constants p_m and l. From (6.25a) and (6.25b), in order to have $\dot{V} < 0$ and $\dot{V}_s < 0$, we need

$$\sqrt{V_s} \leq (k_5/2k_6)\sqrt{V}, \text{ and } \sqrt{V_s} \geq (2\mu k_8/k_7)\sqrt{V} + 2\mu k_9/k_7$$

Considering equality, we have two lines in $(\sqrt{V}, \sqrt{V_s})$, which intersect for sufficiently small μ and the intersection points are given by $\sqrt{V} = \mu k_{10}$ and $\sqrt{V_s} = \mu k_{11}$, for some positive constants k_{10} and k_{11}. Moreover, for sufficiently small μ, on the boundaries $\sqrt{V} = \mu k_{10}$, $\sqrt{V}_s = \mu k_{11}$, we have $\dot{V} < 0$ and $\dot{V}_s < 0$. From which we can conclude that $\dot{V} < 0$ for $V \geq \mu^2 k_{10}^2$ and $\dot{V}_s < 0$ for $V_s \geq \mu^2 k_{11}^2$.

Next we find a compact set $\Omega_x = \{V \leq d\}$, which is contained in Θ. The constant d can be chosen [68] as $d = c_{\min}\tilde{c}^2/\lambda_{\max}(\mathcal{B}\mathcal{B}^T)$, where $\tilde{c} > 0$ is such that for $||\mathcal{B}^T\delta - \mathcal{B}^T\delta^*|| \leq \tilde{c}$, also satisfies $\mathcal{B}^T\delta \in \Theta$. Therefore, for sufficiently small μ, we have $\dot{V} < 0$ on $V = d$ and $\dot{V}_s < 0$ on $V_s = a$, where $a > 0$. Therefore, the set $\Omega = \Omega_x \times \{V_s \leq a\}$ is positively invariant.

Since the reduced-order model and boundary layer are exponentially stable, it follows from

[91, Theorem 11.2] that (6.19) has a unique solution $x(t, \mu)$ on $[0, \infty)$ and

$$x(t, \mu) - \bar{x}(t) = O(\mu) \tag{6.26}$$

holds uniformly for $t \in [0, \infty)$, where $\bar{x}(t) = (\bar{\delta}(t) - \delta^*, \bar{\omega}(t))$ is the solution of the reduced-order model (6.20). Therefore, (6.22) follows from (6.26). ■

6.4 Controller Design Under Unknown Time Varying Power Demand

In this section we proceed with the second step and design the controller when the power demand is unknown.

6.4.1 Extended High-Gain Observer

In the previous section we assumed that each local controller had access to the signal σ_i. However, in practice this signal is typically not available because the power demand is not known beforehand. We use a high-gain observer to estimate the signal σ_i, which can then be used by the dynamic consensus algorithm. The signal σ_i, composed of a time-varying power demand and the power-flow, is estimated using an extended high-gain observer. The extended high-gain observer is constructed as

$$\dot{\hat{\omega}} = -M^{-1}D\hat{\omega} + M^{-1}\hat{\sigma} + M^{-1}u + \frac{\alpha_1}{\epsilon}(\omega - \hat{\omega}) \tag{6.27a}$$

$$\dot{\hat{\sigma}} = \frac{\alpha_2}{\epsilon^2}(\omega - \hat{\omega}) \tag{6.27b}$$

where α_1, α_2 are any positive constants, ϵ is a small positive constant, $\hat{\omega} \in \mathbb{R}^N$, $\hat{\sigma} \in \mathbb{R}^N$ are the estimates of ω and σ. Next we define the scaled estimation errors as

$$\zeta_1 = \frac{\omega - \hat{\omega}}{\epsilon}, \quad \zeta_2 = \sigma - \hat{\sigma}$$

where $\zeta_1 \in \mathbb{R}^N$, $\zeta_2 \in \mathbb{R}^N$. Using (6.4) and (6.27) we write the observer error dynamics as

$$\epsilon\dot{\zeta} = A_0\zeta + \epsilon B_1\zeta + \epsilon B_2\Delta(t, \delta, \omega) \tag{6.28}$$

where $\zeta = \mathrm{col}(\zeta_1, \zeta_2)$, $\Delta(t, \delta, \omega) = -Q^{-1}\mathbf{1}\dot{p}(t) - \nabla^2 U(\delta)\omega$,

$$A_0 = \begin{bmatrix} -\alpha_1 I & M^{-1} \\ -\alpha_2 I & 0 \end{bmatrix}, \; B_1 = \begin{bmatrix} -M^{-1}D \\ 0 \end{bmatrix}, \; B_2 = \begin{bmatrix} 0 \\ -I \end{bmatrix},$$

The eigenvalues of A_0 are given by the roots of the polynomials

$$s^2 + \alpha_1 s + \alpha_2 m_i^{-1}, \text{ for } i = 1, \ldots, N.$$

Since the coefficients of the polynomials are positive it follows that the roots of the polynomials are negative, from which we conclude that A_0 is Hurwitz. To avoid the peaking phenomenon [90], we saturate the observer estimates outside the positively invariant set Ω before using them in feedback control. The signal $\hat{\sigma}$ is saturated as

$$\hat{\sigma}_{is} = M_{is}\mathrm{sat}\left(\frac{\hat{\sigma}_i}{M_{is}}\right)$$

where sat is the saturation function and

$$M_{is} > \max_{\delta\in\Omega,\ ||P(t)||\leq P_m} \sigma_i$$

where P_m represents a measure of the maximum power demand. The distributed dynamic average consensus algorithm using the saturated estimate $\hat{\sigma}_s = \text{col}(\hat{\sigma}_{1s}, \ldots, \hat{\sigma}_{ns})$ is given by

$$\mu\dot{p} = -Lp + L\hat{\sigma}_s \tag{6.29}$$

and the controller is chosen as

$$u = -F_1(\hat{\sigma}_s - p) \tag{6.30}$$

6.4.2 Analysis of the Closed-loop System

By defining the dynamic consensus tracking error as $e = \sigma - p - \dfrac{\mathbf{1}^T\sigma\mathbf{1}}{N}$ and using the change of coordinates $\tilde{e} = T^T e$, the error dynamics is given by

$$\mu\dot{\tilde{e}} = -(T^T LT)\tilde{e} + T^T L(\hat{\sigma}_s - \sigma) + \mu T^T \Pi\dot{\sigma}$$

where $T^T L = \text{col}(0, R^T L)$, from which we have

$$\dot{\tilde{e}}_1 = 0 \tag{6.31a}$$

$$\mu\dot{s} = -\tilde{L}s + R^T L(\hat{\sigma}_s - \sigma) + \mu R^T\dot{\sigma} \tag{6.31b}$$

where $s = \mathrm{col}(\tilde{e}_2, \ldots, \tilde{e}_n)$. Since, we choose $p(0) = 0$, it follows that

$$\tilde{e}_1(t) = 0, \quad \forall\, t \geq 0$$

Next we define the Lyapunov function $V_\zeta = \zeta^T S \zeta$, where S is the solution to the Lyapunov equation $SA_0 + A_0^T S = -I$.

Lemma 6.2: *Let $(\delta(0) - \delta^*, \omega(0), s(0))$ lie in the interior of the set Ω, and let the initial observer states lie in $(\hat{\omega}(0), \hat{\sigma}(0)) \in Y$, where Y is a compact subset of $\mathbb{R}^{2n}$. Then, there exists a positive constant κ_1 such that the set $\Lambda = \Omega \times \{V_\zeta \leq \kappa_1 \epsilon^2\}$ is positively invariant and the trajectory $(\delta(t) - \delta^*, \omega(t), s(t), \zeta(t))$ enters the set Λ in finite time $T(\epsilon) > 0$, where $\lim_{\epsilon \to 0} T(\epsilon) = 0$.*

Proof : We first show that Λ is positively invariant by calculating the derivatives of V, V_s and $V_\zeta = \zeta^T S \zeta$ on the boundaries $V = d$, $V_s = a$ and $V_\zeta = \kappa_1 \epsilon^2$, respectively. The saturation is no longer active when the system trajectory is in Λ, which implies $\hat{\sigma}_{is}(t) = \hat{\sigma}_i(t)$. Taking the time derivative of V_ζ we have

$$\epsilon \dot{V}_\zeta \leq -||\zeta||^2 + \epsilon q_1 ||\zeta||^2 + \epsilon q_2 ||\zeta||$$

where $q_1 = 2||SB_1||$, $q_2 = 2d_u||SB_2||$, and $||\Delta|| \leq d_u$. After some simplifications we have

$$\epsilon \dot{V}_\zeta \leq -(1/4)||\zeta||^2, \ \forall\, ||\zeta|| \geq 4\epsilon q_2$$

By taking $\kappa_1 = 16\lambda_{\max}(S) q_2^2$, we have

$$\epsilon \dot{V}_\zeta \leq -(1/4)||\zeta||^2, \ \forall\, V_\zeta \geq \kappa_1 \epsilon^2$$

Next by taking the time derivative of V and V_s, we have

$$\dot{V} \leq -(k_5/4)V - \frac{k_5}{2}\sqrt{V}\left[\sqrt{V} - \frac{2k_6}{k_5}\sqrt{V_s}\right], \forall\, V \geq \epsilon^2 q_3$$

$$\dot{V}_s \leq -\frac{k_7}{4\mu}V_s - \frac{k_7}{2\mu}\sqrt{V}_s\left[\sqrt{V}_s - \frac{2\mu k_8}{k_7}\sqrt{V} - \frac{2\mu k_9}{k_7}\right]$$

for all $V_s \geq \epsilon^2 q_4$, where q_3, q_4 are positive constants. It can be shown that for sufficiently small μ, $\dot{V} < 0$ for $V \geq \mu^2 q_5$ and $\dot{V}_s < 0$ for $V_s \geq \mu^2 q_5$, for some positive constants q_5 and q_6. Furthermore, we can choose ϵ sufficiently small, such that the set $\{V \leq \epsilon^2 q_3\} \times \{V_s \leq \epsilon^2 q_4\}$ is in the interior of the set $\{V \leq \mu^2 q_5\} \times \{V_s \leq \mu^2 q_6\}$. Therefore, we have $\dot{V} < 0$ on the boundary $V = d$ and $\dot{V}_s < 0$ on the boundary $V_s = a$, which implies Λ is positively invariant.

By following the standard work in high-gain observer theory [90], it can be shown that $(\delta(t) - \delta^*, \omega(t), s(t)) \in \Omega$ for all $t \in [0, \bar{T}]$, where $\bar{T} > 0$ is some finite time independent of μ. The state $\zeta(t)$ enters the set $\{V_\zeta \leq \kappa_1 \epsilon^2\}$ within time $T(\epsilon) > 0$, where $\lim_{\epsilon \to 0} T(\epsilon) = 0$ and therefore by choosing ϵ sufficiently small we have $T(\epsilon) < \bar{T}$, from which we can conclude that $(\delta(t) - \delta^*, \omega(t), s(t), \zeta(t)) \in \Lambda$ for all $t \geq T(\epsilon)$. ■

From Lemma 6.2, we have $\zeta(t) = O(\epsilon), \forall\, t \geq T(\epsilon)$, which implies $\hat{\sigma}_i(t) = \sigma_i(t) + O(\epsilon), \forall\, t \geq T(\epsilon)$ and the closed-loop system for $t \geq T(\epsilon)$ is given by

$$\dot{\delta} = \Pi\omega \tag{6.32a}$$

$$M\dot{\omega} = -D\omega - \nabla U(\delta) - P(t) + u^*(t) - F_1(Rs - \zeta_2) \tag{6.32b}$$

$$\mu\dot{s} = -\tilde{L}s - R^T L\zeta_2 + \mu R^T \dot{\sigma} \tag{6.32c}$$

$$\epsilon\dot{\zeta} = A_0\zeta + \epsilon B_1\zeta + \epsilon B_2\Delta \tag{6.32d}$$

Theorem 6.2: *Consider the closed-loop system (6.32) obtained from the power system model (6.4), the dynamic consensus algorithm (6.29) and the controller (6.30). Let* $(\bar{\delta}(t), \bar{\omega}(t))$ *and* $(\delta(t), \omega(t))$ *be the trajectories of the reduced-order model (6.20) and the closed-loop system (6.32), respectively with* $(\delta(0), \omega(0)) = (\bar{\delta}(0), \bar{\omega}(0))$. *Then given any* $\Xi > 0$, *there exists* $\mu^* > 0$, *and for each* $\mu \in (0, \mu^*]$, $\epsilon^* = \epsilon^*(\mu)$ *exists such that for each* $\mu \in (0, \mu^*]$ *and* $\epsilon \in (0, \epsilon^*(\mu)]$, *all system trajectories are bounded, and*

$$||\delta(t) - \bar{\delta}(t)|| \leq \Xi, \quad ||\omega(t) - \bar{\omega}(t)|| \leq \Xi, \quad \forall\, t \geq 0 \tag{6.33}$$

Proof : The proof is done in three steps where we first show (6.33) during the time period $[\tilde{T}, \infty)$, where $\tilde{T} > 0$ is some finite time followed by $[0, T(\epsilon)]$ and then during $[T(\epsilon), \tilde{T}]$.
Let $\tilde{x}(t) = \mathrm{col}(\delta(t) - \delta^*, \omega(t), s(t))$ be the solution of (6.32) and $\tilde{x}_r(t) = \mathrm{col}(\delta_r(t) - \delta^*, \omega_r(t), s_r(t))$ be the solution of the reduced-order model of system (6.32) obtained by setting $\epsilon = 0$, which is represented by Eq. (6.19), with $\tilde{x}_r(0) = \tilde{x}(0)$. From Theorem 6.1 and Lemma 6.2, given any $\Xi > 0$, there exists $\mu_1 > 0$ and $\epsilon_1 = \epsilon_1(\mu) > 0$ such that for each $\mu \in (0, \mu_1]$ and $\epsilon \in (0, \epsilon_1(\mu)]$

$$||\tilde{x}(t)|| \leq \Xi/4, \quad ||\tilde{x}_r(t)|| \leq \Xi/4, \ \forall\, t \geq \tilde{T}$$

Therefore it follows that

$$||\tilde{x}(t) - \tilde{x}_r(t)|| \leq \Xi/2, \ \forall\, t \geq \tilde{T}$$

Using $\delta(t) - \bar{\delta}(t) = \delta(t) - \delta_r + \delta_r(t) - \bar{\delta}(t)$ and $\omega(t) - \bar{\omega}(t) = \omega(t) - \omega_r + \omega_r(t) - \bar{\omega}(t)$, there exists $\mu_2 > 0$ and $\epsilon_2 = \epsilon_2(\mu) > 0$, such that for all $\mu \in (0, \mu_2]$ and $\epsilon \in (0, \epsilon_2(\mu)]$, we have

$$||\delta(t) - \bar{\delta}(t)|| \leq \Xi, \ ||\omega(t) - \bar{\omega}(t)|| \leq \Xi, \ \forall\, t \geq \tilde{T}$$

Next we show (6.33) during the time period $[0, T(\epsilon)]$. From Lemma 6.2, we know that $(\delta(t) - \delta^*, \omega(t), s(t)) \in \Omega$ during the time period $[0, T(\epsilon)]$. Therefore the right-hand-side of (6.32a)-(6.32b) and (6.19a)-(6.19c) is bounded by a constant independent of ϵ, from which we have

$$||\delta(t) - \delta_r(t)|| \leq 2bT(\epsilon), ||\omega(t) - \omega_r(t)|| \leq 2bT(\epsilon),$$

for all $t \in [0, T(\epsilon)]$, where $\lim_{\epsilon \to 0} T(\epsilon) = 0$ and b is a positive constant. Similar to the first step using $\delta(t) - \bar{\delta}(t) = \delta(t) - \delta_r + \delta_r(t) - \bar{\delta}(t)$ and $\omega(t) - \bar{\omega}(t) = \omega(t) - \omega_r + \omega_r(t) - \bar{\omega}(t)$, there exists $\mu_3 > 0$ and $\epsilon_3 = \epsilon_3(\mu) > 0$ such that for each $\mu \in (0, \mu_3]$ and $\epsilon \in (0, \epsilon_3(\mu)]$, we have

$$||\delta(t) - \bar{\delta}(t)|| \leq \Xi,\ ||\omega(t) - \bar{\omega}(t)|| \leq \Xi, \forall\ t \in [0, T(\epsilon)]$$

Over the time interval $[T(\epsilon), \tilde{T}]$, equations (6.32a)-(6.32c) under output feedback is $O(\epsilon)$ perturbation from the corresponding model (6.19a)-(6.19c). Therefore, it follows from the continuous dependence of solutions of differential equation on initial conditions and parameters [91, Theorem 3.5] and by repeating the arguments in the previous steps that there exists $\mu_4 > 0$ and $\epsilon_4 = \epsilon_4(\mu) > 0$ such that for each $\mu \in (0, \mu_4]$ and $\epsilon \in (0, \epsilon_4(\mu)]$, we have

$$||\delta(t) - \bar{\delta}(t)|| \leq \Xi,\ ||\omega(t) - \bar{\omega}(t)|| \leq \Xi,\ \forall\ t \in [T(\epsilon), \tilde{T}]$$

Therefore, (6.33) follows by choosing $\mu^* = \min\{\mu_1, \mu_2, \mu_3, \mu_4\}$ and $\epsilon^* = \min\{\epsilon_1, \epsilon_2, \epsilon_3, \epsilon_4\}$.

■

6.5 Simulation

We illustrate the performance of the proposed controller on a connected four area network taken from [74]. The area connections taken from [74] is illustrated in Fig. 6.1.

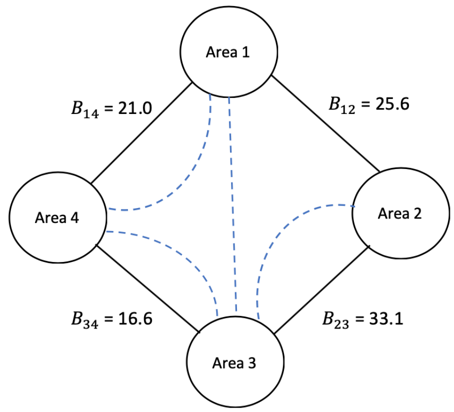

Figure 6.1: Four area network

The four area equivalent network can be obtained for the IEEE New England 39-bus system; see [121]. The parameters of the system in per unit taken from [74], are given by $M = \text{diag}(5.22, 3.98, 4.49, 4.22)$, $D = \text{diag}(1.60, 1.22, 1.38, 1.42)$. All the line voltages are chosen to 1 per unit and line coefficients of the power-flow are taken as $B_{12} = 25.6$, $B_{23} = 33.1$, $B_{34} = 16.6$, $B_{14} = 21$. The generator cost coefficient matrix is given by $Q = \text{diag}(1, 0.75, 1.5, 0.5)$ and the nominal frequency is chosen as $\omega_{\text{ref}} = 120\pi$ rad/s.

6.5.1 Case I : Unknown Constant Power Demand

For the first scenario the power demand is constant which implies $P = \bar{P}$ (per unit). The system is initially at steady-state with $P = [2.00, 1.00, 1.50, 1.00]^T$, $t \in [0, 10)$. At timestep 10 the load is increased for $t \geq 10$ to $P = [2.20, 1.05, 1.55, 1.10]^T$. For the design of the controller (6.30) we choose the parameters as $\alpha_1 = 2$, $\alpha_2 = 1$, $\epsilon = 0.001$, $\mu = 0.01$ and the saturation level as $\hat{M}_{is} = \pm 3$ for $i = 1, 2, 3, 4$. The saturation levels are chosen from simulations to see the maximal values that the trajectories would take when using the controller with the worst case power demand.

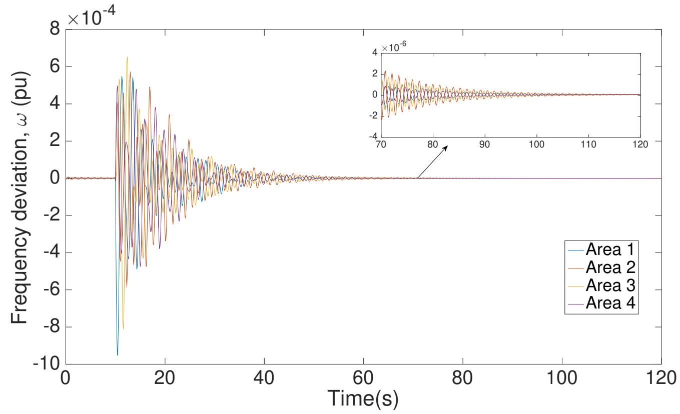

Figure 6.2: Frequency deviation (ω) under unknown constant power demand

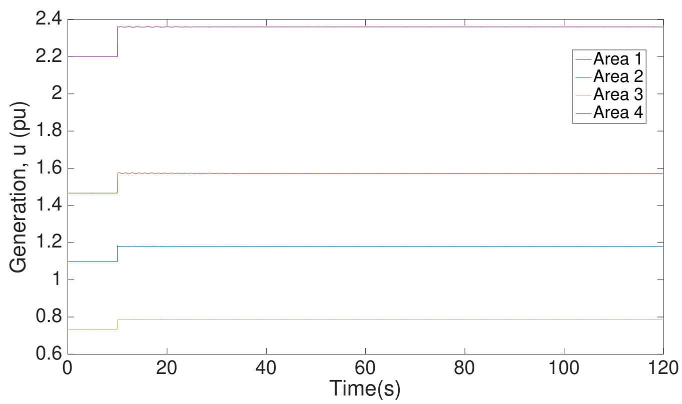

Figure 6.3: Control (u) under unknown constant power demand

Fig. 6.2 and 6.3 illustrates the frequency deviation under the controller (32). Compared to the results in [74], the frequency deviation is roughly ten times smaller. Morever the control signal quickly reaches steady-state as seen from Fig. 6.3.

6.5.2 Case II : Unknown Time-Varying Power Demand with variable Frequency

For the second scenario we consider the unknown power-demand to be time-varying with variable frequency. The power demand is taken as:

$$P(t) = \begin{cases} [2.00, 1.00, 1.50, 1.00]^T, & t \in [0, 10) \\ [2.20, 1.05, 1.55, 1.10]^T + 0.05Q^{-1}\mathbf{1}\tilde{p}_1(t), & t \in [10, 50) \\ [2.20, 1.05, 1.55, 1.10]^T + 0.07Q^{-1}\mathbf{1}\tilde{p}_2(t), & t \in [50, 80) \\ [2.20, 1.05, 1.55, 1.10]^T + 0.09Q^{-1}\mathbf{1}\tilde{p}_3(t), & t \geq 80 \end{cases}$$

where $\tilde{p}_1(t) = \sin\left(\frac{2\pi}{30}t\right), \tilde{p}_2(t) = \sin\left(\frac{2\pi}{20}t\right), \tilde{p}_3(t) = \sin\left(\frac{2\pi}{10}t\right)$.

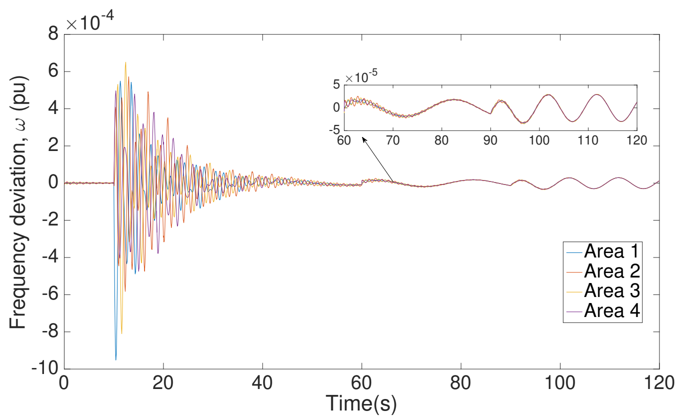

Figure 6.4: Frequency deviation (ω) under unknown time-varying power demand

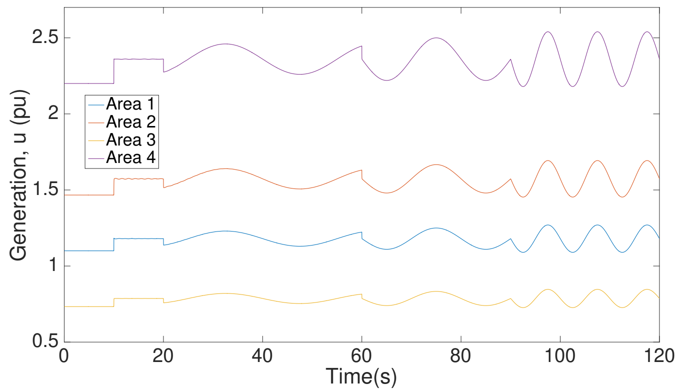

Figure 6.5: Control (u) under unknown time-varying power demand

Fig. 6.4 shows the frequency deviation under the proposed controller (6.30) with $\mu = 0.01$, and $\epsilon = 0.001$. The steady-state error is of the order of 10^{-5} and has oscillations of small amplitude due to the time-varying power demand. Finally, Fig. 6.5 shows the control, which is time-varying, due to the time-varying component of $P(t)$, and it quickly reaches the time-varying steady-state control.

6.6 Conclusion

In this chapter, we presented an observer-based dynamic consensus algorithm to achieve practical frequency synchronization and power-sharing in the presence of unknown time-varying power demand. The proposed approach does not assume that the power demand is generated from a known exosystem compared to the internal model approach [74]. Moreover, the trajectories of the closed-loop system under the controller (6.30) is arbitrarily close to the system trajectories (6.20) under the steady-state controller.

Chapter 7

Conclusion and Future Work

7.1 Overview of Conclusion

This thesis investigated the use of observers in multi-agent systems to reduce information exchange and increase the convergence rate. The conclusion is summarized below.

First, we showed that by adding extended high-gain observers to each agent except the root agent, the convergence rate of the star topology could be increased to match the convergence rate of a complete graph. Furthermore, we showed that the trajectories of the agents under the star topology approach the trajectories of the agents under a complete graph for sufficiently small ϵ.

Second, we design a scalable consensus algorithm for first-order agents using PD control, where the eigenvalues of the closed-loop Laplacian matrix are invariant with respect to the size of the network for general directed graphs. As a result, the convergence of the consensus protocol does not slow down when the network size increases for non-expander graphs. The PD controller is realized using a high-gain observer, and we show that the trajectories of the closed-loop system when the high-gain observer can be brought arbitrarily close to the trajectories under the PD controller. Simulation results were presented to demonstrate the efficacy of the proposed algorithm on a circular directed graph with 100 nodes and two classes of graphs, which show the trend of decrease in the second smallest eigenvalue of the graph

Laplacian with an increase in network size.

Third, motivated by real-world systems akin to power systems with second-order swing dynamics [65], and longitudinal vehicle dynamics [102], and effect of an increase in network size on the performance of nonlinear systems we design a scalable consensus algorithm to achieve practical synchronization in a leader-follower framework for second-order nonlinear heterogeneous systems. The synchronization error can be made arbitrarily small by increasing a controller parameter. We show that the control signal is uniformly bounded with respect to this controller parameter, and therefore by increasing it to achieve an arbitrarily small synchronization error does not increase the magnitude of the control signal. Unlike the previous chapters, we realize the controller using a reduced-order high-gain observer. This is done because we do not use additional controller dynamics, as in the previous chapter. We show that the synchronization error can be made arbitrarily small by tuning a controller and observer parameter, respectively. We show that the control signal is uniformly bounded with respect to these parameters. We demonstrated the efficacy of the proposed controller with two examples i) a network of oscillators on the IEEE-300 bus system and ii) a platoon of vehicles.

Fourth, we design an extended high gain observer-based controller to achieve synchronization in a leader-follower network of nonlinear multi-agent systems having the same relative degree r. The agents have access to only relative output information from their neighbors. The class of systems considered in this chapter is more general than the previous chapters. But unlike the previous chapters, we focus on synchronization with reduced information exchange. An extended high-gain observer based on the relative output exchange is used to estimate the uncertain terms and then using feedback control to cancel them. In other words, we compensate for the heterogeneous dynamics of each agent using extended high-gain observer and feedback control. Finally, simulations were done on the example from [55] and with a network of power systems to show the efficacy of the proposed controller.

Fifth, we design a load-estimator-based consensus algorithm that achieves practical frequency synchronization in the presence of unknown time-varying power demand in a network of lossless, connected and network-reduced power systems. We assume the availability frequency measurement. The controller design procedure is different from the previous chapter as instead of canceling the power system dynamics, we only compensate for the time-varying power demand. We show that the frequency synchronization error can be made arbitrarily small by tuning a controller and observer parameter. Finally, simulations on a network reduced four area network is performed to show the performance of the proposed controller.

Throughout the thesis, we assumed that there is no noise in the measurements. However, the presence of measurement noise puts a constraint on how high the observer gain could be, which results in a trade-off between fast convergence to the state estimates and the error due to measurement noise. In practice, the choice of ϵ is bounded from below by the level of measurement noise in the system. In experimental applications of high-gain observers, typically, a low-pass filter is used to filter out the high-frequency content of the measurement noise before using the measurement in the observer [122], [123].

One of the basic ideas to mitigate the effect of measurement noise is by adjusting the observer gain so that a higher gain is used during the transient period to converge to the state estimate quickly. Then the gain is lowered as the estimation error approaches the steady-state since the effect of measurement noise is notable when the estimation error is small. Based on this idea, some techniques have been developed in the literature, including switching gain between two values [124], adaptive law to adjust gain [125], and using nonlinear gain where the gain reduces when the estimation error is small [126].

7.2 Future Directions

7.2.1 Stability of Networks with Signed Laplacians

Signed graphs appear in a wide range of applications like social networks, power systems, and biological networks. The graphs primarily contain edges where the weights on these edges can be positive or negative. The negative weights have physical interpretations. For example, antagonistic relations in social relations and the presence of critical transmission lines in power systems across which the bus angles difference is greater than $\pi/2$. The current research in this field focuses on the conditions required on signed Laplacian, such that consensus is achieved.

The future research in this area will mainly focus on achieving consensus for any signed graph. Since the scalable consensus controller designed in this thesis can change the closed-loop Laplacian matrix using only relative information. This can help in changing the closed-loop Laplacian of signed networks whose underlying signed Laplacian has positive eigenvalues and, as a result, help in achieving consensus. The main features of using this scalable controller will be:

- The distributed controller will use only local relative information

- The closed-loop system under the proposed controller will behave as a virtual Laplacian, where the non-zero eigenvalues can be assigned to be negative, thus achieving consensus.

One of the main applications of this algorithm will be in the stability analysis of power systems in the presence of critical transmission lines where the bus angles differ by greater than $\pi/2$ and thereby providing solutions to those scenarios where the signed Laplacian is not positive semi-definite.

7.2.2 Scalable Formation Control of Mobile Robots

Formation control of mobile robots is one of the well-studied distributed control problems due to its wide applications in surveillance and searching operations. The mobile robots are generally equipped with omnidirectional range-based proximity sensors, which can measure the relative position or velocity of a neighboring agent if it lies within its proximity disk. The main objective of the formation control algorithm is to maintain a pre-specified distance between the robots while they move or meet at a certain goal point. In the literature, nonlinear consensus algorithms have been developed to maintain connectivity among a group of agents while achieving consensus.

The performance of this algorithm, when the network size increases, needs to be investigated. This is essential since converging to a certain goal within a specific time is very important for applications such as search and rescue. Therefore, there is a need to investigate the performance of these algorithms in large sparse graphs and develop new distributed scalable controllers that can maintain a specific convergence rate with an increase in network size. The presence of proximity sensors, which make consensus algorithm nonlinear, make this work challenging and can explain the lack of research done in this area. Future research in this direction will be the design of new scalable controllers such that performance does not degrade with an increase in network size. The scalable controllers designed in this thesis can help in the design of the new controllers.

7.2.3 Frequency Synchronization in Higher Order Power System Models

The second-order power systems model considered in the thesis was lossless, network-reduced, and the voltage fluctuations were assumed to be constant. As a future direction to this work, a fourth-order model, including the turbine-governor dynamics, will be considered. This research direction will help solve the current practical challenges faced in the frequency synchronization of power systems. The other important directions in this area will include:

- Effects of uncertain mass and damping coefficients
- Effects of loss-of-communication/packet and dropouts/delay.

APPENDIX

Kronecker Product

The Kronecker product of matrices $\bar{A} \in \mathbb{R}^{m\times n}$ and $\bar{B} \in \mathbb{R}^{p\times q}$ is defined as

$$\bar{A} \otimes \bar{B} = \begin{bmatrix} \bar{a}_{11}\bar{B} & \dots & \bar{a}_{1n}\bar{B} \\ \vdots & \vdots & \vdots \\ \bar{a}_{m1}\bar{B} & \dots & \bar{a}_{mn}\bar{B} \end{bmatrix}$$

where $[\bar{A}]_{ij} = \bar{a}_{ij}$ and it satisfies the following properties [6]:

$$(\bar{A} \otimes \bar{B})(\bar{C} \otimes \bar{D}) = (\bar{A}\bar{C} \otimes \bar{B}\bar{D}), \quad (\bar{A} \otimes \bar{B})^T = \bar{A}^T \otimes \bar{B}^T$$

$$\bar{A} \otimes (\bar{B} + \bar{C}) = \bar{A} \otimes \bar{B} + \bar{A} \otimes \bar{C}$$

Moreover if $\bar{A}$ and $\bar{B}$ are nonsingular matrices then

$$(\bar{A} \otimes \bar{B})^{-1} = \bar{A}^{-1} \otimes \bar{B}^{-1}$$

Consensus Algorithm

Consider a group of N agents where each agent is labeled by the index v_i and $v_i \in \mathcal{V}$. Let $\mathcal{G} = \{\mathcal{V}, \mathcal{E}, \mathcal{A}\}$ encode the communication topology connecting the agents. The information available to each agent is given by

$$\zeta_i = \sum_{j=1}^{N} a_{ij}(x_j - x_i) \qquad i = 1, \ldots, N$$

The above form of information is available to the agents implies that it can only measure the relative difference of the states between itself and its neighbors. Each of the agents has single integrator dynamics represented by

$$\dot{x}_i = u_i \qquad i = 1, \ldots, N.$$

We define the total energy of the graph associated with its edges as [19]

$$E_{\mathcal{G}} = \frac{1}{2} \sum_{i,j=1}^{N} a_{ij}(x_j - x_i)^2.$$

The controller is now chosen as the gradient-based feedback law

$$u_i = -\frac{1}{2}\frac{\partial E_{\mathcal{G}}}{\partial x_i} = \sum_{j=1}^{N} a_{ij}(x_j - x_i)$$

for $i = 1, \ldots, N$. The gradient-based feedback law is the standard decentralized controller used for solving the consensus problem as considered in [19].

BIBLIOGRAPHY

BIBLIOGRAPHY

[1] L. Xiao, S. Boyd, and S. Lall, "A scheme for robust distributed sensor fusion based on average consensus," in *IPSN 2005. Fourth International Symposium on Information Processing in Sensor Networks, 2005.* IEEE, 2005, pp. 63–70.

[2] R. Olfati-Saber and J. S. Shamma, "Consensus filters for sensor networks and distributed sensor fusion," in *Decision and Control, 2005 and 2005 European Control Conference. CDC-ECC'05. 44th IEEE Conference on.* IEEE, 2005, pp. 6698–6703.

[3] J. Cortés, S. Martínez, and F. Bullo, "Robust rendezvous for mobile autonomous agents via proximity graphs in arbitrary dimensions," *IEEE Transactions on Automatic Control*, vol. 51, no. 8, pp. 1289–1298, 2006.

[4] W. Ren and R. W. Beard, *Distributed Consensus In Multi-vehicle Cooperative Control.* Springer, 2008.

[5] D. P. Bertsekas and J. N. Tsitsiklis, *Parallel and Distributed Computation: Numerical Methods.* Prentice Hall, Englewood Cliffs, NJ, 1989.

[6] R. A. Horn and C. R. Johnson, *Matrix analysis.* Cambridge university press, 2012.

[7] M. Fiedler, "Algebraic connectivity of graphs," *Czechoslovak mathematical journal*, vol. 23, no. 2, pp. 298–305, 1973.

[8] ——, "A property of eigenvectors of nonnegative symmetric matrices and its application to graph theory," *Czechoslovak Mathematical Journal*, vol. 25, no. 4, pp. 619–633, 1975.

[9] J. Ghaderi and R. Srikant, "Opinion dynamics in social networks with stubborn agents: Equilibrium and convergence rate," *Automatica*, vol. 50, no. 12, pp. 3209–3215, 2014.

[10] H. Zhang and F. L. Lewis, "Adaptive cooperative tracking control of higher-order nonlinear systems with unknown dynamics," *Automatica*, vol. 48, no. 7, pp. 1432–1439, 2012.

[11] J. A. Fax and R. M. Murray, "Information flow and cooperative control of vehicle formations," *IEEE transactions on automatic control*, vol. 49, no. 9, pp. 1465–1476, 2004.

[12] M. Egerstedt and X. Hu, "Formation constrained multi-agent control," *IEEE transactions on robotics and automation*, vol. 17, no. 6, pp. 947–951, 2001.

[13] M. Ji and M. Egerstedt, "Distributed coordination control of multiagent systems while preserving connectedness," *IEEE Transactions on Robotics*, vol. 23, no. 4, pp. 693–703, 2007.

[14] R. Olfati-Saber, "Flocking for multi-agent dynamic systems: Algorithms and theory," *IEEE Transactions on Automatic Control*, vol. 51, no. 3, pp. 401–420, 2006.

[15] W. Ren, R. W. Beard, and E. M. Atkins, "A survey of consensus problems in multi-agent coordination," in *Proceedings of the American Control Conference*, 2005, pp. 1859–1864.

[16] R. Olfati-Saber, J. A. Fax, and R. M. Murray, "Consensus and cooperation in networked multi-agent systems," *Proceedings of the IEEE*, vol. 95, no. 1, pp. 215–233, 2007.

[17] M. Mesbahi and M. Egerstedt, *Graph Theoretic Methods in Multiagent Networks*. Princeton University Press, 2010.

[18] F. Bullo, *Lectures on Network Systems*, 1st ed. CreateSpace, 2018.

[19] R. Olfati-Saber and R. M. Murray, "Consensus problems in networks of agents with switching topology and time-delays," *IEEE Transactions on Automatic Control*, vol. 49, no. 9, pp. 1520–1533, 2004.

[20] C. Godsil and G. F. Royle, *Algebraic graph theory*. Springer Science & Business Media, 2013, vol. 207.

[21] H. Zhang, Z. Chen, and X. Mo, "Effect of adding edges to consensus networks with directed acyclic graphs," *IEEE Transactions on Automatic Control*, vol. 62, no. 9, pp. 4891–4897, 2017.

[22] R. Olfati-Saber, "Ultrafast consensus in small-world networks," in *Proceedings of the 2005, American Control Conference, 2005.* IEEE, 2005, pp. 2371–2378.

[23] L. Xiao and S. Boyd, "Fast linear iterations for distributed averaging," *Systems & Control Letters*, vol. 53, no. 1, pp. 65–78, 2004.

[24] H.-T. Zhang, M.-C. Fan, Y. Wu, J. Gao, H. E. Stanley, T. Zhou, and Y. Yuan, "Ultrafast synchronization via local observation," *New Journal of Physics*, vol. 21, no. 1, p. 013040, 2019.

[25] G. Parlangeli and M. E. Valcher, "Leader-controlled protocols to accelerate convergence in consensus networks," *IEEE Transactions on Automatic Control*, vol. 63, no. 10, pp. 3191–3205, 2018.

[26] R. Aragues, G. Shi, D. V. Dimarogonas, C. Sagüés, K. H. Johansson, and Y. Mezouar, "Distributed algebraic connectivity estimation for undirected graphs with upper and lower bounds," *Automatica*, vol. 50, no. 12, pp. 3253–3259, 2014.

[27] H. A. Poonawala and M. W. Spong, "Decentralized estimation of the algebraic connectivity for strongly connected networks," in *2015 American Control Conference (ACC)*. IEEE, 2015, pp. 4068–4073.

[28] L. Kempton, G. Herrmann, and M. Di Bernardo, "Self-organization of weighted networks for optimal synchronizability," *IEEE Transactions on Control of Network Systems*, vol. 5, no. 4, pp. 1541–1550, 2017.

[29] J. CortéS, "Finite-time convergent gradient flows with applications to network consensus," *Automatica*, vol. 42, no. 11, pp. 1993–2000, 2006.

[30] L. Wang and F. Xiao, "Finite-time consensus problems for networks of dynamic agents," *IEEE Transactions on Automatic Control*, vol. 55, no. 4, pp. 950–955, 2010.

[31] E. Tegling, "Fundamental limitations of distributed feedback control in large-scale networks," Ph.D. dissertation, KTH Royal Institute of Technology, 2018.

[32] E. Tegling, R. H. Middleton, and M. M. Seron, "Scalability and fragility in bounded-degree consensus networks," *IFAC-PapersOnLine*, vol. 52, no. 20, pp. 85–90, 2019.

[33] M. Krebs and A. Shaheen, *Expander families and Cayley graphs: a beginner's guide*. Oxford University Press, 2011.

[34] R. Olfati-Saber, J. A. Fax, and R. M. Murray, "Consensus and cooperation in networked multi-agent systems," *Proceedings of the IEEE*, vol. 95, no. 1, pp. 215–233, 2007.

[35] B. Bamieh, M. R. Jovanovic, P. Mitra, and S. Patterson, "Coherence in large-scale networks: Dimension-dependent limitations of local feedback," *IEEE Transactions on Automatic Control*, vol. 57, no. 9, pp. 2235–2249, 2012.

[36] F. Dörfler, J. W. Simpson-Porco, and F. Bullo, "Electrical networks and algebraic graph theory: Models, properties, and applications," *Proceedings of the IEEE*, vol. 106, no. 5, pp. 977–1005, May 2018.

[37] G. F. Young, L. Scardovi, and N. E. Leonard, "Robustness of noisy consensus dynamics with directed communication," in *Proceedings of the 2010 American Control Conference*. IEEE, 2010, pp. 6312–6317.

[38] T. W. Grunberg and D. F. Gayme, "Performance measures for linear oscillator networks over arbitrary graphs," *IEEE Transactions on Control of Network Systems*, vol. 5, no. 1, pp. 456–468, 2016.

[39] T. Sarkar, M. Roozbehani, and M. A. Dahleh, "Asymptotic network robustness," *IEEE Transactions on Control of Network Systems*, vol. 6, no. 2, pp. 812–821, 2018.

[40] M. Pirani, E. M. Shahrivar, B. Fidan, and S. Sundaram, "Robustness of leader–follower networked dynamical systems," *IEEE Transactions on Control of Network Systems*, vol. 5, no. 4, pp. 1752–1763, 2017.

[41] Y. Kuramoto, "Self-entrainment of a population of coupled non-linear oscillators," in *International symposium on mathematical problems in theoretical physics*. Springer, 1975, pp. 420–422.

[42] J. H. Seo, H. Shim, and J. Back, "Consensus of high-order linear systems using dynamic output feedback compensator: Low gain approach," *Automatica*, vol. 45, no. 11, pp. 2659–2664, 2009.

[43] Z. Li, Z. Duan, G. Chen, and L. Huang, "Consensus of multiagent systems and synchronization of complex networks: A unified viewpoint," *IEEE Transactions on Circuits and Systems I: Regular Papers*, vol. 57, no. 1, pp. 213–224, 2010.

[44] T. Yang, A. A. Stoorvogel, and A. Saberi, "Consensus for multi-agent systems—synchronization and regulation for complex networks," in *American Control Conference (ACC), 2011*. IEEE, 2011, pp. 5312–5317.

[45] L. Moreau, "Stability of multiagent systems with time-dependent communication links," *IEEE Transactions on automatic control*, vol. 50, no. 2, pp. 169–182, 2005.

[46] Y. Su and J. Huang, "Stability of a class of linear switching systems with applications to two consensus problems," *IEEE Transactions on Automatic Control*, vol. 57, no. 6, pp. 1420–1430, June 2012.

[47] W. Ren and R. W. Beard, "Consensus seeking in multiagent systems under dynamically changing interaction topologies," *IEEE Transactions on automatic control*, vol. 50, no. 5, pp. 655–661, 2005.

[48] J. Seo, J. Back, H. Kim, and H. Shim, "Output feedback consensus for high-order linear systems having uniform ranks under switching topology," *IET control theory & applications*, vol. 6, no. 8, pp. 1118–1124, 2012.

[49] Y. Su and J. Huang, "Stability of a class of linear switching systems with applications to two consensus problems," *IEEE Transactions on Automatic Control*, vol. 57, no. 6, pp. 1420–1430, 2012.

[50] T. Yang, H. F. Grip, A. Saberi, M. Zhang, and A. A. Stoorvogel, "Synchronization in time-varying networks of non-introspective agents without exchange of controller states," in *American Control Conference (ACC), 2014*. IEEE, 2014, pp. 1475–1480.

[51] P. Wieland, R. Sepulchre, and F. Allgöwer, "An internal model principle is necessary and sufficient for linear output synchronization," *Automatica*, vol. 47, no. 5, pp. 1068–1074, 2011.

[52] H. F. Grip, T. Yang, A. Saberi, and A. A. Stoorvogel, "Output synchronization for heterogeneous networks of non-introspective agents," *Automatica*, vol. 48, no. 10, pp. 2444–2453, 2012.

[53] H. F. Grip, A. Saberi, and A. A. Stoorvogel, "Synchronization in networks of minimum-phase, non-introspective agents without exchange of controller states: homogeneous, heterogeneous, and nonlinear," *Automatica*, vol. 54, pp. 246–255, 2015.

[54] H. Kim, H. Shim, and J. H. Seo, "Output consensus of heterogeneous uncertain linear multi-agent systems," *IEEE Transactions on Automatic Control*, vol. 56, no. 1, pp. 200–206, 2011.

[55] A. Isidori, L. Marconi, and G. Casadei, "Robust output synchronization of a network of heterogeneous nonlinear agents via nonlinear regulation theory," *IEEE Transactions on Automatic Control*, vol. 59, no. 10, pp. 2680–2691, 2014.

[56] F. D. Priscoli, A. Isidori, L. Marconi, and A. Pietrabissa, "Leader-following coordination of nonlinear agents under time-varying communication topologies," *IEEE Transactions on Control of Network Systems*, vol. 2, no. 4, pp. 393–405, 2015.

[57] Y. Su and J. Huang, "Cooperative semi-global robust output regulation for a class of nonlinear uncertain multi-agent systems," *Automatica*, vol. 50, no. 4, pp. 1053–1065, 2014.

[58] Y. Su, "Semi-global output feedback cooperative control for nonlinear multi-agent systems via internal model approach," *Automatica*, vol. 103, pp. 200–207, 2019.

[59] H. Modares, F. L. Lewis, W. Kang, and A. Davoudi, "Optimal synchronization of heterogeneous nonlinear systems with unknown dynamics," *IEEE Transactions on Automatic Control*, vol. 63, no. 1, pp. 117–131, Jan 2018.

[60] M. Zhang, A. Saberi, A. A. Stoorvogel, and H. F. Grip, "Almost regulated output synchronization for heterogeneous time-varying networks of non-introspective, nonlinear agents without exchange of controller states," in *2015 54th IEEE Conference on Decision and Control (CDC)*, Dec 2015, pp. 2939–2944.

[61] E. Panteley and A. Loría, "Synchronization and dynamic consensus of heterogeneous networked systems," *IEEE Transactions on Automatic Control*, vol. 62, no. 8, pp. 3758–3773, Aug 2017.

[62] L. Scardovi and R. Sepulchre, "Synchronization in networks of identical linear systems," *Automatica*, vol. 45, no. 11, pp. 2557–2562, 2009.

[63] D. Chowdhury and H. K. Khalil, "Synchronization in networks of identical linear systems with reduced information," in *2018 Annual American Control Conference (ACC)*, 2018, pp. 5706–5711.

[64] J. Wu, V. Ugrinovskii, and F. Allgöwer, "Cooperative estimation and robust synchronization of heterogeneous multiagent systems with coupled measurements," *IEEE Transactions on Control of Network Systems*, vol. 5, no. 4, pp. 1597–1607, 2017.

[65] J. Machowski, J. W. Bialek, and J. Bumby, *Power system dynamics: stability and control*. John Wiley & Sons, 2011.

[66] M. Andreasson, D. V. Dimarogonas, H. Sandberg, and K. H. Johansson, "Distributed control of networked dynamical systems: Static feedback, integral action and consensus," *IEEE Transactions on Automatic Control*, vol. 59, no. 7, pp. 1750–1764, July 2014.

[67] C. Zhao, E. Mallada, and F. Dörfler, "Distributed frequency control for stability and economic dispatch in power networks," in *2015 American Control Conference (ACC)*. IEEE, 2015, pp. 2359–2364.

[68] E. Weitenberg et al., "Robust decentralized secondary frequency control in power systems: Merits and tradeoffs," *IEEE Transactions on Automatic Control*, vol. 64, no. 10, pp. 3967–3982, 2018.

[69] D. K. Molzahn et al., "A survey of distributed optimization and control algorithms for electric power systems," *IEEE Transactions on Smart Grid*, vol. 8, no. 6, pp. 2941–2962, Nov 2017.

[70] J. W. Simpson-Porco et al., "Secondary frequency and voltage control of islanded microgrids via distributed averaging," *IEEE Transactions on Industrial Electronics*, vol. 62, no. 11, pp. 7025–7038, Nov 2015.

[71] F. Dörfler, J. W. Simpson-Porco, and F. Bullo, "Breaking the hierarchy: Distributed control and economic optimality in microgrids," *IEEE Transactions on Control of Network Systems*, vol. 3, no. 3, pp. 241–253, Sep. 2016.

[72] M. Andreasson, D. V. Dimarogonas, H. Sandberg, and K. H. Johansson, "Distributed PI-Control with Applications to Power Systems Frequency Control," in *American Control Conference (ACC), 2014*. IEEE, 2014, pp. 3183–3188.

[73] E. Weitenberg, C. De Persis, and N. Monshizadeh, "Exponential convergence under distributed averaging integral frequency control," *Automatica*, vol. 98, pp. 103–113, 2018.

[74] S. Trip, M. Bürger, and C. De Persis, "An internal model approach to (optimal) frequency regulation in power grids with time-varying voltages," *Automatica*, vol. 64, pp. 240–253, 2016.

[75] M. Bürger and C. De Persis, "Dynamic coupling design for nonlinear output agreement and time-varying flow control," *Automatica*, vol. 51, pp. 210–222, 2015.

[76] N. Monshizadeh and C. De Persis, "Agreeing in networks: Unmatched disturbances, algebraic constraints and optimality," *Automatica*, vol. 75, pp. 63–74, 2017.

[77] Z. Wang, S. Mei, F. Liu, S. H. Low, and P. Yang, "Distributed load-side control: Coping with variation of renewable generations," *Automatica*, vol. 109, p. 108556, 2019.

[78] D. Chowdhury and H. K. Khalil, "Fast consensus in multi-agent systems with star topology using high gain observers," *IEEE Control Systems Letters*, vol. 1, no. 1, pp. 188–193, 2017.

[79] J. Yick, B. Mukherjee, and D. Ghosal, "Wireless sensor network survey," *Computer networks*, vol. 52, no. 12, pp. 2292–2330, 2008.

[80] N. e. a. Celandroni, "A survey of architectures and scenarios in satellite-based wireless sensor networks: system design aspects," *International Journal of Satellite Communications and Networking*, vol. 31, no. 1, pp. 1–38, 2013.

[81] X. Zhang and A. Papachristodoulou, "A real-time control framework for smart power networks with star topology," in *2013 American Control Conference*. IEEE, 2013, pp. 5062–5067.

[82] J. Ma, Y. Zheng, and L. Wang, "Lqr-based optimal topology of leader-following consensus," *International Journal of Robust and Nonlinear Control*, vol. 25, no. 17, pp. 3404–3421, 2015.

[83] L. B. Freidovich and H. K. Khalil, "Performance recovery of feedback-linearization-based designs," *IEEE Transactions on Automatic Control*, vol. 53, no. 10, pp. 2324–2334, 2008.

[84] A. N. Atassi and H. K. Khalil, "A separation principle for the stabilization of a class of nonlinear systems," *IEEE Transactions on Automatic Control*, vol. 44, no. 9, pp. 1672–1687, 1999.

[85] P. Kokotović, H. K. Khalil, and J. O'reilly, *Singular perturbation methods in control: analysis and design.* SIAM, 1999.

[86] D. Chowdhury and H. K. Khalil, "Scalable consensus in networks of multi-agent systems using high-gain observers," *IEEE Transactions on Control of Network Systems.*

[87] D. A. B. Lombana and M. Di Bernardo, "Distributed pid control for consensus of homogeneous and heterogeneous networks," *IEEE Transactions on Control of Network Systems*, vol. 2, no. 2, pp. 154–163, 2014.

[88] F. Dörfler, J. W. Simpson-Porco, and F. Bullo, "Electrical networks and algebraic graph theory: Models, properties, and applications," *Proceedings of the IEEE*, vol. 106, no. 5, pp. 977–1005, 2018.

[89] N. Morača, "Bounds for norms of the matrix inverse and the smallest singular value," *Linear algebra and its applications*, vol. 429, no. 10, pp. 2589–2601, 2008.

[90] H. K. Khalil, *High-gain observers in nonlinear feedback control.* SIAM, 2017, vol. 31.

[91] ——, "Nonlinear systems, 3rd," *New Jewsey, Prentice Hall*, vol. 9, 2002.

[92] J. A. Marshall, M. E. Broucke, and B. A. Francis, "Formations of vehicles in cyclic pursuit," *IEEE Transactions on Automatic Control*, vol. 49, no. 11, pp. 1963–1974, 2004.

[93] S. Patterson and B. Bamieh, "Consensus and coherence in fractal networks," *IEEE Transactions on Control of Network Systems*, vol. 1, no. 4, pp. 338–348, 2014.

[94] K. C. Das, "The laplacian spectrum of a graph," *Computers & Mathematics with Applications*, vol. 48, no. 5-6, pp. 715–724, 2004.

[95] W. Yu, G. Chen, M. Cao, and J. Kurths, "Second-order consensus for multiagent systems with directed topologies and nonlinear dynamics," *IEEE Transactions on Systems, Man, and Cybernetics, Part B (Cybernetics)*, vol. 40, no. 3, pp. 881–891, June 2010.

[96] Q. Song, J. Cao, and W. Yu, "Second-order leader-following consensus of nonlinear multi-agent systems via pinning control," *Systems & Control Letters*, vol. 59, no. 9, pp. 553–562, 2010.

[97] M. Zhang, A. Saberi, A. A. Stoorvogel, and H. F. Grip, "Almost output synchronization for heterogeneous time-varying networks for a class of non-introspective, nonlinear agents without exchange of controller states," *International journal of robust and nonlinear control*, vol. 26, no. 17, pp. 3883–3899, 2016.

[98] A. Das and F. L. Lewis, "Distributed adaptive control for synchronization of unknown nonlinear networked systems," *Automatica*, vol. 46, no. 12, pp. 2014–2021, 2010.

[99] ——, "Cooperative adaptive control for synchronization of second-order systems with unknown nonlinearities," *International Journal of Robust and Nonlinear Control*, vol. 21, no. 13, pp. 1509–1524, 2011.

[100] F. L. Lewis, H. Zhang, K. Hengster-Movric, and A. Das, *Cooperative Adaptive Control for Systems with Second-Order Nonlinear Dynamics*. London: Springer London, 2014, pp. 259–278.

[101] D. Chowdhury, "Practical scalable synchronization in leader-follower networks," *Conditionally accepted in IEEE Transactions on Control of Network Systems*.

[102] R. Rajamani, *Vehicle dynamics and control*. Springer Science & Business Media, 2011.

[103] H. K. Khalil, *Nonlinear control*. Pearson, Upper Saddle River, New Jersey, 2015.

[104] H. Zhang, Z. Li, Z. Qu, and F. L. Lewis, "On constructing lyapunov functions for multi-agent systems," *Automatica*, vol. 58, pp. 39–42, 2015.

[105] A. Berman and R. J. Plemmons, *Nonnegative matrices in the mathematical sciences*. SIAM, 1994.

[106] S. Soltan and G. Zussman, "Expose the line failures following a cyber-physical attack on the power grid," *IEEE Transactions on Control of Network Systems*, vol. 6, no. 1, pp. 451–461, 2018.

[107] D. Chowdhury and H. K. Khalil, "Scalable coherence in large scale second-order networks using high-gain observers," in *2020 American Control Conference (ACC)*. IEEE, 2020.

[108] ——, "Practical synchronization in networks of nonlinear heterogeneous agents with application to power systems," *IEEE Transactions on Automatic Control*.

[109] M. Rubenstein, C. Ahler, and R. Nagpal, "Kilobot: A low cost scalable robot system for collective behaviors," in *Robotics and Automation (ICRA), 2012 IEEE International Conference on*. IEEE, 2012, pp. 3293–3298.

[110] L. Wang, A. Isidori, and H. Su, "Output feedback stabilization of nonlinear mimo systems having uncertain high-frequency gain matrix," *Systems & Control Letters*, vol. 83, pp. 1–8, 2015.

[111] Q. Jiao, H. Modares, F. L. Lewis, S. Xu, and L. Xie, "Distributed L_2-gain output-feedback control of homogeneous and heterogeneous systems," *Automatica*, vol. 71, pp. 361–368, 2016.

[112] Z. Li, Z. Duan, and G. Chen, "On $H\infty$ and H_2 performance regions of multi-agent systems," *Automatica*, vol. 47, no. 4, pp. 797–803, 2011.

[113] M. Andreasson, H. Sandberg, D. V. Dimarogonas, and K. H. Johansson, "Distributed Integral Action: Stability Analysis and Frequency Control of Power Systems," in *Decision and Control (CDC), 2012 IEEE 51st Annual Conference on*. IEEE, 2012, pp. 2077–2083.

[114] F. Dörfler and F. Bullo, "Synchronization in complex networks of phase oscillators: A survey," *Automatica*, vol. 50, no. 6, pp. 1539–1564, 2014.

[115] W. Ren, "On consensus algorithms for double-integrator dynamics," *Automatic Control, IEEE Transactions on*, vol. 53, no. 6, pp. 1503–1509, 2008.

[116] G. Rinaldi, P. P. Menon, C. Edwards, and A. Ferrara, "Design and validation of a distributed observer-based estimation scheme for power grids," *IEEE Transactions on Control Systems Technology*, 2018.

[117] M. F. Rahman, L. Zhong, M. E. Haque, and M. Rahman, "A direct torque-controlled interior permanent-magnet synchronous motor drive without a speed sensor," *IEEE Transactions on Energy Conversion*, vol. 18, no. 1, pp. 17–22, 2003.

[118] *Power systems test case archive-30 bus power flow test case.* [Online]. Available: http://www.ee.washington.edu/research/pstca/pf30/pgtca30bus.htm

[119] D. Chowdhury and H. K. Khalil, "Practical frequency synchronization in power systems using extended high-gain observer under unknown time-varying power demand," in *2020 American Control Conference (ACC)*. IEEE, 2020.

[120] S. S. Kia et al., "Tutorial on dynamic average consensus: The problem, its applications, and the algorithms," *IEEE Control Systems Magazine*, vol. 39, no. 3, pp. 40–72, June 2019.

[121] S. Nabavi and A. Chakrabortty, "Topology identification for dynamic equivalent models of large power system networks," in *2013 American Control Conference*. IEEE, 2013, pp. 1138–1143.

[122] H. K. Khalil and S. Priess, "Analysis of the use of low-pass filters with high-gain observers," *IFAC-PapersOnLine*, vol. 49, no. 18, pp. 488–492, 2016.

[123] H. K. Khalil, "High-gain observers in feedback control: Application to permanent magnet synchronous motors," *IEEE Control Systems Magazine*, vol. 37, no. 3, pp. 25–41, 2017.

[124] J. H. Ahrens and H. K. Khalil, "High-gain observers in the presence of measurement noise: A switched-gain approach," *Automatica*, vol. 45, no. 4, pp. 936–943, 2009.

[125] R. G. Sanfelice and L. Praly, "On the performance of high-gain observers with gain adaptation under measurement noise," *Automatica*, vol. 47, no. 10, pp. 2165–2176, 2011.

[126] A. A. Prasov and H. K. Khalil, "A nonlinear high-gain observer for systems with measurement noise in a feedback control framework," *IEEE Transactions on Automatic Control*, vol. 58, no. 3, pp. 569–580, 2012.